A MODEL OF ARTHROFIBROSIS USING INTRA-ARTICULAR GENE DELIVERY OF TRANSFORMING GROWTH FACTOR BETA 1

By

RACHAEL SUSAN WATSON

A DISSERTATION PRESENTED TO THE GRADUATE SCHOOL
OF THE UNIVERSITY OF FLORIDA IN PARTIAL FULFILLMENT
OF THE REQUIREMENTS FOR THE DEGREE OF
DOCTOR OF PHILOSOPHY

UNIVERSITY OF FLORIDA

2010

To my family and friends for their unconditional love, support and friendship!

ACKNOWLEDGMENTS

I would first like to thank my mentor, Dr. Steven Ghivizzani, for accepting me into his lab and presenting me with the necessary skills to become a research scientist. His encouragement, patience, guidance and motivation will not be forgotten. Dr. Ghivizzani's office door was always open for discussions, scientific or otherwise, and his willingness to meet regularly and provide support and insight for my project exemplifies his dedication. I would also like to thank the members of the Ghivizzani lab. The assistance and mentorship from the postdoctoral associate, Padraic Levings, was critical. I would additionally like to thank my fellow graduate students, Marsha Bush and Jesse Kay, for their friendship and camaraderie over the years. Furthermore, I would like to thank the other members of our lab, Anthony Dacanay for his constant humor, Elvire Gouze, Jean-Noel Gouze, and Celine Theodore.

I am especially grateful to my committee members, Dr. Alfred Lewin, Dr. Gregory Schultz, and Dr. Bryon Petersen, for their helpful suggestions, feedback and expertise, and for generously providing materials, resources, and time necessary for me to complete these studies. I would particularly like to thank our collaborators, above all, Dr. Thomas Wright for providing the inspiration for this project as well as for providing invaluable materials and guidance and Dr. Parker Gibbs, Dr. John Reith, and Marda Jorgensen.

Lastly, none of this would be possible without the support of my loving family and friends: my parents, Robert and Susan, my brothers, Alexander and Robert Jr., my sister, Melissa, and my dearest friends Padraic, Lisa, LeeAnn, and Christy; all of whom provided an endless flow of love, humor and guidance.

TABLE OF CONTENTS

page

ACKNOWLEDGMENTS 4

LIST OF TABLES 8

LIST OF FIGURES 9

ABSTRACT 14

CHAPTER

1 INTRODUCTION 16

Idiopathic Adhesive Capsulitis (IAC) 16
Stages of IAC 17
Treatments of IAC are Controversial 18
Tissue Repair and Fibrosis 19
TGF-beta 1 and Fibrogenesis 21
Analysis of TGF-β1 and CTGF Expression in IAC Patients 23
Diabetes, TGF-beta1 and Fibrosis 24
Gene Transfer to Capsular Fibroblasts 27
Significance 29

2 MATERIALS AND METHODS 34

Vector Production 34
Tissue Culture 34
ASO Transfection 35
TGF-β1 ELISA 35
Cell Migration Assay 35
Animal Experimentation 36
For Anti-sense oligonucleotides (ASO) Experiments 36
Induction of Diabetes in Animals 36
Preparation of Total RNA 37
PCR Array 37
Immunohistochemistry 38
Detection of GFP 39
Detection of Reporter ASO 39
Microarray 40
Sample Preparation 40
RNA Amplification, Labeling and Array Hybridization 40

3 GENERATION AND CHARACTERIZATION OF ADENOVIRAL VECTOR 42

In vitro Expression of Adenoviral Vector 42

Overexpression of TGF-β1 *In vivo* Induces Fibrosis 44

4 GENE DELIVERY OF TGF-BETA1 INDUCES ARTHROFIBROSIS AND CHONDROMETAPLASIA OF SYNOVIUM *IN VIVO* 51

Introduction 51
Results 54
Intra-articular Delivery of Ad.TGF-β1 Induces a Dose-Dependent Fibrotic Response: 54
Sustained Overexpression of TGF-β1 in the Joints of Nude Rats Induces Severe Arthrofibrosis and Chondrometaplasia: 55
TGF-β1 Stimulates Expression of Genes for Matricellular Proteins, MMPs, Collagens and Adhesion Molecules 57
Resident Synovial/Capsular Fibroblasts Proliferate to form the Fibrotic Mass . 60
Discussion 61
Expression Profiling is Consistent with an Aggressive Fibrotic and Chondrometaplastic Phenotype 62
Synovial and Capsular Fibroblasts have a High Proliferative Capacity and Innate Plasticity 65

5 EXAMINING THE EFFECTS OF LONG TERM ARTHROFIBROSIS IN IMMUNOCOMPETENT ANIMALS 76

Introduction 76
Results 78
Delivery of Ad.TGF-β1 to the Joints of Immunocompetent Rats Induces Arthrofibrosis and Chondrometaplasia that Resolves with Time 79
Expression Profiles of Genes Stimulated by TGF-β1 Display Altering Patterns of Expression Consistent with the Phenotype of the Tissue 80
Discussion 82

6 EXAMINING THE RELATIONSHIP BETWEEN DIABETES AND ARTHROFIBROSIS 89

Introduction 89
Results 91
D-glucose Stimulates Cell Migration 91
Streptozotocin Diabetic Induction 92
Diabetes Induced Alterations in Gene Expression in Synovial Tissue 93
Diabetic Joints Receiving Ad.TGF-β1 Resulted in an Overall Less Severe Fibrosis 94
Decreases in Gene Expression at Onset of Fibrosis were seen between Diabetic and Non-Diabetic Animals Receiving Ad.TGF-β1 96
Discussion 96

7 ANTISENSE-OLIGONUCLEOTIDES LESSEN SEVERITY OF JOINT FIBROSIS WHEN DELIEVERED AT ONSET OF DISEASE 111

Introduction 111
Results 113
TGF-β1 Knockdown by Specific ELISA 113
Intra-articular Injection of Reporter ASO is Retained in the Joint Space 113
ASOs were Effective at Inhibiting Arthrofibrosis in Animal Model 114
Discussion 115

8 SUMMARY AND FUTURE DIRECTIONS 122

LIST OF REFERENCES 127

BIOGRAPHICAL SKETCH 140

LIST OF TABLES

Table		page
1-1	Stages of Idiopathic Adhesive Capsulitis	31
4-1	Relative Expression Values of ECM and Associated Genes in the Joints of Nude Rats Receiving Ad.TGF-β1	68
5-1	Relative Expression Values of ECM and Associated Genes in the Joints of Wistar rats receiving $5.0*10^7$ Ad.TGF-β1	86
6-1	Mean of blood glucose in diabetic and normal Wistar rats.	100
6-2	Relative signal values of ECM and adhesion genes in the joints of Diabetic Wistar rats compared to non-diabetic normal Wistar joints	101
6-3	Relative signal values of ECM and adhesion genes in the joints of Diabetic Wistar rats receiving Ad.TGF-β1 compared to untreated diabetic Wistar rats	103
6-4	Relative signal values of ECM and adhesion genes in the joints of Diabetic Wistar rats receiving Ad.TGF-β1 compared to non-diabetic Wistar rats receiving Ad.TGF-β1	105
6-5	Arbitrary scale measuring severity of fibrosis by a blinded observer. Scale represents 0 (Normal)-4 (severe fibrosis).	107
7-1	Arbitrary scale in which a blinded observer measured severity of fibrosis. Scale represents 0 (normal)-4 (severe fibrosis).	118

LIST OF FIGURES

Figure		page
1-1	TGF-β/Smad signaling pathway.	32
1-2	Immunohistochemistry analysis for CTGF expression in tissue from patients with adhesive capsulitis	33
3-1	Western blot analysis of CTGF protein	46
3-2	hCTGF specific ELISA.	47
3-3	Cell proliferation assay.	48
3-4	Percentage change in knee diameter relative to day zero of adenovirus injected Wistar rats.	49
3-5	Histolgical H&E stain of Wistar rats knees, four days post intra-articular injection..	50
4-1	Transgene expression following infection of rat synovial fibroblasts with Ad.TGF-β1.	70
4-2	Intra-articular delivery of Ad.TGF-β1 induces joint swelling	71
4-3	Local overexpression of Ad.TGF-β1 in the knee joint induce severe arthrofibrosis.	72
4-4	Capsular fibrosis and chondrogenesis induced by Ad.TGF-β1.	73
4-5	Immunohistochemical staining for MMPs 9 and 13, and α smooth muscle actin (αSMA).	74
4-6	Arthrofibrosis and chondrometaplasia arise from resident synovial and capsular fibroblasts.	75
5-1	Capsular fibrosis and chondrogenesis induced by Ad.TGF-β1 resolves with time.	88
6-1	Glucose stimulates rat synovial fibroblast migration.	108
6-2	Glucose stimulates rat synovial fibroblast migration.	109
6-3	Capsular fibrosis induced by Ad.TGF-β1 in diabetic animals.	110

7-1 Transgene expression following transduction of rat synovial fibroblasts with Ad.TGF-β1 and/or transfection with an antisense oligonucleotide specific for TGF-β1. 119

7-2 Immunohistochemical staining of reporter anti-sense oligonucleotide 120

7-3 Capsular fibrosis induced by Ad.TGF-β1 in Wistar rats is inhibited by co-intra-articular injection of ASO. 121

LIST OF ABBREVIATIONS

α	alpha
αSMA	alpha smooth muscle actin
Ad	Adeno virus
ASO	antisense oligonucleotide
β	beta
ºC	degrees centigrade
cDNA	complementary DNA
CMV	cytomegalovirus
CO_2	carbon dioxide
CCN2/CTGF	connective tissue growth factor
CsCl	cesium chloride
DMEM	Delbecco's modified Eagle's medium
DNA	deoxyribonucleic acid
ECM	extracellular matrix
EDTA	ethylenediaminetetraacetic acid
ELISA	enzyme-linked immunosorbant assay
FBS	fetal bovine serum
FGFR-1	fibroblast growth factor receptor – 1
GFP	green fluorescent protein
H&E	hematoxylin and eosin stain
hr	hour
IAC	idiopathic adhesive capsulitis
IHC	immunohistochemistry
IL-1β	interleukin-1 beta

IL-1Ra	Interleukin-1 receptor antagonist
mg	milligram
μg	microgram
mL	milliliter
μl	microliter
mM	millimolar
MMPs	matrix metalloproteases
ng	nanogram
nM	nanomolar
NSAID	non steroidal anti-inflammatory drug
OA	osteoarthritis
OPN	osteopontin
PBS	phosphate buffered solution
PCR	polymerase chain reaction
PDGFRα	platelet derived growth factor receptor alpha
RA	rheumatoid arthritis
RNA	ribonucleic acid
ROM	range of motion
RSF	rat synovial fibroblast
SEM	standard error of the mean
siRNA	small interfering RNA
STZ	streptozotocin
TGF	transforming growth factor
TIMP	tissue inhibitor of MMP
TNF-α	tumor necrosis factor alpha

UV	ultraviolet
Vp	viral particles
VSV-G	vesicular stomatitis virus G protein

Abstract of Dissertation Presented to the Graduate School
of the University of Florida in Partial Fulfillment of the
Requirements for the Degree of Doctor of Philosophy

A MODEL OF ARTRHOFIBROSIS USING INTRA-ARTCULAR DELVERY OF TRANSFORMNG GROWTH FACTOR BETA-1

By

Rachael Susan Watson

May 2010

Chair: Steven C. Ghivizzani
Major: Medical Sciences— Genetics

Idiopathic adhesive capsulitis (IAC) of the shoulder is a disease of unknown etiology characterized by painful, chronic fibrotic expansion of the synovium and joint capsule, gradually leading to loss of joint motion. Although IAC affects approximately 3-5% of the population, and 20% of diabetics, little is known about its pathogenesis. While the underlying causes are diverse, it is likely that many of the harmful aspects of fibrosis are mediated by transforming growth factor-β1 (TGF-β1), a pleiotropic cytokine. In an effort to establish an animal model of IAC and develop an understanding of the cellular and molecular events contributing to arthrofibrosis, we first used an adenovirus to deliver and over-express TGF-β1 cDNA (Ad.TGF-β1) in the knee joints of athymic nude rats. By 5 days, TGF-β1 induced a rapid increase in knee diameter and the complete encasement of the joints in dense scar-like tissue, locking the joints at 90^{o} of flexion. Histologically, massive proliferation of synovial fibroblasts was seen, followed by their differentiation into myofibroblasts. By day 30 the phenotype of the expanded fibrotic tissue had undergone chondrometaplasia, indicated by tissue and cellular morphology, and matrix composition. Pre-labeling of the articular cells by injection of recombinant lentivirus containing the cDNA for eGFP showed the cells comprising the

fibrotic/cartilaginous tissues appeared to arise almost entirely from the local proliferation and differentiation of resident fibroblasts. These results indicate that TGF-β1 is a potent inducer of arthrofibrosis, and resident articular fibroblasts have immense proliferative potential and are highly plastic. Reduced viral dose and delivery of Ad.TGF-β1 into the joints of immunocompetent animals resulted in a fibrotic pathology that more closely resembled IAC. This model was less severe and gradually resolved over 120 days. To examine the effects of diabetes on this arthrofibrotic model, streptozotocin was used to induce diabetes in animals. Ten days after onset of diabetes, diabetic animals were intra-articularly injected with Ad.TGF-β1 which induced a fibrotic event similar to non-diabetic animals; however, there was markedly less chondrogenic differentiation, and tissue appeared to be less resolved at the end of the experiment. Alterations in ECM and adhesion genes were seen in the joint synovium, suggesting a reason why diabetics are prone to development of IAC and why diabetic animals may take longer to resolve fibrosis.

CHAPTER 1
INTRODUCTION

Idiopathic Adhesive Capsulitis (IAC)

Also known as Frozen Shoulder Syndrome, IAC is a disease of unknown etiology that is characterized by both primary and secondary capsulitis. Primary capsulitis is manifested as intense pain, shoulder stiffness and a loss of passive and active shoulder rotation due to a thickening contraction and adhesion of the capsule, synovium, and surrounding structures. Secondary capusilits is histopathologically similar, but associated with an extrinsic or intrinsic condition such as diabetes, autoimmune disease, stroke or myocardial infarction[1]. Affecting 2-5% of the population and 20% of diabetics, this disease is commonly recognized, but poorly understood. It usually begins in the sixth decade of life and affects more women than men[2]. This idiopathic disease is typically self-limiting, lasting 1-3 years, and the non-dominant shoulder is most commonly afflicted. Less than 20% of patients incur similar disease in the opposite shoulder within five years of the resolution of the originally affected shoulder[2].

In this disease, synovitis, dense adhesions and capsular constriction are found intra-articularly, causing severe restriction of motion. The diagnosis for IAC is mainly clinical, and shoulders are examined through radiographs and scapular rotation. Normal scapular rotation is 90 degrees; however, the scapular rotation of an affected individual is at 60 degrees with active abduction of the shoulder[3]. IAC is associated with significant morbidity; the shoulder becomes so stiff that everyday movements, such as raising the arm or rotating the humerus, are difficult to perform. Patients also suffer considerable loss of productivity due to pain and the inability to sleep, and are often unable to adequately perform at work. After 20-30 months, the fibrosis will “thaw” and

many patients will have minimal pain and will have regained most, but not all, of the use of the affected shoulder[4]. However, some individuals, usually diabetic patients, never work their way out of the painful and stiff stages and remain permanently disabled.

There is some disagreement whether the underlying pathologic process is an inflammatory condition or one of fibrosis. Patient histories are consistent with the view that IAC arises initially from a persistent synovial inflammation which, in turn, chronically stimulates tissue repair pathways whose dysregulation leads to the development of capsular fibrosis.

Stages of IAC

Based on clinical and arthroscopic examination, and histologic appearance of capsule biopsy specimens, adhesive capsulitis can be divided into four stages. These do not represent discrete, well-defined steps, but rather, a continuum of disease progression (Table 1-1). The following description is based on that provided by Hannafin et al[1].

In *Stage 1*, symptoms have typically been present for less than 3 months. Patients present with an aching pain in the shoulder, which becomes sharp at the extreme ranges of motion. Pain is usually associated with a loss of internal rotation, forward flexion and adduction, as well as a more subtle loss of external rotation in adduction. Arthroscopic and histologic examinations of the joint tissues demonstrate the presence of a hypertrophic vascular synovitis covering the entire capsular lining which itself appears normal. Under anesthesia the range of motion (ROM) is nearly normal, indicating that at this early stage, the loss in ROM is primarily attributable to painful synovitis rather than actual capsular contraction. In *Stage 2*, symptoms have been present for 3 to 9 months, with progressive loss of ROM and persistence of the pain

pattern described above. Manipulation of the joint under anesthesia reveals that the loss of motion is increasingly attributable to loss of capsular volume. Examination of the joint tissues reveals a hypervascular synovitis with capsular fibroplasia and deposition of disorganized collagen fibrils, and a hypercelluar appearance. Typically an inflammatory infiltrate is not present with either Stage 1 or 2. In *Stage 3*, symptoms have been present for 10-20 months or greater, and have changed noticeably with time. Patients present with a history of painful stiffening of the shoulder and a significant loss of ROM. Often reported is an extremely painful phase that has resolved, resulting in a relatively pain-free but very stiff shoulder. Increased ROM is not achieved under anesthesia reflecting a persistent loss of capsular volume, and fibrosis of the glenohumeral joint capsule. Examination of the joint tissues reveals a synovial thickening and a dense hypercellular collagenous tissue. *Stage 4*, is marked by a "thawing" of IAC, and is characterized by the slow, steady recovery of ROM resulting from capsular remodeling. Little histologic information is available regarding these patients as they rarely have surgery or capsular biopsy.

Treatments of IAC are Controversial

Despite its prevalence and debilitating effects, frozen shoulder has received little research attention because it is generally self-limiting, often disappearing within 2-3 years without specific medical or physical action. Since the underlying causes of IAC remain unknown, no specific treatment has been shown to cure IAC or have a long-term advantage. Treatments are aimed at reducing pain and maintaining shoulder mobility; therefore, all stages of IAC require physical therapy[5-7] to enhance/preserve ROM and relax the muscles. NSAIDS[8, 9] have been shown to reduce inflammation and relieve pain, and oral corticosteroids[10] as well as intra-articular injections[6, 11-13] aid in physical

therapy and also pain relief. For patients in more advanced stages of IAC, surgical intervention, particularly manipulations under anesthesia to break up the adhesions, and post-surgical rehabilitations, are the most common treatments. In addition, arthroscopic release is recommended for patients who have not improved after several months of physical therapy. To date, there have been no studies in which patients were assigned randomly to treatment groups and followed from diagnosis, through treatment, and for a significant time downstream.

Tissue Repair and Fibrosis

Little is known of the etiology or the biology that drives the pathologic fibrosis of IAC; however, tissue fibrosis is a prominent feature of progressive disease in several other organs such as the skin, liver, lung and kidney. Important clues to the pathogenesis of IAC are likely to come from parallels with these conditions. In many fibrotic diseases, pathology is thought to arise from tissue repair responses to chronic injury such as from alcohol abuse and viral hepatitis in the liver.

Fibrogenesis is a normal part of wound healing and occurs in response to tissue injury. Many factors that mediate normal tissue repair also participate in pathologic fibrosis. Following injury, there is an early inflammatory step characterized by hemorrhage of the vasculature and coagulation of the blood. During this phase, platelets degranulate and release numerous growth factors into the local environment that help to attract inflammatory cells, particularly monocytes and granulocytes, to the site of injury. These infiltrating cells release protein factors that initiate the repair process, including platelet derived growth factor, insulin-like growth factor, endothelins, angiotensin I, transforming growth factor beta 1, among others[14]. Elevated levels of these cytokines stimulate the recruitment, activation and proliferation of fibroblasts and

fibroblast-like cells as well as the synthesis by these cells of extracellular matrix (ECM) components, which serve to replace the provisional fibrin matrix of the coagulated blood[15]. Fibroblasts present early in the repair process appear immature; however, as the repair proceeds, a number of the fibroblastic cells acquire features of smooth muscle cells and are termed myofibroblasts. These cells contain cytoplasmic bundles of microfilaments consisting of alpha smooth muscle-actin (αSMA) which, with mechanisms similar to smooth muscle, enable cellular contraction.

During the granulation phase of healing, the contractile properties of myofibroblasts are responsible for facilitating wound closure[16]. Adhesions from the myofibroblasts in the ECM allow them to pull on the matrix and transmit force to neighboring cells. This retraction is stabilized by new deposition of matrix components such as collagens I and III resulting in overall tissue shortening. A direct correlation exists between the level of αSMA in fibrotic tissue and its contractility. Myofibroblasts also express other SM cytoskeletal proteins including caldesmon, desmin, and SM-myosin heavy chains, but their roles in these cells are not fully understood.

In the resolution phase of healing, there is a reduction in the overall cellularity of the repair tissue, particularly of myofibroblasts and inflammatory cells. Much of this reduction is attributable to apoptosis; however, a portion of the myofibroblastic cells may undergo a reversion to the normal fibroblastic phenotype. The fibroblasts that remain after the wound is closed possess a quiescent, noncontractile phenotype lacking the αSMA microfilament bundles.

The overall phenotype of the repair tissue changes from a synthetic/contractile mode with reduced matrix metalloproteinases (MMPs) and increased tissue inhibitors of

metalloproteinases (TIMPS) to one of remodeling, with increased MMPs and reduced TIMP production. The signal that triggers the loss of myofibroblastic cells is unknown but may be related to reduced levels of growth factors in the resolving wound or changes in the balance of MMPs and TIMPs[16].

Pathologic fibrosis may similarly begin with a tissue insult and initiation of repair mechanisms. However, as the process loses its inflammatory component, there is no accompanying reduction in myofibroblastic cells and thus the contractile fibrotic state persists. It is thought that mechanisms that continually stimulate myofibroblast differentiation or conversely those that specifically inhibit apoptosis or phenotypic reversion in these cells are responsible for their persistence.

TGF-beta 1 and Fibrogenesis

Several cytokines have been found to be central to the process of fibrogenesis, in other tissues including transforming growth factor-beta 1(TGF-β1), connective tissue growth factor (CCN2/CTGF), platelet derived growth factor (PDGF) and fibroblast growth factor-2 (FGF-2, or basic FGF), among others[14, 17-20].

While the underlying causes are diverse, it is likely that many of the harmful aspects of fibrosis are mediated by the effects of Transforming Growth Factor- beta 1 (TGF- β1)[17]. TGF-β1 is a secreted homodimeric protein that participates in a broad array of biological activities, such as normal development, wound repair and regulation of inflammation. It directs numerous cellular responses, including proliferation, differentiation, migration and apoptosis[21]. It also is a potent inducer of ECM protein synthesis. TGF-β1 is the prototypic member of the TGF-β superfamily which consists of over 35 structurally related pleiotropic cytokines that includes TGF-β2, TGF-β3, the

Bone Morphogenetic Proteins, the Activins and Nodals. Members of the TGF-β superfamily have crucial roles in development and tissue homeostasis. Perturbation of their signaling has been implicated in numerous developmental disorders and in a variety of human diseases including cancer, autoimmune disease, and fibrosis as discussed here[22, 23].

Most of TGF-β is secreted as homodimer complexed with latency associated peptide (LAP) and is stored in the ECM. Activation of TGF-β involves a complex process[24] involving the cleavage of LAP by various proteases, or the physical interaction of LAP with proteins, such as thrombospondin-1. Cell signaling by TGF-β family members, diagrammed in Figure 1-1, occurs through type I and type II serine/threonine kinase receptors (TGF-βRI and TGF-βRII, respectively). Upon binding of its TGF-β ligands, TGF-βRII recruits TGF-βRI into an activated heterotetrameric receptor complex. TGF-βRII phosphorylates TGF-βRI leading to subsequent phosphorylation of its intracellular effector molecules, receptor-regulated Smad proteins 2 and 3. Following phosphorylation, Smads-2 and -3 bind a co-Smad (Smad-4) and translocate to the nucleus, where they interact with transcription factors and coactivators to stimulate transcription of responsive target genes[24-26]. Inhibitory Smads (I-Smads: Smad-6 and Smad-7) act in an opposing manner to receptor-regulated Smads to regulate TGF-β activity. They recruit ubiquitin ligases (Smurfs) to the activated type I receptor, which sequentially leads to receptor ubiquitination, degradation and the termination of signaling.

On a molecular level, TGF-β1 is known to regulate several genes involved in fibrogenesis including connective tissue growth factor (CCN2/CTGF)[27], plasminogen

activator inhibitor-1 (PAI-1)[28], JunB[29], c-Jun[29], Smad-7[30], platelet-derived growth factor β-chain[31] and integrin β5[32]. Moreover, several ECM encoding genes are direct Smad targets, including collagen types I, III, V, VI, VII and X, fibronectin and proteoglycans[33-35]. ECM production by TGF-β1 is thought to be enhanced by its inhibitory effect on MMP synthesis and stimulation of increased production of protease inhibitors such as TIMP-1 and PAI-1[35].

TGF-β1 mRNA and protein are increased in tissue biopsies of fibrotic lesions in most fibrotic conditions. Because TGF-β1 controls both the expression of components of the ECM network and the expression of protease inhibitors, it is a crucial regulator of ECM deposition, and a key growth factor in the development of tissue fibrosis. Indeed, type I collagen and ECM deposition are the unifying histopathologic hallmarks of fibrotic disorders, such as renal sclerosis, liver cirrhosis, keloid scars, and systemic sclerosis. TGF-β1 is also a chemoattractant for fibroblasts and myofibroblasts[36]. It serves to maintain the fibrotic state by stimulating myofibroblast differentiation and suppressing apoptosis in these cells[37, 38].

Analysis of TGF-β1 and CTGF Expression in IAC Patients

Few studies have addressed the involvement of specific growth factors in IAC; however, Rodeo et. al in 1997, demonstrated positive staining for TGF-β1 in synovial cells from tissues of patients with IAC, whereas none was detected in synovial cells derived from normal tissues[39]. As TGF-β1 has been suggested to be a primary mediator of fibrotic pathology in tissues throughout the body, its positive detection in frozen shoulder tissues implicates its involvement in the fibrotic development of IAC.

Additionally, our research colleagues, Drs. Wright and Schultz, initiated preliminary experiments to determine the contribution of CTGF, believed to be the downstream pro-fibrotic mediator of TGF-β1, in the pathophysiology of IAC (Figure 1-2). For this, tissue biopsies from patients undergoing surgery for IAC were processed for immunohistochemical staining, using a monoclonal antibody directed against human CTGF. As seen in Figure 1-2 A and B, CTGF was found at high levels in the fibroblastic cells of the synovium of IAC patients. Diffuse staining was also seen in the ECM of these tissues. Similar tissue samples obtained from patients without IAC did not exhibit detectable CTGF staining (Figure 1-2, C and D). To quantify CTGF protein levels, biopsy tissues were homogenized and analyzed for CTGF content by specific ELISA. In the tissue samples analyzed to date, CTGF was found to be expressed between 3 and 10 ng/mg protein in capsular tissues of IAC patients. Those from control patients without IAC showed less than 0.02ng/mg. The potential for CTGF and TGF-β1 to induce pathologic fibrosis in the joints of rats will be examined in the present study. These studies implicate TGF-β1 and CTGF in the pathogenesis of IAC and their roles in arthrofibrosis will be further examined in the present study.

Diabetes, TGF-beta1 and Fibrosis

As previously mentioned, approximately 20% of diabetic patients not only suffer with IAC, but have a more persistent and severe case. It is possible that their inability to properly regulate blood glucose may be a contributing factor. Diabetes mellitus is a medical condition associated with abnormally high levels of glucose in the blood. Normally, blood glucose levels are controlled by insulin; however, destruction (type I) or dysfunction (type II) of beta cells, leads to diabetes. Type I diabetes, insulin-dependent

diabetes, accounts for 10% of all cases of diabetes and results from the autoimmune destruction of insulin-producing beta cells in the pancreas by CD4+ and CD8+ T cells and macrophages infiltrating the islets[42]. Afflicting over 150 million people world wide, type II diabetes, non-insulin-dependent diabetes, NIDDM, is an incurable metabolic disorder characterized by insulin resistance, decreased beta-cell function, and hyperglycemia[43].

Wound healing deficiencies in diabetic patients are common. Normal wound healing typically takes 3-14 days and occurs in three phases: inflammation, proliferation and remodeling. During the inflammatory phase, macrophages and neutrophils phagocytize bacteria and other debris. During the proliferative phase, fibroblasts lay down a collagen matrix, and blood vessels move into the new granulation tissue. During the remodeling phase fibroblasts reorganize the collagen matrix and many transform into myofibroblasts involved in wound contraction. Diabetics have impaired wound healing, due to decreased growth factor production[44], macrophage function[45], collagen accumulation[46], fibroblast migration and proliferation, bone healing[47], and an imbalance between accumulation and remodeling of the ECM[48], among others.

Significant research efforts have gone into studying diabetes, its associated morbidities, and the effects of hyperglycemia. Much of this research has focused on examining the relationship between high glucose and the cytokines involved in fibrogenesis both *in vivo* and *in vitro*, including TGF-β1. TGF-$\beta 1$ is upregulated in diabetes and has been proven to mediate many of the pathological changes in the diabetic kidney[63]. TGF-$\beta 1$ promotes production of excess ECM in kidney cells and causes renal cell hypertrophy. Once activated TGF-$\beta 1$ induces mRNA and protein

production of ECM molecules and impairs ECM degradation. A significant activation of the intracellular Smad pathway, which transduces the TGF-β signal, was noted in the diabetic kidney, as well as upregulation of renal TGF-β type II receptor[54, 64].

High levels of ambient glucose have been shown to stimulate the production of extracellular matrix components, via TGF-β1 signaling[46]. Both TGF-β1 and CCN2/CTGF have been shown to be elevated in plasma[49], secreted in the urine[50], and found in kidney tissues[49, 51, 52] of patients who suffer from diabetic nephropathy: a fibrotic condition which causes kidney function impairment, leading to end-stage renal disease. Research in both type I and type II diabetic animal models further demonstrates the involvement of TGF-β1 and CTGF in diabetes. Increased levels of both CTGF[49, 51, 52] and TGF-β1[53] mRNA and protein have been found in kidney tissues of experimental diabetic animal models, along with an activated Smad signaling pathway, transducing the TGF-β signal[53, 54].

Additionally, both cell culture and animal studies have shown that a high glucose environment induces many of the signaling cascades involved in cell proliferation and fibrogenesis. Decreased expression of MMPs, increased expression of TIMPs[55], an accumulation of fibronectin, laminin, and types I and IV collagen have all been shown to occur in high glucose environments when compared with cells grown in the presence of low glucose[56-58]. In most renal cell types, treatment with a TGF-β1 antagonist, such as a neutralizing monoclonal antibody[57] or anitisense oligonucleotides[59], reverses the rise in ECM expression due to high glucose. This indicates that TGF-β1 is a mediator of the profibrotic effects of high glucose on the kidney[57]. Similar studies have been performed *in vivo* that show treatment with neutralizing monoclonal antibodies against TGF-β1

prevents mRNA increases of TGF-β1, type IV collagen, and fibronectin in diabetic mice,[60] and anti-TGF-β1 antibody therapy prevented mesangial matrix expansion and renal insufficiency[61].

Many features of the diabetic state stimulate TGF-β1 production. A self-maintaining cycle has been proposed whereby an overexpression of Glut-1 leads to an increase in glucose uptake and activation of metabolic pathways that result in an excess of TGF-β1 production, which in turn maintains overexpression of Glut-1[62]. Glut-1 is a ubiquitously expressed molecule that resides on the cell plasma membrane and mediates the rate of glucose transport into the cell. It is a high-affinity and low capacity transporter that is near saturation at physiologic glucose levels. Therefore, an increase in basal glucose uptake would be the result of an increase in the number of Glut-1 molecules. High glucose concentrations in mesangial cells increase Glut-1 expression via a TGF-β1-dependent mechanism[61].

Gene Transfer to Capsular Fibroblasts

Significant portions of the laboratory component of this dissertation involve the delivery of exogenous cDNAs and expression cassettes to fibroblastic cells of the synovium and sub-synovium *in vitro* and *in vivo*, procedures with which our research group has considerable experience. Our efforts in this area were originally directed toward the development of an improved drug delivery system for the treatment of rheumatoid arthritis[73, 74]. It was reasoned that if exogenous cDNAs encoding anti-arthritic proteins could be delivered to cells that line the joint capsule, these cells could be adapted to become factories for the sustained, localized production of the therapeutic gene products. Indeed, we and others have exhaustively demonstrated the

proof-of-concept, and have established its effectiveness in several experimental models of arthritis and two clinical trials.

The first embodiment of intra-articular gene transfer involved an *ex vivo* approach whereby fibroblastic cells from the synovium and capsular tissues were genetically modified *in vitro*, then injected into the joint space where they engrafted and secreted the transgene products into the synovial fluid and surrounding tissues[75, 76]. In subsequent studies our lab has found that several viral vector systems provide efficient gene delivery following direct intra-articular injection, enabling genetic modification of a high percentage of fibroblastic cells within the synovium and joint capsule. Following injection of a recombinant adenovirus containing a marker gene (cell associated alkaline phosphatase) into the knee joint of a rabbit, the virus is capable of transducing cells several layers deep within the lining[74]. We have found this technology to be extremely useful for evaluating the effects of putative anti-arthritic protein products in diseased joints. We have also used it to constitutively overexpress gene products associated with the pathogenesis of disease as a means to study the effects of their sustained presentation on the biology of the articular environment[77].

Although we found that we can generate exceptionally high, biologically relevant levels of transgenic expression following intra-articular gene transfer, the window of expression was brief, persisting only for several days. We have since dedicated a considerable research effort into understanding the biology of the joint tissues as targets for gene delivery, and the factors that limit transgenic persistence. We have found that the joint tissues are highly immune sensitive to the expression of foreign antigens, both non-homologous transgene products as well as viral proteins. Thus, in normal animals,

transduced cells that express non-native gene products are rapidly eliminated by T-cell mediated cytotoxicity. In recent work we have found that in the joints of immunocompromised animals, such as in athymic nude rats, which lack the T-cell arm of the immune system, expression of foreign transgene products will persist for the lifetime of the animals[78]. These animals thus provide an opportunity to examine the effects of long-term expression of foreign gene products on the joint tissues. Within this system, both integrating lentiviral vectors which encode no viral proteins, and first generation adenoviral vectors whose genome remains episomal, are similarly capable of sustaining transgenic expression intra-articularly in the nude rat. In the work described herein, these vector systems will be used for gene transfer of TGF-β1, and CCN2/CTGF to capsular fibroblast cultures, and intra-articularly in the knees of nude and Wistar rats.

Significance

Although adhesive capsulitis is a relatively common disease which causes prolonged pain and morbidity, very little is known about its underlying causes or pathogenesis. This study was designed to initiate a focused research effort to examine IAC from a biological perspective. By undertaking this project we hoped to draw clinical relevance to our laboratory investigations while extending discoveries regarding the cellular and molecular basis of IAC into the formulation of novel therapeutic strategies for clinical application.

Our laboratory hypothesis is that TGF-β1 is a primary cytokine mediator of pathology in IAC. Our investigatory strategy will be comprehensive in scope, enabling a fundamental characterization of the pathobiology of this disease. We will develop an

animal model of arthrofibrosis by local delivery and overexpression of TGF-β1 cDNA in the knee joints of rats and characterize the molecular and cellular events leading to joint fibrosis. We will also examine the relationship between diabetes and fibrotic signaling in cell culture of synovial cells and in our model of IAC. Moreover, by further testing our hypothesis in an animal model of articular fibrosis we will draw parallels between the effects of intra-articular cytokine signaling and clinical pathology. It is intended that at the completion of this work we will have a greater understanding of IAC and be well-positioned to develop effective strategies for therapeutic intervention.

Table 1-1. Stages of Idiopathic Adhesive Capsulitis

Stage 1	
	Duration of symptoms: 0 to 3 months Pain with progressive loss of motion Hypertrophic vascular synovitis Rare inflammatory infiltrate Normal underlying capsule
Stage 2	
	Duration of symptoms: 3 to 9 months Persistence of pain with loss of range of motion Loss of capsular volume with hypervascular synovitis No inflammatory infiltrate
Stage 3	
	Duration of symptoms: >10 to 20 months Minimal pain with stiff shoulder Residual synovial thickening without hypervascularity Dense fibrotic capsule
Stage 4	
	Duration of symptoms: 15 to 30 months Minimal pain Slow, steady recovery of range of motion

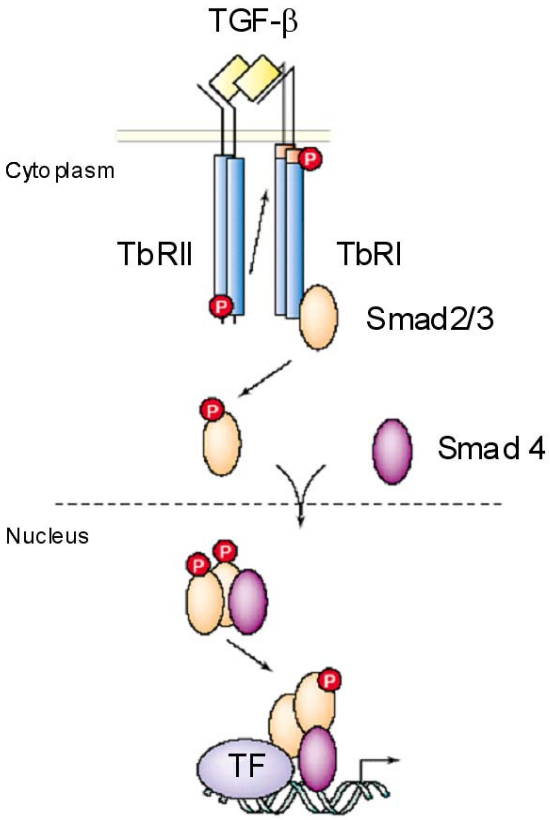

Figure 1-1. TGF-β/Smad signaling pathway. TGF-β binds first to the constitutively active TGF-β type II receptor (TβRII) and then the ligand-receptor complex associates with the type I receptor (TβR1). TβRII phosphorylates TβRI on specific serine and threonine residues in the GS domain. Activated TβRI propagates the signal downstream by directly phosphorylating Smad2 and Smad3 that form heterotrimeric or dimeric complexes with Smad4 and translocate into the nucleus. Interaction of these complexes with transcription factors (TF) regulates transcription. *Adapted from Dijke et al., Trends in Biochemical Sciences, 2004.*

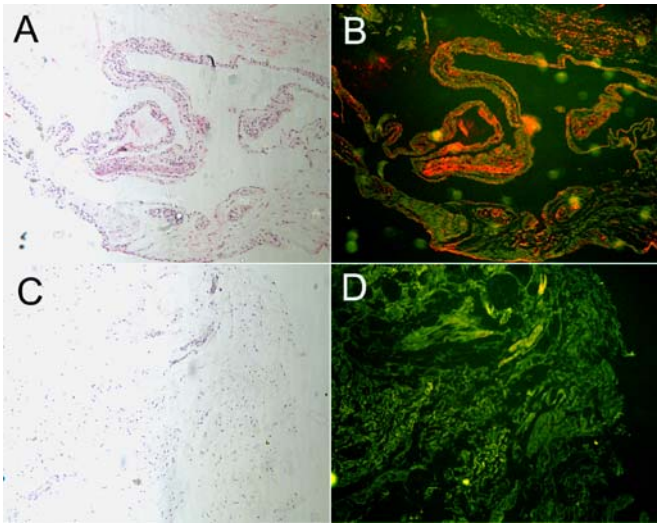

Figure 1-2. Immunohistochemistry analysis for CTGF expression in tissue from patients with adhesive capsulitis (A,B) or normal joints (C,D) visualized under bright field (A,C) and fluorescence (B,D) microscopy. Positive CTGF expression can be detected in tissue from patients with adhesive capsulitis (B) and not in normal joints (D).

CHAPTER 2
MATERIALS AND METHODS

Vector Production

The adenoviral vectors (Ad.GFP, Ad.TGF-β1, Ad.CTGF) used in this study originated from replication-deficient type 5 adenovirus lacking *E1* and *E3* loci. The respective cDNAs were inserted in place of the *E1* region, with expression driven by the human cytomegalovirus early promoter/enhancer[79]. High-titer suspensions of recombinant adenovirus were prepared by amplification in 293 cells, and purified using three consecutive CsCl gradients as previously described[80]. Titers were determined by optical density at 260nm.

Vesicular stomatitis virus G-protein (VSV-G) pseudotyped lentiviral vectors were produced by transient transfection, using Lipofectamine (Invitrogen, Carlsbad, CA), of 293FT cells with the Virapower™ packaging plasmids, pLP1, pLP2 and pLP/VSVG, containing gag-pol, Rev, and VSV-G protein envelope (Invitrogen, Carlsbad, CA) with expression driven by the human cytomegalovirus early promoter/enhancer. The tansducing vector (pCDH1-GFP IRES NEO) was generated by insertion of the cDNA for GFP into the multiple cloning site on the pCDH1-vector. At 48 and 72 hours, the conditioned media were harvested, filtered through a 0.45 μm filter (Steri-cup; Millipore, Billerica, MA), and centrifuged at 20,000 rpm in a swinging bucket rotor for two hours. The viral pellets were resuspended in Opti-Mem (Invitrogen, Carlsbad, CA) and stored in -80°C.

Tissue Culture

Early passage primary rat synovial fibroblasts (RSF), obtained from normal male Wistar rats, were cultured at 37°C in 5% CO_2 atmosphere in Dulbeccos Modified

Medium (DMEM) (Invitrogen, Carlsbad, CA) supplemented with 10% fetal bovine serum and 1% penicillin/ streptomycin (Invitrogen, Carlsbad, CA).

ASO Transfection

Briefly, RSFs were grown to confluence and treated with either 100mM or 300mM of antisense oligonucleotide (ASO; ISIS Pharmeceuticals, Carlsbad, CA) (TGF-β1 ASO, ISIS #105204; Scramble ASO, ISIS #110410; CTGF ASO, ISIS #124212) and 10 μg/ml of Lipofectamine (Invitrogen, Carlsbad, CA) for 1 hour. Medium was added to each well and the cells were grown for 24 hrs. Cells were washed and grown in serum free medium for an additional 24 hrs before harvesting medium for specific ELISA.

TGF-β1 ELISA

RSF's were seeded into flat-bottom twelve well plates in complete medium containing 10% FBS. Upon confluency, cells were transduced with 4.0 x 10^8 vp - 2.0 x 10^9 vp of Ad.TGF-β1. After 24 hrs of incubation, medium was replaced with serum-free medium. Supernatants were collected at 48 hrs and TGF-β1 levels were measured using a solid-phase ELISA with TGF-β1 ELISA kits for humans (R&D Systems) according to the manufacturer's instructions. Four replicate wells were used to obtain all data points and the mean of all samples were calculated.

Cell Migration Assay

Fibroblasts were seeded in 6-well dishes with conditioned medium until cells reached visual confluence. To block proliferation cells were treated with 1 ml of 5μg/ml of mitomycin C (Sigma, St. Louis, MO), in Optimem (Invitrogen, Carlsbad, CA) for one hour. After the cells were washed three times in phosphate buffered saline (PBS), the bottom of each well was vertically scratched using a one ml pipette tip. The cells were then treated with either 2 ml of medium supplemented with D-glucose (Sigma, St. Louis,

MO) with or without varying amounts of either Ad.TGF-β1, Ad.CTGF, or Ad.GFP. For this, cells were placed in a minimal amount of media for one hour with the appropriate virus before supplementing with an additional 2 ml of media/well. Digital images were then taken at 24 and 48 hrs post mitomycin C treatment. Analysis was performed using computer software (GraphPad Prism; GraphPad Software Inc.) at individual time points using a one-way analysis of variance (ANOVA).

Animal Experimentation

Experiments were carried out on 6-7 week old male athymic nude rats and male Wistar rats weighing 150-170g (Charles River Laboratories, Wilmington, MA) housed two per cage with free access to standard laboratory food and water. All animal procedures were approved by the Institutional Animal Care and Use Committee of the University of Florida. Gene delivery vectors were injected into the joint space of the knee through the infrapatellar ligament. At periodic intervals after intra-articular injection, animals were killed by CO_2 asphyxiation followed by thoracic puncture. The joint tissues were then harvested for analysis.

For Anti-sense oligonucleotides (ASO) Experiments

ASOs were co-injected into the knee joint at a concentration of 10μg/μl with Ad.GFP, Ad.CTGF, Ad.TGF-β1 or PBS. ASOs were a generous gift provided by Nick Dean of Excaliard Pharmaceuticals (Carlsbad, CA) and ISIS Pharmaceuticals (Carlsbad, CA). ISIS TGF-β1=105204; ISIS Scramble=110410; ISIS CTGF=124212.

Induction of Diabetes in Animals

Adult Wistar rats weighing 150-170g (Charles River Laboratories, Wilmington, MA) housed two per cage were used for inducing diabetes. The animals were fasted 4 hours

before diabetes was induced using streptozotocin (STZ) (Sigma, St. Louis, MO.). Rats received two intraperitoneal injections of 45mg/kg of STZ, 72 hours apart. STZ was freshly prepared and dissolved in 0.05M citrate buffer, pH 4.5 and injected within 15 minutes of preparation. Blood glucose measurements were performed on a weekly basis using blood obtained from the tails of non-fasting rats using OneTouch® Ultra® (LifeScan Inc, CA). Rats whose blood glucose levels were above 250 mg/dl were considered diabetic. Animals were killed periodically and tissues were harvested. Those animals who were diabetic for longer than 2 months received a single subcutaneous implantation of Linplant (LinShin Canada Inc, Canada) and every two months after as needed to prevent ketoacidosis.

Preparation of Total RNA

Total RNA was isolated from treated and control synovial and capsular tissues using the RNeasy mini kit (Qiagen, Valencia, CA). Briefly, tissues were harvested and stored in RNALater (Qiagen, Valencia, CA) until RNA extraction was performed, at which time the tissues were frozen in liquid nitrogen and pulverized using a mortar and pestle. The pulverized tissue was added to lysis Buffer RLT (Qiagen, Valencia, CA), homogenized using a 20-gauge needle, and RNA was harvested using RNeasy spin columns following manufacturer's protocol (Qiagen, Valencia, CA).

PCR Array

The Extracellular Matrix and Adhesion Molecules PCR Array for rat (SABiosciences, Frederick, MD) was used to examine the expression of over 80 related genes. One µg of RNA was DNase treated and reverse-transcribed using the RT^2 First Strand Kit following manufacturer's protocol (SABiosciences, Frederick, MD). The resulting cDNA template was mixed with SYBR Green PCR master mix

(SABiosciences, Frederick, MD) and 25µl of the mixture was equally aliquoted into each well of the 96-well plate already containing individual PCR primer sets. Differential analysis was performed using software provided by SABiosciences (SABiosciences, Frederick, MD). Briefly, the ΔΔCT method was used for data analysis to determine fold-increase and decrease in expression between treated and control tissues. The student's *t* test was used to determine statistical significance. Each time point represents n=3.

Immunohistochemistry

5µm sections of formalin-fixed, decalcified, paraffin-embedded blocks were cut and mounted on plus charged slides (Fisher Scientific, Pittsburgh, PA). Slides were deparaffinized and rehydrated through a series of xylenes and graded alcohols and blocked in 3% peroxide/methanol for 10 minutes at room temperature. Appropriate sections were stained with hematoxylin and eosin (H&E) or toluidine blue. If required, heat mediated antigen retrieval was performed in Dako Target Retrieval Solution (DakoCytomation, Carpinteria, CA) for 20 minutes at 95°C. Nonspecific binding was blocked in 15% normal serum matched to the secondary antibody species. Slides were incubated overnight at 4°C with commercially available antibodies: mouse anti-αSMA at 1:1000 dilution (Sigma, St. Louis, MO) (no retrieval), goat anti-MMP-9 at 1:50 (Santa Cruz Biotechnology, Santa Cruz, CA), mouse anti-MMP-13 at 1:15 (Santa Cruz Biotechnology, Santa Cruz, CA). The appropriate biotinylated secondary antibody (Vector Labs, Burlingame, CA) was applied to samples for 30 minutes at room temperature at a dilution of 1:200, followed by detection with an avidin-biotin-based peroxidase kit (ABC Elite; Vector Laboratories, Burlingame, CA). The antigen-antibody

complex was observed by reaction with 3,3'-diaminobenzidine (DAB) and slides were counterstained with hematoxylin and coverslipped.

Detection of GFP

5μm sections collected from decalcified, paraffin embedded blocks were manually immunostained using rabbit anti-GFP (dilution 1:1000, ab290, Abcam; Cambridge, MA). Slides were heat retrieved in 10mM citra buffer (BioGenex, San Ramon, CA), pH 6.0 before blocking with normal serum and staining overnight at 4°C. Positive signal was detected with anti-rabbit Alexafluor 488 (dilution 1:500; Molecular Probes, Eugene, OR). Controls consisting of isotype and concentration matched immunoglobulin were included for each section.

Detection of Reporter ASO

Intraarticular injection of 10μg/μl of reporter ASO (generously provided by Dr. Schultz and Dr. Dean) was performed. Tissues were harvested 10 days post injection, and paraffin embedded. 5μm paraffin sections from joints were stained for the reporter ASO using the following two-step horseradish peroxide (HRP) immunohistochemistry technique. The slides were pretreated with DAKO Blocking solution (Carpenteria, CA, USA), and DAKO Proteinase K solution followed by incubation with the primary antibody 2E1-B5 (Berkeley Antibody Company, Berkeley, CA, USA) which recognizes CG or TCG motif in phosphorothiate ASO. Secondary antibody incubation was with Zymed Anti-IgG1 isospecific HRP conjugated secondary (San Francisco, CA, USA). Positive staining was detected with DAB as the chromogen and revealing agent (DAKO Carpenteria, CA, USA). Sections were counterstained with haematoxylin and then photographed to document cellular localization of reporter ASO expression.

Microarray

Sample Preparation

Human tissue samples from patients with IAC and from control human shoulder were obtained post-surgery from Dr. Thomas Wright, University of Florida, and stored at -80 degrees in RNALater® (Company, city). For RNA extraction, the tissues were frozen in liquid nitrogen and pulverized using a mortar and pestle. Pulverized tissue was added to lysis Buffer RLT (Qiagen, Valencia, CA), homogenized using a 20-gauge needle, and RNA was harvested following manufacturers protocol using the RNAeasy Mini kit (Qiagen). RNA concentration was determined using the NanoDrop ND-1000 spectrophotometer (NanoDrop Technologies, Wilmington, DE). RNA integrity and quality were estimated on an Agilent 2100 Bioanalyzer (Agilent Technologies, Palo Alto, CA). RNA integrity number (RIN) index was calculated for each sample using the Agilent 2100 Expert software. RIN provides a numerical assessment of the integrity of RNA and facilitates the standardization of interpretation of RNA quality. To reduce experimental bias in data analysis due to poor RNA quality, only RNAs with RIN number >7.0 were further processed.

RNA Amplification, Labeling and Array Hybridization

For RNA amplification and labeling, 500 ng of total RNA were linearly amplified and labeled with Cy3-dCTP following the Agilent One-Color Microarray-Based Gene Expression Analysis protocol. To monitor the microarray analysis workflow a mixture of 10 different viral polyadenylated RNAs (Agilent Spike-In Mix) was added to each RNA sample before amplification and labeling. Labeled cRNA was purified with the Qiagen RNAeasy Mini Kit (Qiagen, Valencia, CA), and sample concentration and specific activity (pmol Cy3/μg cRNA) were measured in a NanoDrop ND-1000

spectrophotometer. Hybridization was performed by the ICBR Core at the University of Florida.

CHAPTER 3
GENERATION AND CHARACTERIZATION OF ADENOVIRAL VECTOR

In vitro Expression of Adenoviral Vector

To study and evaluate the role of CTGF in arthrofibrosis, we used adenovirus as a mechanism for gene delivery. Adenoviruses infect both resting and dividing cells of many types and highly purified solutions of virus can easily be produced with high titres. Both the Ad.TGF-β1 and Ad.GFP vectors used in these studies were generated and characterized previously by our research group. The Ad.CTGF vector was generated for this project. For this, both the rat and human CTGF cDNAs were subcloned into the AdLox plasmid construct and packaged into adenovirus using Cre recombinase method described by Hardy et.al[79]. Briefly, 293 cells constitutively expressing bacteriophage Cre recombinase were co-transfected with recombinant AdLox vector plasmid carrying the CTGF cDNA and with ψ5 helper virus DNA. Following the formation of cytopathic effects, the cell lysates were used to infect cultures of 293 cells to amplify the recombinants. Vector particles were purified using CsCl density gradient purification.

To determine the functionality of this vector, characterization of the adenovirus containing CTGF began with western blot analysis. Fibroblasts in culture were transduced with either Ad.CTGF or Ad.GFP at varying concentrations and cell lysates and conditioned media were run on 15% pre-cast SDS-polyacrylamide gels (BioRad). For detection of CTGF protein, a biotin anti-Human CTGF C-terminus antibody (R&D BAF 660) was used. It is known that the human CTGF protein resolves at multiple sizes including the full length peptide at 38KD, and partial proteolytic fragments between 10-20KD that represent the degradation of the full length peptide by intracellular proteases within the ER or Golgi[82]. As indicated by the arrow in Figure 3-1, the presence of a 38

KD band is clearly visible in both Ad.hCTGF and Ad.rCTGF and absent in our control, confirming the presence of our proteins. Additionally, an approximately 20KD band from the human CTGF protein is detectible, which is consistent with the literature. The band at 45KD is most likely due to non-specific binding as it is seen in both our negative control and in our Ad.hCTGF and Ad.rCTGF lanes. Western blot of the supernatant and cell lysate revealed the same pattern of bands; however, a higher concentration of protein was found in the lysate (not shown).

To further characterize this virus, a specific ELISA for human CTGF, using antibodies generously provided by Dr. Schultz, was performed. For this, rabbit HIG-82 cells were transduced with equal amounts of Ad.hCTGF, Ad.rCTGF, or Ad.GFP control. As seen in Figure 3-2, Ad.hCTGF expression was confirmed by specific ELISA, further confirming the functionality of our virus. Additional tests will need to be performed to verify the expression of the Ad.rCTGF virus.

Lastly, a cell proliferation assay, using Ad.hCTGF was performed by Edith Sampson in Dr. Schultz's lab, using the CellTiter 96® AQ_{ueous} One Solution Cell Proliferation Assay from Promega. For this, human corneal fibroblast (HCF) cells were seeded in a 96 well plate, grown to 70-80% confluency and serum starved for 48 hours, after which time, virus was serially diluted in each well and assayed 48hours post infection. As shown in Figure 3-3, as increasing amounts of virus was added to cells, an increase in fibroblast proliferation occurred, which is characteristic of the CTGF gene. From these data the Ad.hCTGF, described from here on as Ad.CTGF, appears to be functional and will be examined *in vivo*.

Overexpression of TGF-β1 *In vivo* Induces Fibrosis

After characterizing and confirming the functionality of the Ad.CTGF vector *in vitro*, we further characterized its activities *in vivo* to determine its role in fibrotic induction within the joint. Studies were carried out in the knee joints of Wistar rats to determine effects of CTGF, GFP, and TGF-β1 overexpression intra-articularly. For this, 3.6×10^8 vp (viral particles) of Ad.GFP, Ad.hCTGF, or Ad.hTGF-β1 were injected into both knee joints of Wistar rats, four rats per group. Afterward, the rats were analyzed daily for weight, knee diameter and vigor. Results in Figure 3-4 represent the percentage change in knee diameter relative to day zero. Ad.GFP animals did not have an increase in knee diameter and fluctuated within 7% of the value at day zero. A mild increase in knee diameter, about 20% relative to day zero, was observed immediately after Ad.CTGF injection and gradually leveled off to near normal levels. The greatest effect was observed in those rats receiving Ad.TGF-β1. These rats experienced a ~37% increase one day after injection and continued to increase to ~45% relative to day zero, maintaining an elevated knee diameter throughout the study.

At 4 and 8 days post injection, animals were sacrificed and tissues were harvested and processed for histology. H&E histological staining 4 days post injection, as shown in Figure 3-5, reveals a mild inflammatory response in Ad.GFP infected animals, most likely due to the immunogenic effects of adenovirus. Animals injected with Ad.CTGF revealed a modest increase in fibroblast proliferation, as seen in Figure 3-5, with the image representing the most dramatic changes seen within this group. Additionally, histology from 8 days post injection showed little to no synovial fibroblast proliferation indicating the effects of Ad.CTGF were transient (not shown). Overall, while fibroblast proliferation seen in the Ad.CTGF injected animals was minimal and transient. The most

striking response was observed in animals injected with Ad.TGF-β1. Histology from these animals demonstrated a severe hypercellular response, primarily of fibroblastic cells, resulting in synovial joint thickening. This synovial fibrotic expansion could be seen 8 days post injection (not shown). From this experiment, it appears that while CTGF may play a role in other fibrotic conditions or act as an important co-factor in fibrogenisis, its effects within the joint space are minimal and transient, and it does not appear to be a primary inducer of joint fibrosis. On the contrary, TGF-β1 induced a severe fibrotic response similar to that described in stage 3 IAC. Therefore, for further experiments to model arthrofibrosis, Ad.TGF-β1 was delivered to the knee joints of rats.

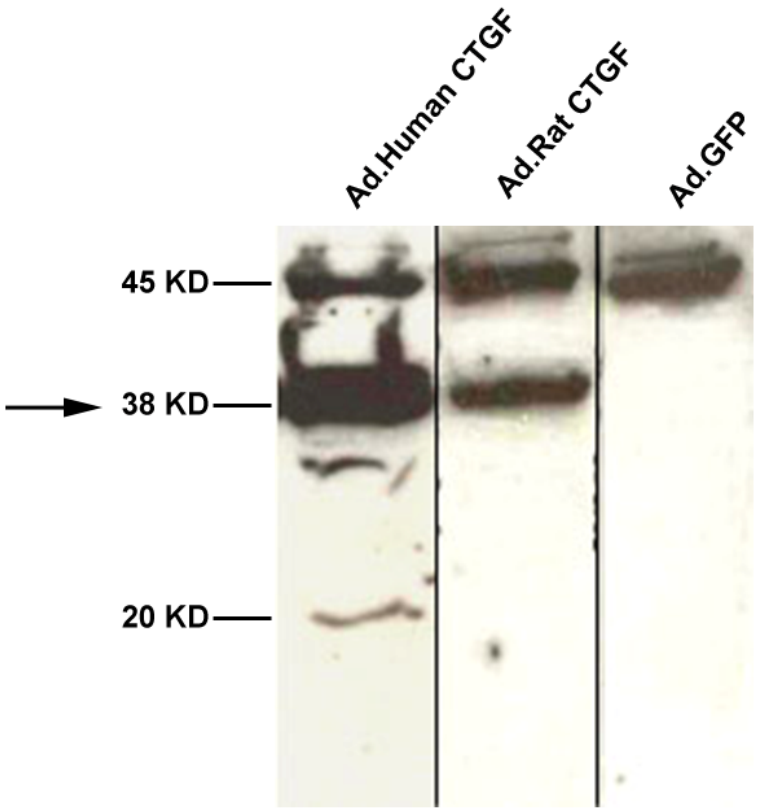

Figure 3-1. Western blot analysis of CTGF protein. HIG-fibroblast cells in culture were infected with Ad.hCTGF, Ad.rCTGF, and Ad.GFP control. Western blot analysis revealed the full length 38kDa protein in both Ad.rCTGF and Ad.hCTGF, as well as, a 20kDa proteolytically cleaved fragment in Ad.hCTGF and non-specific bands at 45kDa.

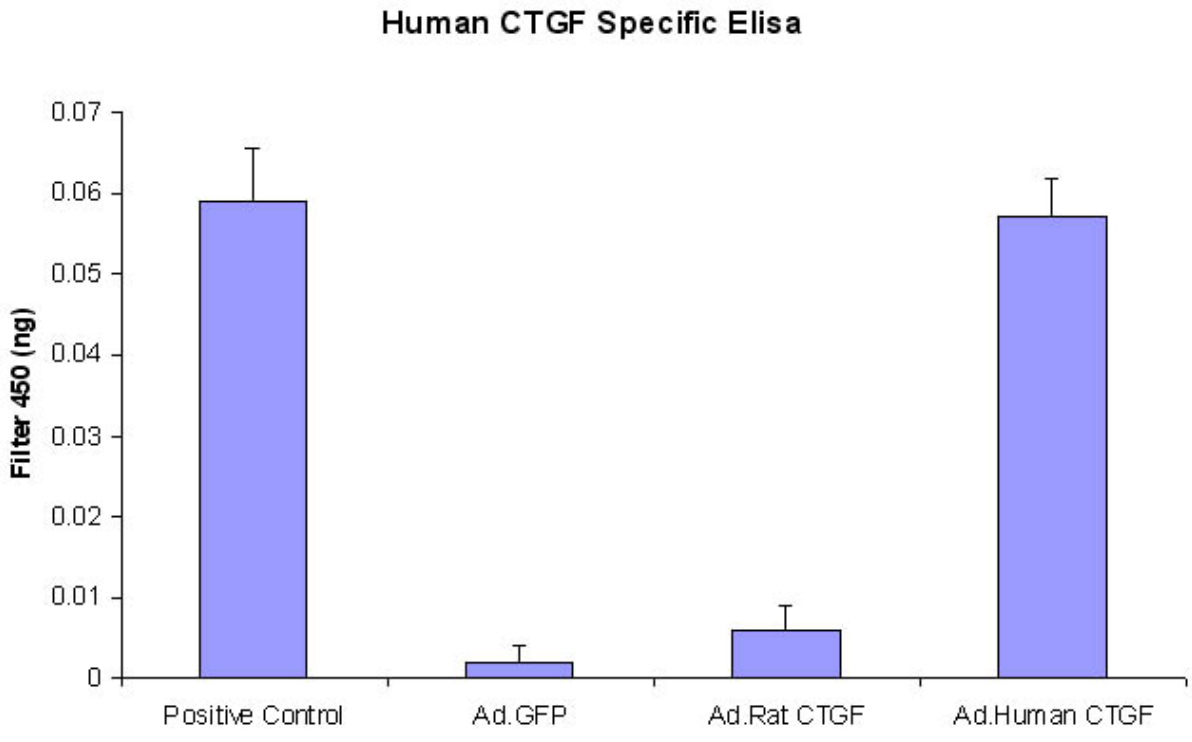

Figure 3-2. hCTGF specific ELISA. Fibroblasts in culture were infected with Ad.GFP control, Ad.rCTGF and Ad.hCTGF. An ELISA, using antibodies specific for hCTGF, confirmed its expression.

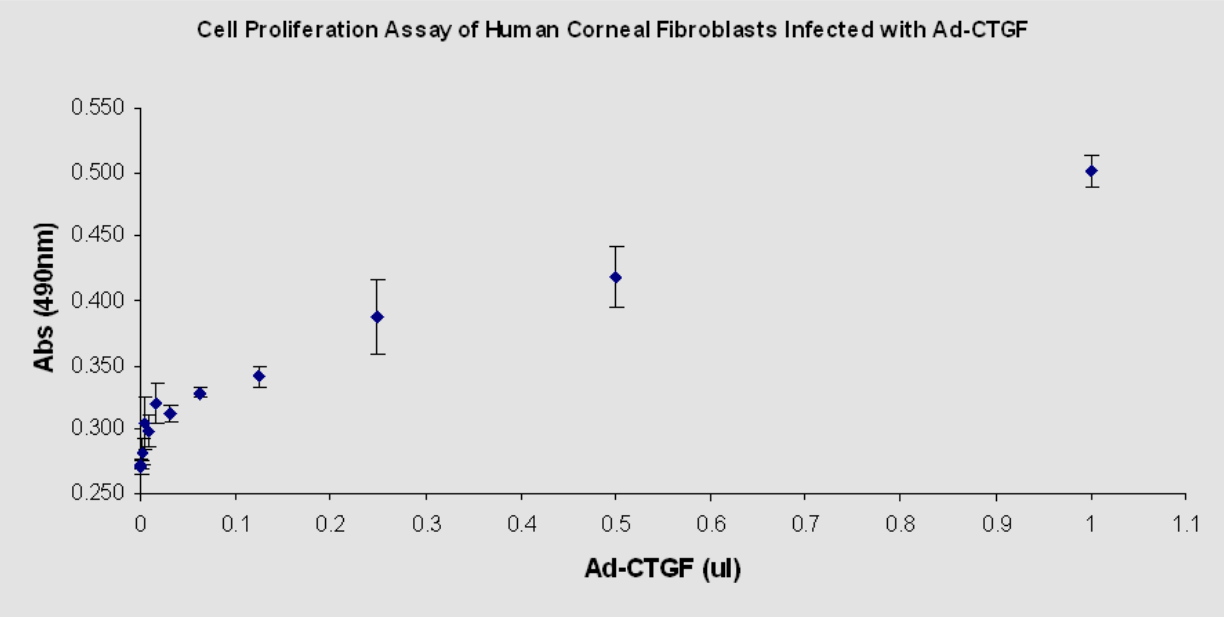

Figure 3-3. Cell proliferation assay. Fibroblasts in culture in a 96-well plate were infected with Ad.hCTGF and serially diluted among the wells. An MTS assay showed an increase in cell proliferation with increasing amounts of virus.

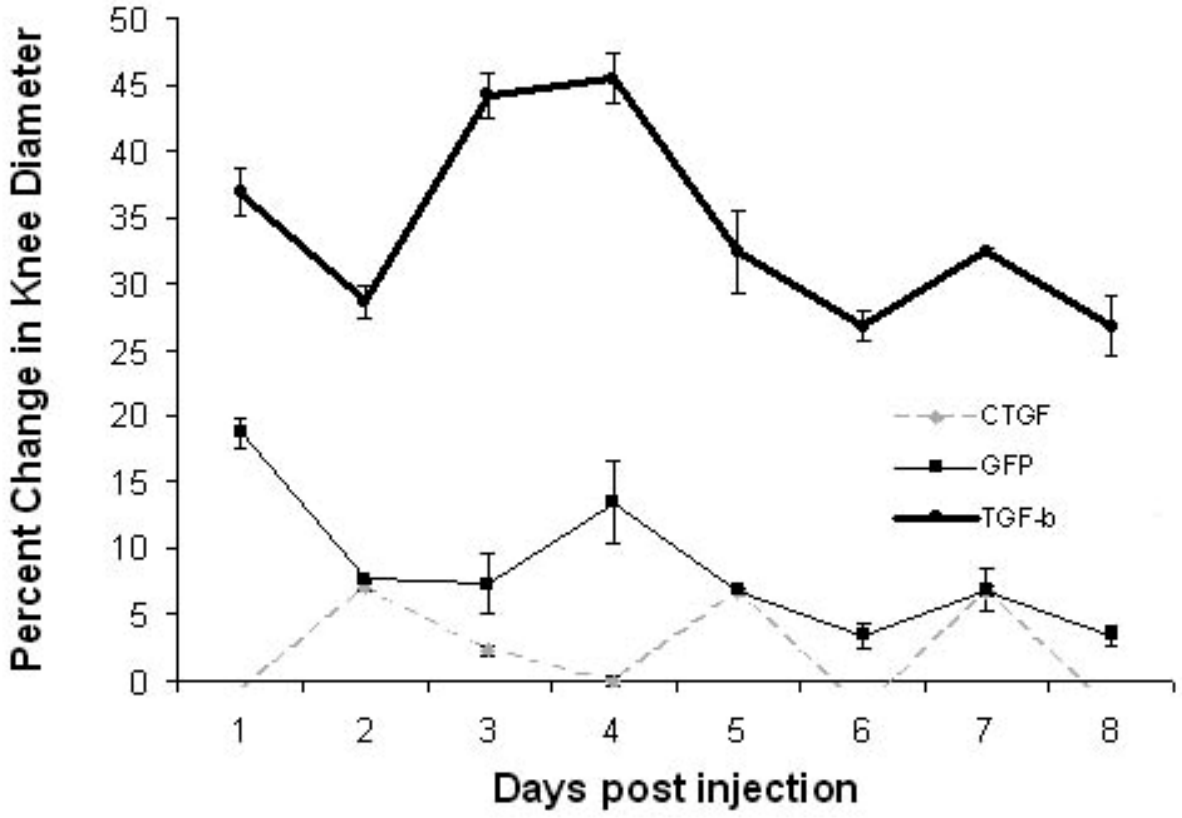

Figure 3-4. Percentage change in knee diameter relative to day zero of adenovirus injected Wistar rats.

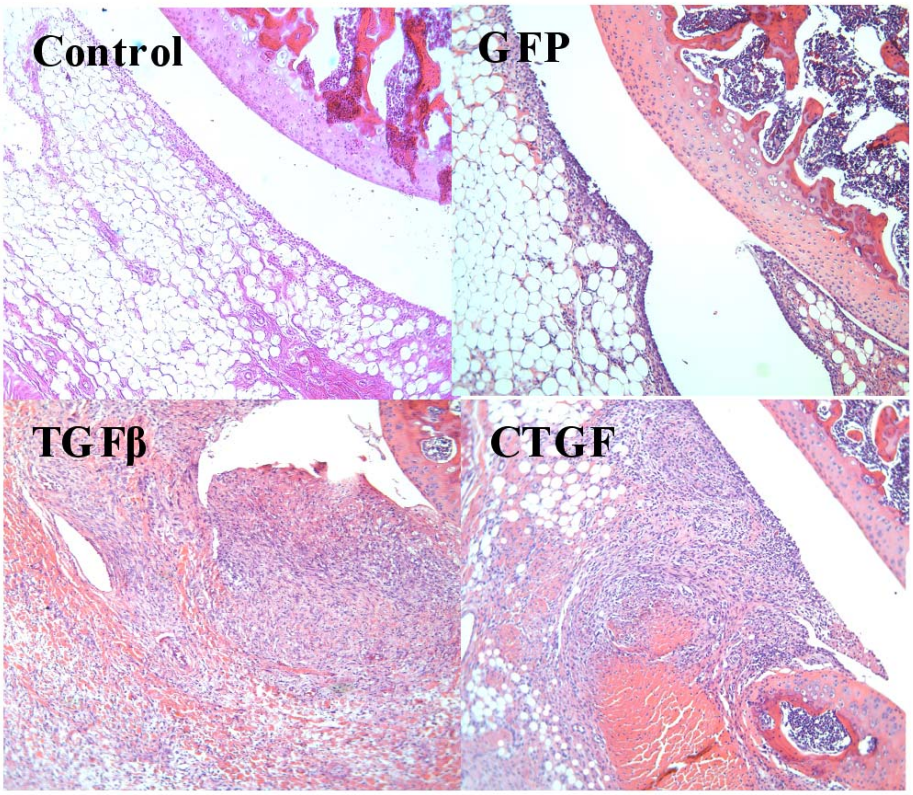

Figure 3-5. Histolgical H&E stain of Wistar rats knees, four days post intra-articular injection. Mild synovial inflammation could be seen following Ad.GFP injection, compared to normal control. Modest fibroblast proliferation was observed in Ad.CTGF injected animals. Ad.TGF-β1 animals displayed severe fibrotic expansion and proliferation. Images shown at 20x magnification.

CHAPTER 4
GENE DELIVERY OF TGF-BETA1 INDUCES ARTHROFIBROSIS AND CHONDROMETAPLASIA OF SYNOVIUM *IN VIVO*

Introduction

Arthrofibrosis is a condition that arises from the development of excess fibrous tissue intra-articularly which leads to chronic joint pain and loss of range of motion. It can occur in most joints and frequently onsets following injury, surgery, diabetes or immobilization; however, the precise etiology remains unclear[83, 84, 85, 86]. A particularly common example is adhesive capsulitis of the shoulder, also known as frozen shoulder syndrome. It is characterized by a painful fibrotic expansion of the synovium and joint capsule, which gradually results in the loss of active and passive motion of the joint.[87, 2] Although the disease is generally self-limiting, it can persist for 2-3 years, leaving patients disabled with limited use of the affected arm[87, 1]. Since the underlying causes remain unknown, no specific pharmacologic or non-surgical therapy has been shown to cure arthrofibrosis or provide significant long-term benefit.

Pathologic fibrosis is a prominent feature of chronic disease in several organs, including the skin, liver, lung and kidney, and often begins with local injury and activation of normal repair mechanisms[88, 89]. Following tissue damage, there is a need for local synthesis of reparative connective tissue, which involves the migration of fibroblasts to the wound site and their proliferation. These cells then synthesize abundant levels of extracellular matrix proteins, including collagens, proteoglycans and fibronectin. Many of these fibroblasts differentiate into myofibroblasts, which express high levels of α-smooth muscle actin (α-SMA) that confers contractile activity to facilitate wound closure. In pathologic fibrosis, as the healing process loses its inflammatory component, there is no accompanying reduction in the myofibroblasts, as would occur

during normal healing, and a contractile fibrotic state persists. It is thought that mechanisms that continually stimulate myofibroblast differentiation, or, conversely, those that specifically inhibit apoptosis or phenotypic reversion in these cells, are responsible for their persistence and that of the fibrotic condition[90].

While the initiating causes of pathologic fibrosis are likely diverse, the protein factors that mediate wound healing and tissue repair are considered to play central roles. In this regard, transforming growth factor-beta 1 (TGF-β1) has been implicated as a participant in a majority of fibrotic conditions[17]. This pleiotropic cytokine induces a broad array of biological activities, such as cellular proliferation, differentiation, regulation of inflammation and tumor progression[91, 92]. TGF-β1 is also a potent mediator of extracellular matrix (ECM) protein synthesis, and its expression is increased in numerous fibrotic conditions[21].

Active TGF-β1 binds to a heteromeric receptor complex consisting of TGF-β type I and type II receptors, and signals intracellularly through transcriptional activators, Smads 2 and 3, as well as Smad independent pathways. Most of the profibrotic effects, fibroblast proliferation, myofibroblast differentiation, enhanced synthesis of matrix proteins and inhibition of collagen breakdown, are thought to be mediated through Smad signaling[93]. Indeed, several ECM genes are direct Smad targets, including collagen types I, III, V, VI, VII and X, and fibronectin[33-35]. TGF-β1 is also known to regulate expression of other proteins thought to drive fibrogenesis, including connective tissue growth factor (CCN2/CTGF), which is often considered to be a downstream mediator of TGF-β1-induced fibrosis[27].

Whereas other fibrotic conditions have received considerable research attention, there are comparatively few reports regarding the pathogenesis of arthrofibrosis. This can be partially attributed to the scarcity of relevant animal models, as well as a lack of available human tissue from early stage disease for detailed analysis. Arthroscopy, due to its invasiveness, is not a diagnostic tool and is only used to remove fibrotic adhesions from late-stage immobilized joints that have proven resistant to other forms of therapy. Few studies have addressed the involvement of specific growth factors in arthrofibrosis; however, it has been shown using immunohistochemical staining and ELISA, that increased levels of TGF-β1 are found in synovial and capsular tissues and diffusely in the fibrotic ECM[1, 39, 41].

We hypothesized that sustained over-production of TGF-β1 intra-articularly drives chronic arthrofibrosis. To test this, we used a recombinant adenovirus to deliver and locally overexpress the cDNA for human TGF-β1 in the joints of athymic nude rats and examined the effects of chronic stimulation on the local biology of the capsular tissues. Using this approach, we found TGF-β1 gene transfer rapidly induced a severe and persistent fibrotic condition that encased and immobilized the injected joint. Histologic examination, as well as focused expression arrays of the joint tissues, suggest that the developing fibrotic tissue possesses many of the molecular features of an aggressive tumor. Important findings regarding the proliferative and plastic nature of resident capsular fibroblasts were also revealed.

Results

Intra-articular Delivery of Ad.TGF-β1 Induces a Dose-Dependent Fibrotic Response:

Prior to undertaking *in vivo* experiments, we first characterized the Ad.TGF-β1 vector for transgene expression in cultures of synovial fibroblasts isolated from the joints of rats. The cells were incubated with increasing doses of virus, and 48 hours later, the levels of human TGF-β1 in the conditioned media were determined by specific ELISA. As shown in Figure 4-1, TGF-β1 was expressed in a dose-dependent manner and achieved a maximum of ~1 μg/ml at 2.0 x 10^9 viral particles (vp). Vector doses exceeding this were found to be toxic to the cells.

After confirming the ability of the Ad.TGF-β1 construct to deliver and express the transgene in the target cells, we performed preliminary studies *in vivo* to determine a vector dose that would provide a significant biological response without being detrimental to the health of the animals when expressed long term. We initially used Wistar rats, which are immunologically competent, but enable sustained expression of adenovirally delivered transgenes for about 7-10 days[94]. For these experiments, groups of rats were injected in both knees with low (1.0 x 10^9 vp), medium (2.0 x 10^9 vp), or high (4.0 x 10^9 vp) doses of virus. Rats receiving 4.0 x 10^9 vp of Ad.GFP were used as controls for the pathological effects of viral delivery. The experiment was scheduled for 7 days, at which time the animals would be sacrificed and the tissues harvested for analysis.

Within three days, the knees receiving the Ad.TGF-β1 virus became visibly enlarged, increasing in size with the vector dose. At four days post injection the rats receiving the highest dose of Ad.TGF-β1 were sacrificed due to health concerns. They

were lethargic, did not eat and showed labored respiration. Although the animals at the lower doses showed a prominent increase in joint diameter, they were otherwise healthy with normal appetite. Dissection of the joints from the animals killed at day 4, and those of the remaining groups sacrificed at day 7, showed that the increase in joint size was due to the overgrowth of a dense scar-like tissue that encased the joints and effectively occluded joint motion.

Sustained Overexpression of TGF-β1 in the Joints of Nude Rats Induces Severe Arthrofibrosis and Chondrometaplasia:

After observing the initial fibrotic response to overexpression of Ad.TGF-β1 and identifying a working range of virus, we next wanted to determine the effects of sustained TGF-β1 over-expression for a prolonged period of time. We injected the medium dose (2.0×10^9 vp) of Ad.TGF-β1 into both knee joints of a group of nude rats. As a control for viral administration, we delivered a similar dose of Ad.GFP into a parallel group. Animals in each group were euthanized at 5, 10, and 30 days post injection and the joint tissues were harvested for analysis.

As seen in Figure 4-2, by day 5 the knee joint diameter in the animals receiving Ad.TGF-β1 increased by about 40% relative to controls, and this increase was maintained throughout the course of the experiment. Following sacrifice and removal of the skin, gross inspection showed that the knee joints were completely enveloped in fibrotic tissue such that the normal features of the joint were not discernable (similar to that shown in Figure 4-3C). Consistent with the pilot experiments, by day 5 the knee joints had become immobilized, and remained locked at 90^o flexion for the duration of the experiment. During dissection of the day 5 animals, the fibrotic encasement was easily cut from the bone to expose the intact structures beneath. At each successive

time point, however, the fibrotic tissue became progressively more dense and aggresssive, such that by day 30 it appeared to penetrate and fuse with the bony architecture of the knee joint, making it difficult to distinguish pre-existing anatomy (Figure 4-3D).

Histologic analysis of the harvested tissues showed that injection of Ad.GFP caused a slight increase in the number of leukocytes in the synovial intima at day 5, but otherwise the tissues appeared normal (Figure 4-4, control). In stark contrast, injection of Ad.TGF-β1 stimulated a dramatic fibrotic response intra-articularly that, over time, changed and progressed into an aggressive fibrocartilaginous metaplasia. By day 5 there was an extensive proliferation of reactive-appearing stellate and spindled fibroblasts effacing much of the normal intra- and periarticular connective tissues (Figure 4-4, day 5). The fibroblasts replaced the normal subsynovial adipose tissue, and radiated outward from the joint space without altering the articular cartilage, which maintained its amphophilic appearance on toluidine blue stains. The fibroblastic proliferation also extended into adjacent skeletal muscle, where it invaded between myocytes. There was little accompanying inflammatory component early and no metaplastic bone or cartilage was identified at 5 days.

At 10 days, the fibroblastic proliferation had essentially replaced all of the normal anatomic structures in and surrounding the joint and began to fuse with articular cartilage, subperiosteal cortical bone, and ligamentous and capsular fibrous tissue (Figure 4-4, day 10). At these sites of fusion, the cells began to lose their once spindled morphology, instead appearing as rounded, chondrocyte-like cells.

At thirty days, the normal microscopic anatomy of the joint was not recognizable, and the resident joint and capsular structures were displaced (Figure 4-4, day 30). The fibroblastic component was considerably less cellular and more densely fibrotic, and large areas were now composed of cartilaginous tissue. The majority of the articular cartilage was replaced by metaplastic fibrocartilaginous tissue, confirmed by the deeply amphophilic appearance of the tissue on toluidine blue stain. There was no clear delineation between the fibrous component and the cartilaginous component. These cartilaginous masses penetrated the entire joint space leaving an abundant deposition of matrix enriched for proteoglycans.

TGF-β1 Stimulates Expression of Genes for Matricellular Proteins, MMPs, Collagens and Adhesion Molecules

In an attempt to determine the protein mediators responsible for driving the pathologic changes in the cells and tissues, RNA isolated from the capsular/synovial tissues of control rats and those receiving Ad.TGF-β1 was analyzed by PCR-array for expression of 84 genes associated with cellular adhesion, extracellular matrix synthesis and remodeling.

Differential analyses of the expression patterns, as seen in Table 4-1, strikingly illustrated the extent to which prolonged exposure to TGF-β1 activates the articular tissues. Numerous genes showed significantly enhanced expression, many exceeding 100-fold, while only modest reductions in expression were observed sporadically in a handful of the genes. Analyzed over the course of the experiment, the most extensive and consistent changes in gene expression were observed among the collagens, the matricellular proteins, and the proteolytic enzymes.

Consistent with the early fibrotic expansion, collagen types I, III and V were elevated from 3 to 10 fold at days 5 and 10. As the hypercellular tissue began to differentiate and transition to a cartilaginous phenotype at day 10, expression of collagen type II and hyaluronan and proteoglycan link protein 1 (HAPLN1/cartilage link protein) dramatically increased, with both genes showing >100 fold increase by day 30. Modest increases in expression of collagens VI and VIII were also observed at different time points.

Supporting the highly proliferative, expansive response of the capsular tissues, expression of the matricellular protein genes, as a group, was elevated at all time points. Those most profoundly induced were osteopontin (30-100 fold), followed by thrombospodins 1 and 2, tenascin-C and periostin. Expression of other matricellular protein genes, such as CCN2/CTGF and secreted protein acidic and rich in cysteine (SPARC/osteonectin), was also modestly elevated throughout the study and only achieved statistical significance at certain time points.

Characteristic of the expansive and invasive properties of the capsular tissues, expression of the MMPs was broadly induced at all time points. Expression of MMP-12 (elastase) showed the greatest sustained induction ranging from ~100 to 200-fold over controls. This was followed by the collagenases, MMPs-13 and -8, which were also elevated throughout the experiment, but showed >200-fold enhanced expression at days 10 and 30, respectively. MMPs-9 and -2 (the gelatinases), MMP-7 (matrilysin), MMP-11 (a member of the stromelysin family), and MMPs-14 and -16 (also termed membrane type; MT-MMPs-1 and -3) also showed significant increases in expression, ranging between ~3-80 fold induction throughout the course of the experiment.

ADAMTS1 showed evidence of enhanced expression at each time point, but this was not statistically significant.

A variety of cellular adhesion molecules also showed increased expression in the expanded capsular tissues. Of note, E-, N- and P-cadherins (epithelial, neural, and placental, respectively) were each up-regulated at day 5; however, only N-cadherin remained highly expressed for all 30 days. Interestingly, this was paralleled by heightened expression of neural-cell adhesion molecule (NCAM). Both NCAM and N-cadherin are thought to coordinately interact during cellular condensation in chondrocytic differentiation as well as in tumor cell proliferation. Several integrin receptor molecules showed increased expression during the early stages of the experiment, including α_L and β_3 subunits at day 5, and α_L, α_M, β_2 and β_3 at day 10. Increased expression of β-catenin was also seen at day 10 and L-selectin showed ~16-fold enhanced expression at day 30.

Several other genes showed enhanced expression; the most notable being Emilin-1 whose expression was increased >180-, 87- and 36-fold at days 5, 10 and 30. Emilin-1 is a connective tissue glycoprotein associated with elastic fibers, and is thought to contribute to cell motility, tissue differentiation and morphogenesis.[95] Certain laminins also showed increased expression, particularly the laminin α1 chain at day 30 and laminin γ1 at day 10. Fibronectin was also moderately enhanced at days 10 and 30.

To solidify these data, we used immunohistochemistry to examine the tissues for the presence of MMP-13 and MMP-9 at the protein level, as well as α smooth muscle actin (αSMA), a myofibroblast marker (Figure 4-5). Consistent with the expression patterns above, staining for MMP-13 was visible throughout the fibrotic matrix at the

later time points, with darker staining in the more cartilaginous tissues. Likewise, staining for MMP-9 was consistent with RNA analysis and appeared throughout the fibrotic synovium. The darkest staining was observed at day 10 at the borders between the newly expanded fibrotic tissues and cartilaginous regions. As expected, dark staining for αSMA was detected at day 5 in the heavily fibrotic regions.[96] At days 10 and 30, as the cells appeared to differentiate toward a chondrocytic phenotype, αSMA staining was significantly reduced.

Resident Synovial/Capsular Fibroblasts Proliferate to form the Fibrotic Mass

In fibrotic conditions of several tissues, such as liver, lung and kidney, a level of uncertainty has surrounded the origin of the fibroblastic cells causing the pathology. In certain models, it remains unresolved as to whether the fibrosis arises from the local proliferation and differentiation of resident fibroblasts or from infiltrating progenitor cells originating from bone marrow, or elsewhere.

To determine the origin of the cells responsible for generating the pathologic fibrotic and cartilaginous tissues in the joint, a lentiviral vector containing the cDNA for GFP (LV-GFP), was injected into the knees of nude rats 48 hrs prior to injection of Ad.TGF-β1. We have shown previously that lentivirus-based vectors, when delivered at sufficient titer, will transduce a significant proportion of the fibroblastic cells resident in the normal joint[97]. Therefore, by using a lentivirus to deliver the cDNA for GFP we could stably mark the fibroblastic cells that were pre-existent in the capsular tissues; furthermore, since the lentiviral vector integrates its genetic payload into the genome of the transduced cell, any progeny that arise from the transduced cell will likewise contain the transgene and fluoresce green[78, 97]. By pre-labeling the resident capsular cells in

this manner, if the cells comprising the fibrotic mass arise from resident fibroblast populations, then a large percentage should fluoresce green. Alternatively, if the fibroblastic cells arise from circulating myofibroblasts or progenitor cells, then the bulk of the cell mass would be negative for GFP expression.

Consistent with earlier experiments, delivery of LV-GFP in normal control joints, generated a uniform layer of fluorescent cells across the entire expanse of the synovial lining and penetrated several cell layers deep (Figure 4-6A)[78, 97]. In the joints of animals that subsequently received Ad.TGF-β1, examination at day 5 showed that the entire depth of the fibrotic synovial tissue was filled with elongated fluorescent fibroblastic cells. At day 10 the cells appeared more organized with a mixture of fluorescent elongated fibroblasts and more rounded chondrocytic cells (Figure 4-6C). By day 30, the cells in the cartilaginous tissues, as confirmed by toluidine blue staining, were also predominantly GFP+ (Figure 4-6D). These results demonstrate that in arthrofibrosis, myofibroblasts arise from fibroblastic cells resident in the connective tissues of the joint. These cells have a high proliferative capacity and the ability to transdifferentiate into chondrocytic cells.

Discussion

Our investigations present a vivid demonstration of the stimulatory capacity of TGF-β1 and its potential as a pro-fibrotic cytokine in joint disease. Sustained overexpression of TGF-β1 in the knee joints of nude rats induced a severe fibrotic response arising from the rapid proliferation of synovial fibroblasts, their differentiation into myofibroblasts and the synthesis of fibrillar collagenous matrix. Much like the adhesions associated with arthrofibrosis in humans, the fibrotic tissue progressively

developed an aggressive phenotype and began to attach and fuse with the cartilaginous and bony surfaces. Fibrotic regions in contact with articular cartilage began to undergo chondrometaplasia. Following 30 days of TGF-β1 over-expression, sections of the expanded fibro-cartilaginous tissue had penetrated the articular cartilage and subchondral bone. Large portions of the hypertrophied expanse had differentiated into hyaline-like cartilage, progressing in some regions toward osteogenesis.

Although our data provide an extraordinarily severe representation of joint fibrosis, the pathologies observed are entirely consistent with those seen in clinical cases of arthrofibrosis that occur following joint surgery[98]. Procedures involving the knee, such as anterior cruciate ligament reconstruction and high tibial osteotomy, are particularly vulnerable to the development of this type of fibrosis[98]. Histological examination of tissues recovered from fibrotic knee joints following surgical release frequently identifies fibrosis, vascular proliferation and synovial chondrometaplasia[99]. In many cases the fibro-chondrogenic tissues also contain endochondral bone formations[100-102]. The similarities between the tissue phenotype of the rat TGF-β1 overexpression model shown here and human arthrofibrosis, indicate that the data generated in the rat knee have relevance to the human condition. As such, our results support the role of TGF−β1 as a primary mediator of the pathogenesis in arthrofibrosis and therefore, as a primary target in the prevention of fibrotic conditions of the joint.

Expression Profiling is Consistent with an Aggressive Fibrotic and Chondrometaplastic Phenotype

The expression data from the PCR-arrays support the macroscopic and histologic findings, and provide insight into the molecular events through which TGF-β1 drives the fibrotic hypertrophy and cartilaginous morphogenesis of the tissues. Overall, the profile

reflected in Table 4-1 is in accord with a highly mobile, aggressive tissue that produces large quantities of ECM protein. Similar to the histologic profile, the pattern of gene expression bears many similarities to that of an aggressive tumor.

Consistent with the fibrotic phenotype observed at days 5 and 10, there was an accompanying increase in expression of various laminins and ECM proteins, including interstitial collagens type I and III, and pericellular type V collagen. Further, as the tissue transitioned to hyaline-like cartilage, there was a dramatic enhancement of expression of collagen type II, the predominant structural protein of articular cartilage. This was paralleled by an increase in transcription of cartilage link protein (HAPLN1), which serves to stabilize aggrecan and hyaluronan aggregates in the articular cartilage matrix and contributes to chondrocyte differentiation and maturation[103].

Beyond cellular proliferation and expression of structural proteins, the changes in tissue phenotype observed in response to TGF-β1 stimulation require extensive degradation of pre-existing matrix as the emerging fibrotic tissue is generated and expands, and later as the fibrous mass becomes invasive and is replaced by cartilaginous tissue. In accordance with this, some of the more striking increases in gene expression were seen among the MMPs. Fibrosis has often been considered to be a process dominated by TIMPs, whereby increased inhibition of MMPs is thought to permit the accumulation of ECM proteins, leading to fibrotic hypertrophy.[104, 105] Although TIMPs modulate MMP proteolysis, it is also known that TIMPs-1 and -2 facilitate the activation of certain MMPs[106]. While we saw an early, but relatively modest, increase in TIMP-1 expression at day 5, dramatic increases were seen in MMPs -2, -7 -8, -9, -11, -

12, -13, -14 and -16, which further increased at day 10. At various time points in the experiment, expression of certain MMPs was increased by 80 to 300-fold.

MMPs are known to participate in numerous diverse activities, including extracellular matrix remodeling, basement membrane disruption, epithelial apoptosis, cell migration, and angiogenesis[107]. Their roles in these processes occur either by direct matrix molecule cleavage or by generating bioactive mediators and biologic regulators[104, 107]. Due to the complex and dynamic nature of the articular tissues over the 30-day experiment, it is not possible to discern the contributions of individual MMPs in arthrofibrosis. However, our results suggest that the induction and maintenance of arthrofibrosis does not hinge upon the activity of any single MMP, but instead represents an orchestrated, interactive network between numerous MMPs and TIMPs.

Also notable was the marked increase in expression of matricellular protein genes. These non-structural, secreted glycoproteins interact with cell surface receptors, the ECM and soluble extracellular factors (e.g. growth factors and MMPs) to modulate cell function as well as regulate the activity or availability of proteins sequestered in the matrix[108]. As a group, matricellular proteins are known to enhance cellular mobility, ECM synthesis, cellular differentiation and migration[109-113]. They are expressed at high levels during development, but in healthy adults are typically only synthesized during active tissue remodeling, such as in wound repair and disease, particularly in cancer. Within this family, osteopontin showed the greatest induction throughout. Consistent with our expression data, osteopontin is known to bind and activate MMPs-2 and -3 even in the presence of TIMPs[114-117]. Somewhat surprisingly, despite the dramatic effects of TGF-β1 on the joint tissues, expression of CCN2/CTGF remained relatively

unchanged. CCN2/CTGF is thought to be a major activator of TGF-β1 activity and mediator of fibrosis in other tissues[21, 118, 119]. Its low induction here and relatively poor response of rat joint tissue to Ad.CTGF suggests that CCN2/CTGF may not play a major role in arthrofibrosis, and that its absence may be compensated for by other members of this group.

The increased expression of both N-cadherin and NCAM throughout the 30 day experiment is consistent with the development of chondrometaplasia in the fibrotic tissues. These adhesion molecules are expressed during embryonal chondrogenesis, where they contribute to early mesenchymal cell condensation[120]. Their enhanced expression is also in agreement with the aggressive phenotype of the expanded synovial tissues, as both molecules are known to contribute to enhanced cellular motility and migration and are associated with increased invasiveness in several types of cancer[121, 122].

Synovial and Capsular Fibroblasts have a High Proliferative Capacity and Innate Plasticity

Following lentiviral-mediated delivery of the cDNA for GFP to the knees of rats, a large percentage of fibroblasts resident in the synovial lining, subsynovium and fibrous capsule were fluorescently tagged. In previous work we have shown that VSV-G pseudotyped lentiviral vectors primarily infect CD90+ and CD29+ fibroblasts in the synovium and capsular tissues[94]. After stimulation with TGF-β1, these GFP+ cells massively proliferated, and differentiated into myofibroblasts, and later chondrocytic cells, such that the vast majority of cells in the expanded tissues fluoresced green. By stably pre-labeling the articular cells in this manner we showed that the immense fibrotic

expansion of the synovium (and subsequent differentiation of the cells into chondrocytes) arises from cells resident to the joint space.

For pathologic fibrotic conditions in organs, such as the lung, kidney and liver, the fibroblast/myofibroblast populations responsible for generating the fibrotic mass are thought to originate variously from: (1) local, resident mesenchymal cell populations, (2) epithelial cells that undergo epithelial to mesenchymal transition, and/or (3) circulating mesenchymal progenitors from bone marrow that home to sites of injury[123-127]. With regard to arthrofibrosis, our data strongly support the first scenario, and largely exclude the other two as having a meaningful role. Further, our data provide a striking demonstration of the proliferative capacity, innate plasticity and chondro/osteogenic potential of synovial and capsular fibroblasts. They also confirm the potency of TGF-β1 as an inducer of proliferation and chondrogenic differentiation in these cells.

The existence of mesenchymal progenitor cells in human synovium has been recognized since 2001, and the natural potential of these cells to spontaneously generate ectopic cartilaginous/osteogenic tissue is reflected in diseases such as chondromatosis and arthrofibrosis[128-130]. The utility of these cells in therapies for cartilage and bone repair is currently being investigated, and several preclinical studies point to synovial-derived fibroblasts as being superior to bone marrow and adipose-derived mesenchymal progenitors for these purposes[131, 132]. The apparent facility with which articular fibroblasts differentiate along chondrogenic and osteogenic pathways suggest they are predisposed to these lineages and should be strongly considered as candidates for regenerative and tissue engineering strategies for connective tissue disorders. The application of TGF-β1 as a chondrogenic agent *in vivo*, either as a

recombinant protein or transgene product, however, should be more cautiously considered. Our results serve to emphasize the sensitivity of connective tissue fibroblasts to growth factor stimulation, and that protocols designed to induce cellular differentiation in cartilage and bone repair *in vivo* should be aware of the high capacity for toxic side effects in adjacent tissues.

Table 4-1. Relative Expression Values of ECM and Associated Genes in the Joints of Nude Rats Receiving Ad.TGF-β1

Gene	Day 5	Day 10	Day 30
Structural Proteins			
Collagen, type 1, alpha 1	*4.5	**9.7	*3.7
Collagen, type 2, alpha 1	6.4	**160.3	**223.3
Collagen, type 3, alpha 1	1.8	6.1	1.9
Collagen, type 4, alpha 1	1.1	2.3	*-2.1
Collagen, type 4. alpha 2	1.1	4.2	-1.1
Collagen, type 4, alpha 3	**-3.1	-1.7	-2.6
Collagen, type 5, alpha 1	**4.0	**5.8	2.6
Collagen, type 6, alpha 1	1.7	*4.8	*2.2
Collagen, type 8, alpha 1	*7.6	5.1	*3.3
Hapln 1	2.3	**33.8	**106.5
Versican	**4.6	2.9	*4.5
Matricellular Proteins			
CCN2/CTGF	3.0	3.6	*4.4
Osteopontin 1	**32.8	**118.0	**130.0
Periostin	** 9.3	*7.3	**6.9
Sparc	*2.8	*7.4	2.1
Spock 1	1.4	3.7	1.4
Tenascin-C	**9.5	**8.9	**9.6
Thrombospondin 1	**26.1	*7.5	**20.0
Thrombospondin 2	**12.6	**8.8	**14.5
Cell Adhesion Proteins			
E-Cadherin	**4.5	9.6	3.4
N-Cadherin	**10.7	**29.8	**10.1
P-Cadherin	**8.4	2.6	3.0
R-Cadherin	*-5.4	3.8	-3.6
Catenin, alpha 1	1.2	3.7	-1.2
Catenin, alpha 2	1.7	1.9	1.4
Catenin, beta 1	2.0	*5.1	1.4
Contactin 1	*-3.2	2.0	-2.1
Icam-1	-1.0	3.4	2.0
Integrin, alpha 2	-1.1	2.6	1.0
Integrin, alpha 3	-1.8	1.8	-2.0
Integrin, alpha 4	1.2	5.6	1.8
Integrin, alpha 5	1.8	4.2	1.2
Integrin, alpha D	1.5	3.7	1.0
Integrin, alpha E	1.6	5.0	1.3
Integrin, alpha L	*2.6	*9.9	1.6
Integrin, alpha M	1.5	*4.4	-1.6
Integrin, alpha V	1.4	4.4	-1.1
Integrin, beta 1	2.2	2.9	1.9
Integrin, beta 2	1.5	*5.8	-2.8
Integrin, beta 3	*2.3	*5.2	1.6
Integrin, beta 4	-1.5	3.6	-1.4
Ncam 1	** 25.3	**15.0	**15.1
Ncam 2	1.3	2.1	1.6
Pecam	-1.0	1.6	1.3

Table 4-1. Continued

	Gene	Day 5	Day 10	Day 30
	E-Selectin	1.4	-1.7	1.8
	L-Selectin	3.6	14.3	**15.83
	P-Selectin	2.2	3.1	2.0
	Vcam 1	-2.0	1.2	-1.7
	Vitronectin	-1.8	1.3	-2.3
Extracellular Matrix Proteins				
	Fibronectin 1	1.3	*3.4	*2.7
	Laminin alpha 1	*5.7	5.1	**25.0
	Laminin alpha 2	-2.2	2.3	1.4
	Laminin alpha 3	1.1	*3.5	-1.3
	Laminin beta 2	-2.4	3.5	-1.4
	Laminin beta 3	-1.5	*3.8	*2.9
	Laminin gamma 1	21.6	*72.4	3.3
	Tgfbi	**6.9	*9.3	**3.9
Metaolloproteinases and Inhibitors				
	Adamts 1	12.2	26.7	15.3
	Adamts 2 (RGD1565950)	2.0	** 4.3	*3.8
	Adamts 5	-1.0	2.3	1.3
	Adamts 8	*-4.4	-2.4	-3.9
	MMP 1a	3.5	3.6	2.6
	MMP 2	** 5.7	**9.3	**6.3
	MMP 3	-1.1	2.0	4.6
	MMP 7	** 13.2	**20.8	*9.0
	MMP 8	*10.4	*229.9	*39.2
	MMP 9	*11.0	*79.5	3.1
	MMP 10	3.2	11.2	8.3
	MMP 11	*2.9	**17.9	**4.4
	MMP 12	** 97.3	**182.9	**198.1
	MMP 13	19.3	*58.9	*300.3
	MMP 14	** 7.0	**5.0	**6.4
	MMP 15	-1.4	1.3	-2.1
	MMP 16	*3.2	*9.6	**5.70
	TIMP 1	**10.8	1.1	**6.8
	TIMP 2	2.9	1.5	*2.5
	TIMP 3	** -4.1	3.1	-1.5
Elastic Fiber Proteins				
	Emilin 1	* *181.3	*87.0	*36.1
	Fibulin 1	1.4	3.4	*3.1
	Extracellular matrix protein 1	-1.5	3.8	1.5
Other				
	Synaptotagmin I	3.1	3.0	9.2
	CD44 Antigen	-2.4	-1.5	-3.1
	Sarcogycan	1.3	3.4	1.1
	NTPDase-1 (CD39)	1.9	3.0	1.6

Values with an asterisk represent $p<0.05$. Values with two asterisks represent $p<0.01$. n=3 for each time point.

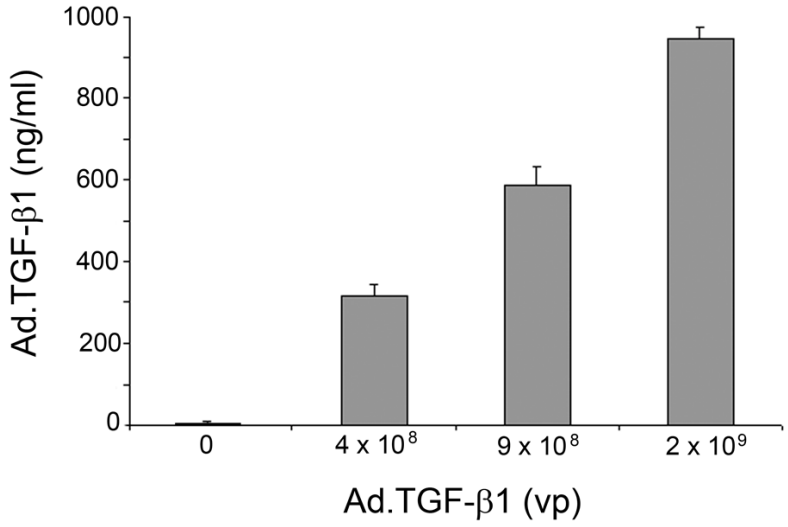

Figure 4-1. Transgene expression following infection of rat synovial fibroblasts with Ad.TGF-β1. Following isolation of fibroblasts from rat synovium, the cells were grown in monolayer in 12-well plates and infected with increasing doses of Ad.TGF-β1. At 24hrs post infection, the medium was replaced by 0.5 ml of serum-free medium. At 48hrs post infection, the conditioned medium was harvested and TGF-β1 content measured by specific ELISA. Results are expressed in ng/ml as the mean of 3 replicates. Error bars represent ± S.E.M.

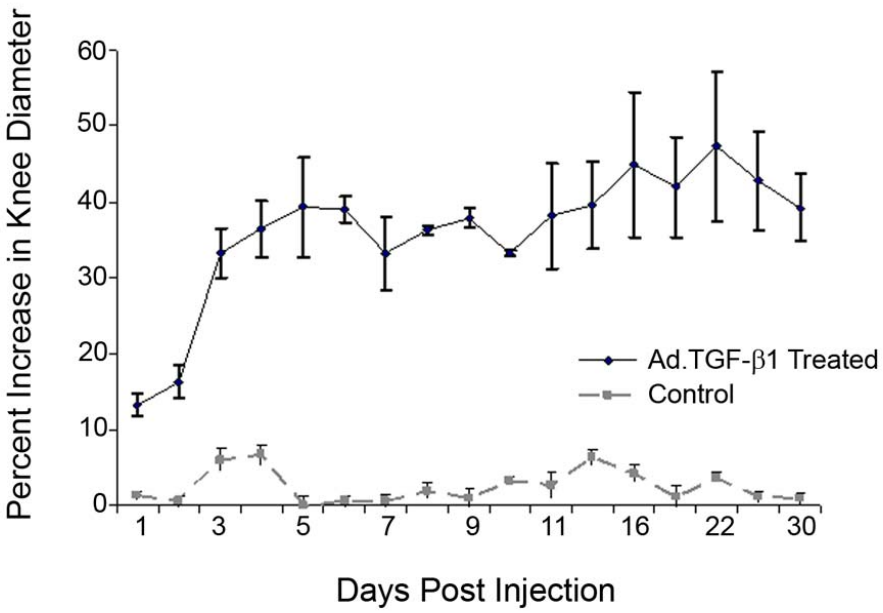

Figure 4-2. Intra-articular delivery of Ad.TGF-β1 induces joint swelling. The knees of nude rats were injected with 2.0 x 10^9 vp of Ad.TGF-β1, and the diameter of the joints was measured periodically with calipers. Injection of Ad.TGF-β1 rapidly induced joint thickening, and animals showed increased knee diameter throughout the experiment. For the Ad.TGF-β1 treated group, days 0 and 5 represent n=16 knees, days 5-10 represent n=8 knees, and days 10-30 represent n=4 knees. For all time points normal control represents an n=8 knees. Values represent the mean of measurements for all knees in each group. Error bars represent + S.E.M.

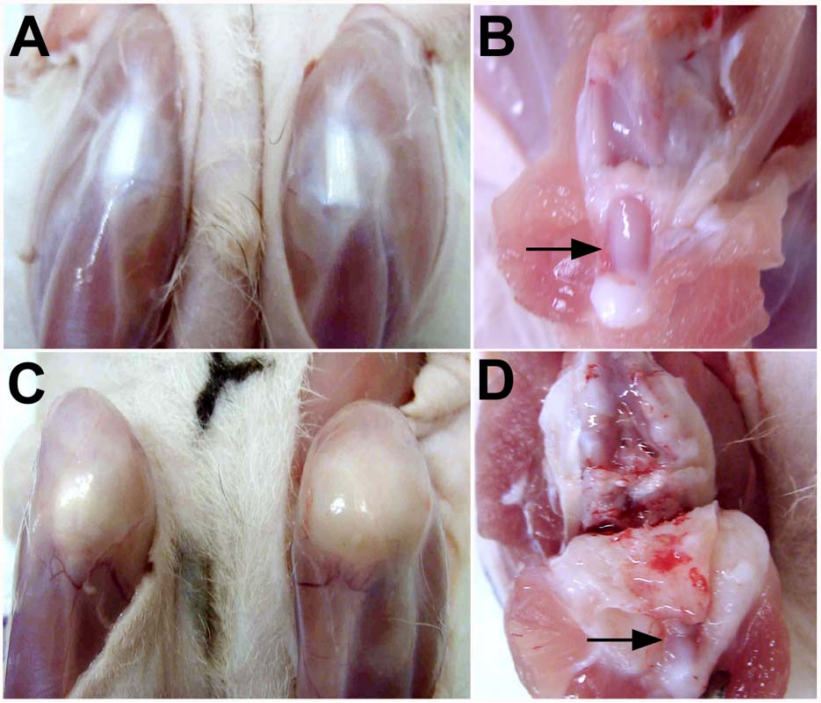

Figure 4-3. Local overexpression of Ad.TGF-β1 in the knee joint induce severe arthrofibrosis. Groups of rats were injected intra-articularly with 2.0 x 10^9 vp of Ad.TGF-β1 (panels A and B) or Ad.GFP (panels C and D) and were killed periodically thereafter, as described. Images shown are representative of those sacrificed at day 30. (A and C) External views of knee joints after removal of the skin. (B and D) Internal views of the joints following dissection. For joints receiving Ad.TGF-β1 there was a visible increase in joint size, and the knees became encased in a dense, scar-like tissue. Upon dissection, the fibrotic tissue was observed to override the joint space and displace pre-existing structures. Arrows indicate the location of the patella.

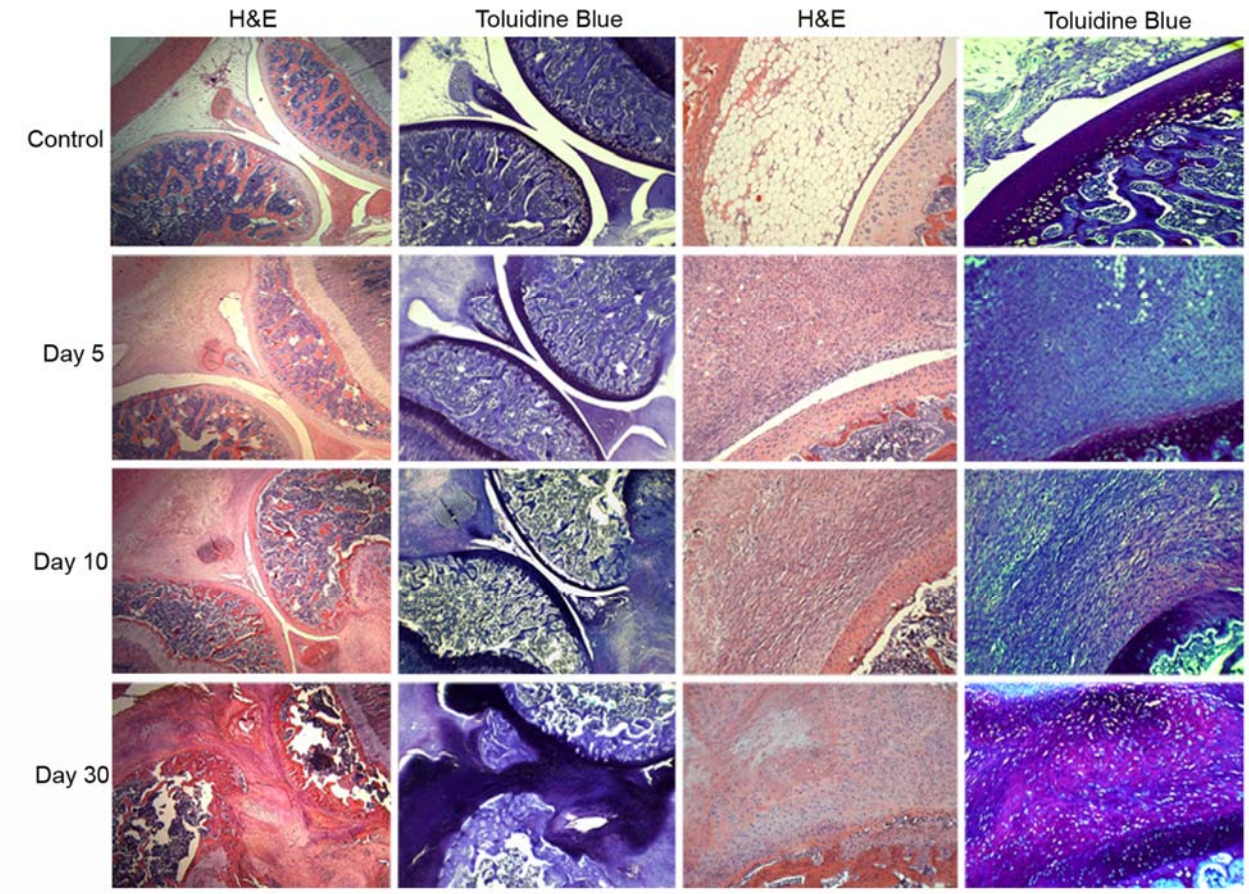

Figure 4-4. Capsular fibrosis and chondrogenesis induced by Ad.TGF-β1. Knees of nude rats receiving Ad.TGF-β1 were harvested at various time points, decalcified and processed for histology. Sections were stained with H&E or toluidine blue as indicated. Images at day 0 show the Ad.GFP treated joint with a thin synovial lining supported largely by adipose tissue. At 5 days post injection, an expansion of fibroblastic cells from the synovial lining generated the bulk of the fibrotic mass, occluding the adipose layer. 10 days post injection, formation of chondrocyticic cells can be seen within the fibrotic tissue. By day 30, the majority of fibroblastic cells had differentiated into chondrocytes, as seen in the toluidine blue stain, invading neighboring tissues and displacing existing structures. Images in left two columns are at a magnification of 2.5x, and images in the right columns are at a magnification of 20x.

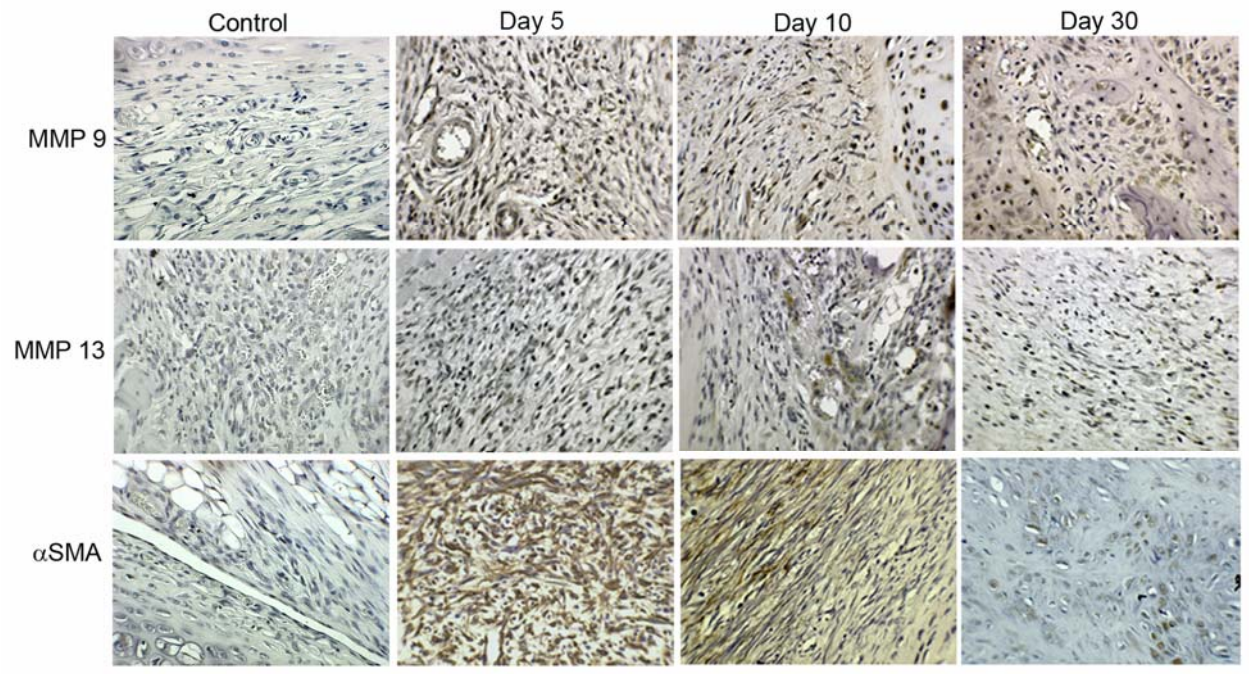

Figure 4-5. Immunohistochemical staining for MMPs 9 and 13, and α smooth muscle actin (αSMA). The knee joints of nude rats receiving Ad.GFP control and Ad.TGF-β1 were harvested at days 5, 10 and 30, paraffin embedded, sectioned and immunologically stained for the presence of MMP 9, MMP 13 or αSMA as indicated.

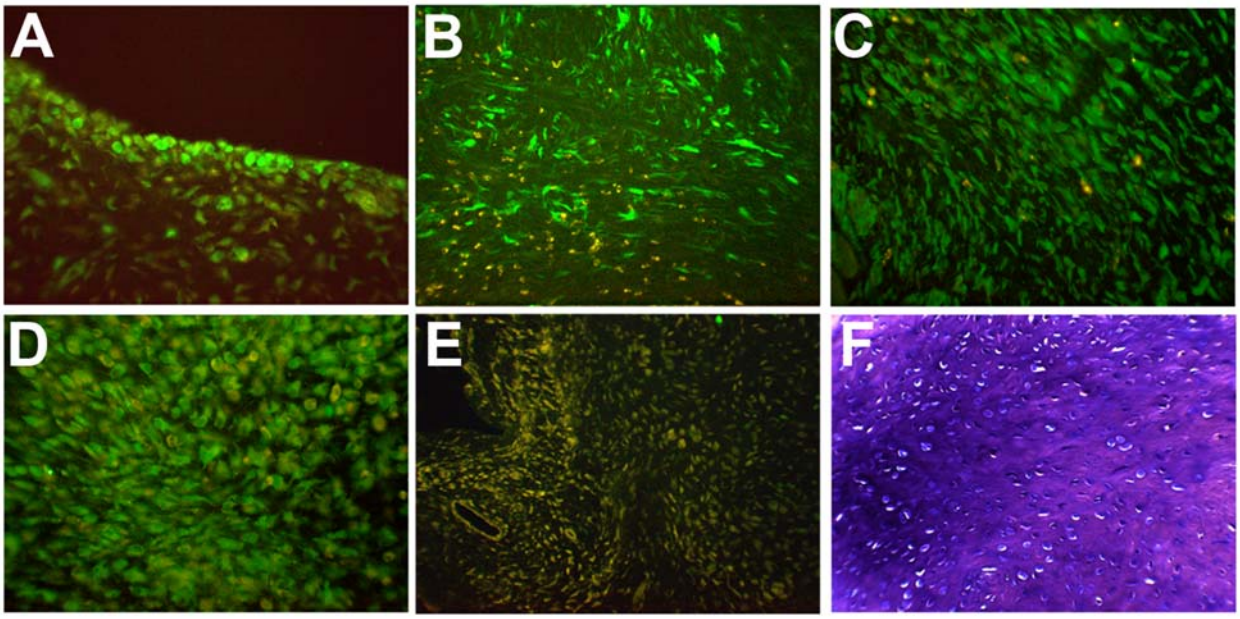

Figure 4-6. Arthrofibrosis and chondrometaplasia arise from resident synovial and capsular fibroblasts. A) Fibroblastic cells in the synovium and joint capsule of nude rats were fluorescently labeled following intra-articular injection of recombinant lentivirus containing the cDNA for GFP (LV.GFP). 48 hours after delivery of LV.GFP, Ad.TGF-β1 was injected into the joint, and the rats were killed periodically thereafter. (B) Day 5 post Ad.TGF-β1 injection showed a fibrotic cell mass composed primarily of GFP+ cells. (C) At day 10 the GFP labeled cells began to acquire a chondrocytic appearance. (D) By day 30, the GFP+ cells had differentiated into a chondrocytic phenotype as evidenced by the rounded morphology. E) Joints receiving only Ad.TGF-β1 show no evidence of GFP expression. F) The cartilaginous phenotype of tissues in panel D is confirmed by metachromatic staining of proteoglycan with toluidine blue.

CHAPTER 5
EXAMINING THE EFFECTS OF LONG TERM ARTHROFIBROSIS IN IMMUNOCOMPETENT ANIMALS

Introduction

IAC is characterized by a painful fibrotic expansion of the synovium and joint capsule, which gradually results in the loss of active and passive motion of the joint. It typically begins over several months and progresses in stages[87]. The disease is generally self-limiting. Some individuals, however, mostly diabetics, never recover from the painful and stiff stages and remain permanently disabled. Since the underlying causes of IAC remain unknown, no specific pharmacologic or non-surgical therapy has been shown to cure IAC or provide significant long-term benefit. A primary reason for the absence of literature regarding the pathogenesis of IAC is the lack of available tissue from early stage disease for detailed analysis. Few studies have addressed the involvement of specific growth factors in IAC.

Pathologic fibrosis is a prominent feature of chronic disease in several organs, including the skin, liver, lung and kidney, and often begins with local injury and activation of repair pathways. While the physical causes of pathologic fibrosis vary, the protein factors that mediate wound healing and tissue repair are considered to play central roles. TGF-β1 has been implicated in a majority of fibrotic conditions[17]. Previously, we chronically overexpressed TGF-β1 at high levels in the knee joints of immunocompromised nude rats, which led to very severe arthrofibrosis (see Chapter 4). The amount of virus delivered in these experiments represented an extreme response to stimulation with TGF-β1. While relevant to various diseases of the joint, including

synovial chondromatosis, chondrometaplasia, osteosarcoma and chondrosarcoma, it showed no signs of resolving.

Therefore, in an effort to understand the biological processes that contribute to the development and resolution of arthrofibrosis and frozen shoulder, we wanted to establish an animal model that more closely reflected the level of disease in humans. As cells expressing nonhomologous transgenic proteins are immunologically cleared from the joints of immunocompetent Wistar rats within 21 days[94], we used this system to examine the effects of short term production of TGF-β1 intra-articularly, with the goal of inducing a fibrotic event that will more closely mirror the stages of IAC. By observing animals over the course of 120 days and delivering a low dose of Ad.TGF-β1, we hypothesized that the animals would undergo a remodeling process similar to stage 4 IAC. To follow the changes in gene expression over the course of disease in the capsular tissues, we used real-time PCR technology and histologic analysis. Using PCR arrays, we were able to establish the signaling patterns occurring throughout this process, which should be of use in future studies comparing these data to expression data obtained from humans with IAC.

We found that TGF-β1 gene transfer very rapidly induced a fibrotic condition that completely encased and immobilized the injected joint, induced a chondrogenic response, and over the course of the 120 day experiment, gradually resolved into a less aggressive, less fibrotic, and overall less cellular tissue. Histologic examination, as well as focused expression arrays of the joint tissues over time, suggested the developing fibrotic tissue adopted a phenotype similar to that of IAC and gradually remodeled with time.

Results

We hypothesized that over-production of TGF-β1 intra-articularly contributes to, and may be the cause of, chronic arthrofibrosis seen in patients with IAC. The goal of our experiments was to establish a less severe model of arthrofibrosis more similar in intensity to that of IAC. In doing so, we could more accurately model its onset and progression as well as the factors affecting its resolution.

Immunocompetent Wistar rats received a single intra-articular injection of Ad.TGF-β1or Ad.GFP into both knee joints (5.0×10^7 vp). Groups of rats were killed periodically over the course of 120 days, and the tissues were harvested and analyzed. Within three days, rats developed a robust fibrotic response. The knees became swollen and were slightly immobilized the joint. Although the animals showed a prominent fibrotic response, they were otherwise healthy with normal appetite.

Animals receiving Ad.TGF-β1 showed an increase in knee diameter at day 10 relative to controls, and the increased joint size persisted throughout the course of the experiment. Physical manipulation of the knee showed the joints were stiff, and while not as seen in the nude rat receiving a higher dose, range of motion was notably limited. While not quite as severe as previously seen (Figure 4-3), gross inspection of the joint tissues at the times of sacrifice reveled that knee joints were encased in fibrotic tissue, obscuring the normal features of the joint. Also, similar to immunocompromised animals in Chapter 4, early in the time course this fibrotic encasement could easily be dissected away from the bone and structures beneath; however as the fibrosis developed, the tissue became more dense, making it difficult to distinguish pre-existing anatomical structures.

Delivery of Ad.TGF-β1 to the Joints of Immunocompetent Rats Induces Arthrofibrosis and Chondrometaplasia that Resolves with Time

The normal rat knee joint is surrounded by a thin layer of synovium, only a few cell layers thick, overlying a layer of adipose tissue. Following stimulation of the synovium with TGF-β1, there was a massive proliferation of elongated fibroblastic synovial cells surrounding the joint. These fibroblastic cells from the synovium actively proliferate and are surrounded by collagen fibers, generating the bulk of the fibrotic mass replacing all of the adipose tissue seen in the normal joint (Figure 5-1, Day 10). By day thirty, the hypertrophied fibrotic tissue extends outward to fill the entire joint space, displacing resident joint and capsular structures (Figure 5-1, Day 30). The fibrotic tissue began to adhere to the articular cartilage displaying a blending together of elongated fibroblastic cells and rounded cartilage cells, so much so, that toluidine blue staining of the matrix composition and cell morphology reveal the predominant phenotype of the cells overrunning the joint had changed to that of articular cartilage.

Reminiscent of the resolution phase described in human IAC, by day 90, the overall phenotype of the joint space of these animals was less severe and less cellular than that seen at day 30; however, much of the chondrogenic tissue remained (Figure 5-1, Day 90). As opposed to the highly proliferative state seen at days 10 and 30, by days 90 and 120, the joint appeared to resolve much of the fibrotic and chondrogenic mass that developed. At day 120, the majority of fibrotic overgrowth had been eliminated, there was an overall reduction in cellularity, and adipose tissue could be seen surrounding the joint space. While some fibrotic and cartilaginous tissue remained, the overall architecture of the joint began to once again resemble that of a normal joint (Figure 5-1, Day 120).

Expression Profiles of Genes Stimulated by TGF-β1 Display Altering Patterns of Expression Consistent with the Phenotype of the Tissue

Using this overall less severe model of IAC, we wanted to examine the expression profile over the course of the 120 day experiment, to observe changes in expression of ECM and adhesion molecules, using RNA isolated from the capsular/synovial tissues of control rats and those receiving Ad.TGF-β1. Differential analyses of the expression patterns can be seen in Table 5-1.

Similar to our earlier experiment and consistent with the early fibrotic expansion seen histologically, collagen types I, III and V were elevated from 2 to 6 fold at day 10. As the hypercellular tissue transitioned into a cartilaginous phenotype at days 10 and 30, expression of collagen type II and hyaluronan and proteoglycan link protein 1 (HAPLN1/cartilage link protein) dramatically increased, with both genes showing >100 fold increase by day 10 and >45 and ~20-fold increase by day 30, respectively. Interestingly, at days 90 and 120 expression of all structural proteins decrease, including Collagen II and Hapln1, consistent with the remodeling observed histologically.

Supporting the highly proliferative, expansive response of the capsular tissues, expression of the matricellular protein genes, as a group, were highly elevated at the early time points, days 10 and 30. Those most profoundly induced were osteopontin (15-100 fold), followed by thrombospodins 1 and 2, tenascin-C and periostin. As a whole, the matricellular proteins gradually decreased in expression as the tissue continued to remodel through day 120 into a less aggressive and less fibrotic phenotype. The exception was Spock-1, also known as testican-1. While the exact functions of this matricellular protein are not fully understood, it is speculated to

participate in the regulation of matrix turnover in cartilage and inhibition of membrane-type MMPs, consistent with the remodeling seen in this tissue.

Characteristic of the expansive and invasive properties of the capsular tissues, expression of the MMPs was broadly induced at all time points. Interestingly, for many of MMPs, expression levels not only peaked at the induction of fibrosis at day 10, but also during the reduction phase seen at day 120. Expression of MMP-12 (elastase) showed the greatest levels of expression at days 10 and 30 ranging from >250 to >150-fold over controls and decreased to a 45 fold induction by day 120. This was followed by the collagenases, MMPs-13 and -8, which were elevated throughout the experiment, showed >100-fold and >60-fold enhanced expression at day 10, respectively. Additionally, both MMP-12 and -13 showed increases in expression at day 120, during remodeling. MMP-9 (gelatinase), MMP-7 (matrilysin), MMP-11 (a member of the stromelysin family), and MMPs-14 and -16 (also termed membrane type; MT-MMPs-1 and -3) also showed significant increases in expression, ranging between ~2-50 fold induction throughout the course of the experiment. Similarly, ADAMTS-2, -5, and -8 increased in expression as the tissue remodeled at days 90 and 120, but not all points were statistically significant.

A variety of cellular adhesion molecules also showed increases in expression in the expanded capsular tissues during fibrotic induction. Heightened expression of neural-cell adhesion molecule (NCAM) peaked at day 10 and remained increased from >20 to 2-fold, throughout the experiment. Interestingly, both NCAM and N-cadherin are thought to coordinately interact during cellular condensation in chondrocytic differentiation as well as in tumor cell proliferation; however decreases are seen in N-

cadherin at days 10 and 30. Several integrin receptor molecules showed increased expression during the early stages of the experiment, including α_L, α_E and β_3 subunits at day 10 and 30. While most cell adhesion molecules peak at onset of fibrosis integrin $\beta 1$ and E-selectin peak in expression during remodeling at day 120.

Several other genes showed enhanced expression at onset of fibrosis and an overall reduction during remodeling; the most notable being Emilin-1 whose expression peaked at day 10 and gradually diminished. Emilin-1 is a connective tissue glycoprotein associated with elastic fibers, and is thought to contribute to cell motility, tissue differentiation and morphogenesis.[95] Certain laminins also showed increased expression at onset, particularly the laminin $\alpha 1$ chain at day 30 and laminin $\gamma 1$ at days 10 and 30.

Discussion

Patients with IAC generally experience an extremely painful stage when the adhesions are developing within the joint capsule, followed by a frozen/adhesive phase, during which time the pain subsides but the glenohumeral joint remains stiff with limited rotation, and finally a thawing/resolution phase. The spontaneous resolution can take up to 42 months and patients see an improvement in the range of motion as the adhesions resolve. Since not much is known about what causes the glenohumeral joints of patients to “freeze” or to “thaw”, we examined by histology and by gene expression analysis the differences that occur in a model of joint fibrosis in rodents.

During the onset of fibrosis observed at day 10, there was an accompanying increase in expression of various ECM proteins, including interstitial collagens type I, II and III. As the tissue transitioned to hyaline-like cartilage, dramatic enhancement of

expression of collagen type II, the predominant structural protein of articular cartilage along with an increase in transcription of cartilage link protein (HAPLN1) could be seen. As the tissue resolved over the 120 day experiment, there was an overall phenotypic decrease in the chondrometaplastic tissue and concurrent decreases in both collagen type II and cartilage link protein.

While not examined in the present study, apoptosis of fibrotic synovial cells may contribute to the resolution of fibrosis by acting as a mechanism for removing the cell population responsible for both producing the fibrotic matrix and protecting the matrix from degradation via their production of TIMPs. Evidence suggests that a major mechanism mediating the loss of cells that are unwanted after a pathological process is apoptosis[133-136]. However, the loss of activated synovial fibroblasts is not in itself sufficient to allow a remodeling of the existing excess collagens, which requires matrix degradation to be upregulated. MMPs are key enzymes in the breakdown of the ECM. Collagenases, MMP-1, -8, -13, are members of the MMP family that degrade fibrillar collagens types I, II, and III. MMP-13 is the major collagenase that degrades collagens in connective tissues in rats along with MMP-8, which is expressed in articular chondrocytes[137], synovial fibroblasts[138], osteoblasts and osteocytes[139], among other locations.

Our results indicate that in the MMP-8 expression peaks at the development of fibrosis showing >60 fold, when the tissue is expanding and differentiating into an articular cartilage-like phenotype, and tapers off throughout the experiment as the tissue remodels so that by day 120 its expression had decreased. MMP-13 mRNA expression levels peaked both at the onset of fibrosis and when the most remodeling of the joint

space seemed to be occurring. At days 10 and 120 MMP-13 levels showed >100 fold increases and at days 30 and 90 expression levels were >50 and >65, respectively. TIMPs-1 and -2 expression went from >25-70 fold increases seen during the peak of fibrosis at days 10 and 30, to an approximate ~2-fold increase at days 90 and 120 consistent with the extensive remodeling and degradation of fibrotic tissue. While MMP activity was highly expressed throughout the experiment, several of the MMPs peaked during both the fibrotic induction at day 10, and the resolution at day 120. These data suggest important factors for promoting the matrix remodeling are the enhanced MMP synthesis and the removal of the inhibitory influences of the TIMPS on collagenase activity.

Intra-articular delivery of a low dose of virus in immunocompetent Wistar rats observed over 120 days, resulted in a rapid and severe fibrotic induction that was less intense than previous experiments (see Chapter 4), and remodeled into an overall less fibrotic tissue with time. The resulting pathology more closely resembled that described in patients with IAC. An initial synovial fibrotic proliferation caused the joint to become stiff. However, areas of the synovium transformed into hyaline-appearing cartilage, which is observed in various forms of arthrofibrosis within the knee joint, not necessarily in IAC. The formation of synovial chondrometaplasia could be due to the anatomical site of the intra-articular injections. This shortcoming is not easily remedied as it is not feasible to inject into the shoulder joint of rodents. This dense fibrotic chondrometaplastic tissue resolved to a large extent over the course of 120 days. While the cartilaginous tissues were not completely eliminated by the end of this study, normal joint features were once again visible, and one would predict that this tissue would

completely resolve at a longer time point. Ultimately, these data will be compared to global expression patterns of RNA extracted from tissue samples of human patients undergoing surgery for IAC. Comparing the expression profiles of what is seen in our model of arthrofibrosis to that in human patients, will provide a valuable insight into the signaling of this disease and, perhaps, highlight potential targets for therapy.

Table 5-1. Relative Expression Values of ECM and Associated Genes in the Joints of Wistar rats receiving $5.0*10^7$ Ad.TGF-β1

Gene	Day 10	Day 30	Day 90	Day 120
Structural Proteins				
Collagen, type 1, alpha 1	**6.3	*3.3	-1.0	1.5
Collagen, type 2, alpha 1	**106.3	48.2	**14.2	2.9
Collagen, type 3, alpha 1	**2.9	1.9	-3.0	-1.4
Collagen, type 4, alpha 1	1.0	*-2.0	-3.1	-2.3
Collagen, type 4. alpha 2	1.7	-1.5	-3.5	-2.5
Collagen, type 4, alpha 3	-1.6	-2.4	1.8	2.6
Collagen, type 5, alpha 1	**2.7	2.1	-2.3	-1.2
Collagen, type 6, alpha 1	**2.4	1.5	-1.2	1.5
Collagen, type 8, alpha 1	**7.6	*5.1	2.0	**2.4
Hapln 1	**165.4	*21.7	*21.9	6.0
Versican	-1.2	*5.6	2.0	2.9
Matricellular Proteins				
CCN2 (CTGF)	*3.0	2.0	2.1	2.0
Osteopontin 1	**100.6	*49.2	**80.4	15.9
Periostin	**6.0	2.6	-4.4	-1.2
Sparc	*2.1	1.7	-2.8	-1.6
Spock 1	-1.1	*6.3	7.7	8.1
Tenascin-C	**7.9	1.9	1.8	2.8
Thrombospondin 1	**14.4	**11.9	3.1	2.5
Thrombospondin 2	**11.1	*7.6	2.5	3.2
Cell Adhesion Proteins				
E-Cadherin	**2.9	**5.5	2.2	1.2
N-Cadherin	*-2.8	*-6.6	2.8	1.7
P-Cadherin	1.9	3.0	1.1	1.8
R-Cadherin	**-12.7	1.4	-1.4	-1.9
Catenin, alpha 1	-1.1	1.1	-2.3	-1.2
Catenin, alpha 2	-2.1	*19.6	12.6	3.4
Catenin, beta 1	**2.5	1.7	-1.3	1.3
Contactin 1	-2.1	-1.1	-1.3	2.2
Icam-1	-1.2	1.1	-1.0	1.7
Integrin, alpha 2	1.6	1.1	-1.2	1.2
Integrin, alpha 3	**-3.2	*-3.4	-1.2	1.5
Integrin, alpha 4	**2.7	1.7	-1.7	-1.1
Integrin, alpha 5	**1.6	1.1	-1.8	1.1
Integrin, alpha D	-1.5	2.1	-1.6	1.3
Integrin, alpha E	**31.5	**58.7	1.9	4.5
Integrin, alpha L	*2.9	*3.1	-2.8	-1.4
Integrin, alpha M	1.7	1.7	-1.5	1.4
Integrin, alpha V	1.7	-1.1	-2.7	-1.3
Integrin, beta 1	**-3.1	**-4.8	*21.3	**18.1
Integrin, beta 2	1.2	1.1	-2.2	-1.2
Integrin, beta 3	*4.12	1.1	-2.1	-1.2
Integrin, beta 4	-1.6	-1.4	-1.5	1.1
Ncam 1	**24.3	*11.2	2.0	*4.7
Ncam 2	-3.0	4.9	2.9	1.5

Table 5-1. Continued

	Gene	Day 10	Day 30	Day 90	Day 120
	Pecam	1.5	1.4	2.0	*3.0
	E-Selectin	-2.1	-2.9	*15.0	**20.7
	L-Selectin	**-9.8	-6.0	1.4	1.9
	P-Selectin	1.7	1.6	-1.7	1.5
	Vcam 1	-1.2	-1.5	1.3	1.5
	Vitronectin	*-4.4	-6.7	3.4	2.5
Extracellular Matrix Proteins					
	Fibronectin 1	**-2.0	*-3.5	3.3	*3.7
	Laminin alpha 1	3.1	*17.7	3.7	3.7
	Laminin alpha 2	-1.6	1.3	-1.7	1.2
	Laminin alpha 3	-1.0	-1.0	-1.8	-1.4
	Laminin beta 2	-1.2	1.3	-2.1	-1.3
	Laminin beta 3	**-9.2	**-6.8	1.1	1.5
	Laminin gamma 1	10.0	18.4	1.8	1.9
	Tgfbi	**6.3	*4.1	-2.1	1.0
Metaolloproteinases and Inhibitors					
	Adamts 1	*2.7	12.7	-1.5	1.4
	Adamts 2 (RGD1565950)	*1.7	1.6	2.7	**5.0
	Adamts 5	-1.7	-1.2	4.8	*5.6
	Adamts 8	-1.8	-2.6	6.0	8.9
	Mmp 1a	-1.9	21.8	7.2	2.3
	Mmp 2	**1.7	1.3	-2.5	1.6
	Mmp 3	*4.5	**39.4	3.1	3.8
	Mmp 7	-1.5	*10.1	1.6	*16.8
	Mmp 8	**61.8	*24.4	16.8	*9.2
	Mmp 9	*51.9	11.5	9.3	14.0
	Mmp 10	2.5	20.1	11.5	7.6
	Mmp 11	**7.7	**5.8	1.3	*3.1
	Mmp 12	**258.9	*157.3	6.9	*45.0
	Mmp 13	105.5	51.1	*66.4	*112.2
	Mmp 14	**7.6	*2.9	2.2	4.3
	Mmp 15	**-3.8	-**5.3	1.3	2.4
	Mmp 16	**4.6	*4.5	1.5	2.4
	Timp 1	**35.3	**49.8	2.3	2.9
	Timp 2	**74.5	**35.8	2.1	3.1
	Timp 3	-1.9	-2.2	-2.2	-1.8
Elastic Fiber Proteins					
	Emilin 1	*49.29	32.8	6.3	*10.4
	Fibulin 1	1.4	2.8	-1.1	1.9
	Extracellular matrix protein 1	2.1	1.3	1.3	2.1
Other					
	Synaptotagmin I	-2.0	5.7	3.2	1.7
	CD44 Antigen	*-2.5	-1.9	2.0	*2.8
	Sarcogycan	-1.4	1.1	-1.6	1.0
	NTPDase-1 (CD39)	*4.9	1.8	1.6	2.5

Values with an asterisk represent $p<0.05$. Values with two asterisks represent $p<0.01$. n=3 for each time point.

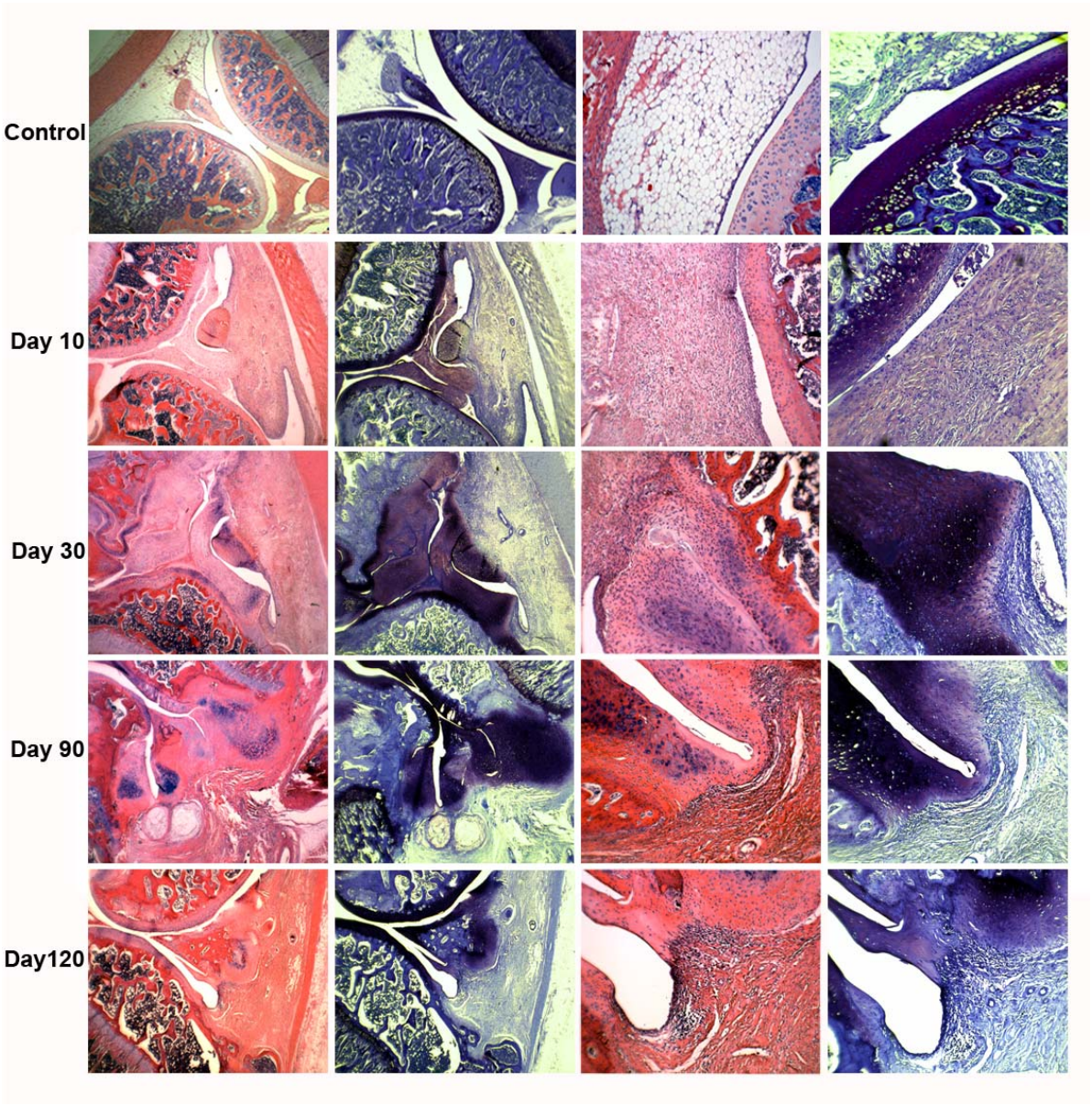

Figure 5-1. Capsular fibrosis and chondrogenesis induced by Ad.TGF-β1 resolves with time. Knees of Wistar rats receiving Ad.TGF-β1 were harvested at various time points, decalcified and processed for histology. Sections were stained with H&E or toluidine blue. Control images, in the upper panel, show Ad.GFP treated joint with a thin synovial lining supported largely by adipose tissue. 10 days post injection, an expansion of fibroblastic cells from the synovial lining generated the bulk of the fibrotic mass, occluding the adipose layer and formation of chondrocyticic cells can be seen within the fibrotic tissue. By day 30, the majority of fibroblastic cells had differentiated into chondrocytes, as seen in the toluidine blue stain, invading neighboring tissues and displacing existing structures. Day 90 histology shows signs of remodeling with a less aggressive tissue and reduction in cellularity. By day 120, much of the fibrotic and chondrogenic tissue has resolved. Images in left two columns are at a magnification of 2.5x, and images in the right columns are at a magnification of 20x.

CHAPTER 6
EXAMINING THE RELATIONSHIP BETWEEN DIABETES AND ARTHROFIBROSIS

Introduction

According to statistics from the Centers for Disease Control and Prevention, in 2007, 23.6 million people (7.8% if the population) in the United States were living with diagnosed or undiagnosed diabetes. Diabetes mellitus is a medical condition associated with abnormally high levels of glucose in the blood. Normally, blood glucose levels are controlled by insulin. In type I diabetes, destruction of beta cells, leads to hyperglycemia. Type I diabetes (insulin-dependent), accounts for 10% of all cases and results from the autoimmune destruction of insulin-producing beta cells in the pancreas by CD4+ and CD8+ T cells and macrophages infiltrating the islets[42]. Afflicting over 150 million people worldwide, type II diabetes, (non-insulin-dependent (NIDDM)), is an incurable metabolic disorder characterized by insulin resistance, decreased beta-cell function, and hyperglycemia[43].

Approximately 20% of diabetic patients not only suffer with IAC, but have a more persistent and severe case. Their inability to properly regulate blood glucose may be responsible. Hyperglycemic conditions are known to stimulate elevated expression of TGF-β1[53, 60]. Acute and chronic high glucose exposure stimulates TGF-β1 transcription, leading to an increased pool of bioactive TGF-$\beta 1$[140]. High levels of ambient glucose have been shown to stimulate the production of extracellular matrix components, including collagens, via TGF-β1 and CTGF signaling[46]. Diabetic animals displayed increased levels of TGF-β1[53] mRNA and protein in kidney tissues, along with an activated Smad signaling pathway, transducing the TGF-β1 signal[53, 54].

TGF-β1 has been shown to be elevated in plasma[49], secreted in the urine[50], elevated in the circulation[141], and found in kidney tissues[51, 52] of patients who suffer from diabetic nephropathy, a fibrotic condition that causes kidney function impairment, leading to end-stage renal disease. All three isoforms of TGF-β[142] and TGF-β1 mRNA are markedly increased in renal biopsy specimens from patients with diabetic kidney disease[143].

Data from tissue culture and animal models has demonstrated that elevated glucose levels stimulate signaling cascades involved in cell proliferation and fibrogenesis. Compared with low glucose, high glucose environments decrease expression of MMPs, increase expression of TIMPs[144], and lead to accumulation of fibronectin, laminin, and types I and IV collagen[56]. In several renal cell types, treatment with a TGF-β1 antagonist, such as a neutralizing monoclonal antibody[57] or antisense oligonucleotides[59], largely eliminated the rise in ECM expression due to high glucose. This pointed to TGF-β1 as a mediator of the profibrotic effects of high glucose on the kidney[53]. Similar studies showed treatment with neutralizing monoclonal antibodies against TGF-β1 prevented mRNA increases of TGF-β1, type IV collagen, and fibronectin in diabetic mice[60] and anti-TGF-β1 antibody therapy prevented mesangial matrix expansion and renal insufficiency[145].

While the specific reason remains unknown, diabetics are prone to the development of IAC and often suffer from a more persistent, prolonged case[146]. We hypothesize that this is due to increased levels of blood sugar that stimulate the release of TGF-β1 and other profibrotic cytokines that serve to exacerbate the fibrotic condition.

To test this we examined the effects of TGF-β1 overexpression on the knee joints of rats with experimental diabetes induced by streptozotocin.

Results

D-glucose Stimulates Cell Migration

Prior to undertaking experiments in our animal model of IAC, we examined the effects of elevated glucose on the function of TGF-β1 in RSF *in vitro*. To determine if elevated glucose enhanced cellular migration, RSF cells were grown to confluence in 6-well dishes prior to treatment with mitomycin C, which alkylates DNA and produces interstrand DNA cross-links, thereby inhibiting DNA synthesis and fibroblast proliferation[147-151]. The RSF cells were then transduced with 1.3 x 10^7 vp of the appropriate viral construct, either Ad.TGF- β1 or Ad.CTGF. Afterward, the medium in certain wells was supplemented with D-glucose. Using a pipette tip, a scratch was made in the cellular monolayer to simulate a tissue lesion, and cell migration into the mock wound space was assayed at 48 hours post treatment.

In normal medium, overexpression of CTGF induced cellular migration approximately 2 fold over that of control, while TGF-β1 increased motility approximately 3-fold. In the presence of elevated D-glucose, migration into the mock wound space was also enhanced approximately two-fold at each concentration tested: 8, 25 and 75 mM (Figure 6-1 and Figure 6-2). An additive effect could be seen in the presence of elevated glucoses with TGF-β1 or CTGF where migration was increased approximately 3x and 4x that of control, respectively. This assay shows the potential for extracellular glucose to enhance the effects of TGF-β1 and CTGF-induced cellular migration in RSF cells.

Streptozotocin Diabetic Induction

Noting the effect elevated glucose had on stimulating cellular migration of rat joint cells in culture, we wanted to examine the role that increased circulating glucose plays in our animal model. Based on these data, we hypothesized the presence of high glucose would enhance the effects of TGF-β1, leading to a more severe and prolonged case of arthrofibrosis. To test this, animals were rendered diabetic by injection streptozotocin (STZ). The STZ-induced diabetic rat is one of the most commonly employed animal models used to study diabetes and its associated complications. STZ is a glucosamine-nitrosourea compound that is particularly toxic to beta cells, the insulin-producing cells of the pancreas. The diabetes that results is similar to type I insulin-dependent diabetes mellitus in humans, and animals exhibit behavioral and biochemical signs consistent with the onset of diabetes.

Male Wistar rats weighing approximately 175 g were fasted up to 6hrs prior to diabetic induction. Animals received two intra-peritoneal injections of freshly prepared STZ, at a dose of 45 mg/kg, 72 hours apart. Animals were supplied 10% sucrose water for 48 hours post injection and body weights and blood glucose levels were measured 72 hours after second STZ injection, followed by measurement at weekly intervals, to identify onset and continued presence of diabetic hyperglycemia. Diabetic animals were euthanized at 10, 30, 90 and 120 days after onset of diabetes, and joint tissues were harvested. As seen in Table 6-1, mean diabetic glucose was 480 mg/dL compared to 108 mg/dL in non-diabetic, normal animals. Blood glucose levels exceeding 250 mg/dL were considered diabetic.

Diabetes Induced Alterations in Gene Expression in Synovial Tissue

Diabetic and normal control rats were killed at days 10, 30, 90 and 120 and the joint tissues were harvested for examination. No phenotypic differences were observed by gross visual inspection or in H&E stained tissue sections among the diabetic animals compared to non-diabetic animals (data not shown). To determine the effect of hyperglycemia on normal tissue homeostasis in the joint at the molecular level, RNA was isolated from the capsular tissues of diabetic induced animals and age-matched non-diabetic control rats was analyzed by PCR-array for differential expression of genes associated with cellular adhesion, extracellular matrix synthesis and remodeling.

Numerous alterations were seen in gene expression patterns in the synovium of diabetic animals compared to non-diabetic animals particularly at the onset of diabetes, as shown in Table 6-2. Among the structural proteins, the majority of the collagens displayed decreased expression throughout the experiment; however, collagens 4, 6, 8 were increased at the later time points. Consistent with these data, kidney tissues from animal models of diabetes and humans show an upregulation of Collagen IV[58, 144]. Of the matricellular proteins, only Spock1 showed enhanced expression at each of the four time points examined.

Expression patterns reminiscent of that observed in the Ad.TGF-β1 fibrotic tissues in earlier chapters, were seen for several groups of genes, including expression TIMP-1 and -2, which were increased throughout the course of the experiment, along with proteases MMP 1a, 3, 7, 8, 10, and 11. Interestingly, ADAMTS-5 and -8 and MMP-3, -7, -10, and -12 all had increased expression levels at the onset of hyperglycemia and some were increased by the later time points. Many cell adhesion proteins, including

integrins α3 and β1, E- and L-selectins, N-cadherin, VCAM1 and vitronectin also displayed expression patterns similar to that seen in fibrotic tissues. Expression patterns of laminin γ1, α1 and fibronection were also similar.

Most of the extracellular matrix and adhesion genes examined, were either increased or decreased in diabetic joints compared to normal joints. Although no phenotypic differences were observed between non-diabetic and diabetic animals, many of the alterations in gene expression are somewhat similar to animals receiving overexpression of TGF-β1 in Chapter 5, albeit to a lesser extent. These results suggest that increased circulating levels of blood glucose lead to synovial expression patterns similar to that seen in fibrotic tissues. As these animals have altered levels of expression in many ECM and proteolytic genes, they could be more susceptible to development of fibrosis in the presence of an appropriate stimulus suggesting a possible explanation for the prevalence of IAC in diabetic patients.

Diabetic Joints Receiving Ad.TGF-β1 Resulted in an Overall Less Severe Fibrosis

After onset of diabetes, groups of diabetic and non-diabetic Wistar rats were intra-articularly injected with $5.0x10^7$ vp of Ad.TGF-β1 or Ad.GFP control in both knees. Animals were euthanized at 10, 30, 90 and 120 days post injection and joint tissues were harvested for analysis.

After vector injection, there was an increase in knee diameter, and the joints showed modest decrease in ROM. Gross appearance and overall knee diameter did not differ between diabetic and non-diabetic. Tissues were examined histologically using H&E staining to determine differences in fibrotic phenotype and severity. As shown in Figure 6-3, no observable differences could be seen in the histology between normal

and diabetic control joints. However, mild differences were observed between diabetic compared to non-diabetic animals receiving Ad.TGF-β1, for both groups. After 10 days, expansion of fibroblasts within the synovium replaced all adipose tissue, filling the entire joint space, and the fibrotic tissue began to fuse with articular cartilage. Interestingly, at these sites of fusion in non-diabetic animals, the cells began to lose their spindled morphology, instead appearing as rounded, chondrocyte-like cells. However, at these same junctions in diabetic animals, there was no transition into a chondrocytic phenotype and cells retained their fibroblastic morphology.

At thirty days, in both groups of animals, the normal microscopic anatomy of the joint was not recognizable and the resident joint and capsular structures were displaced. Large areas of neo-cartilaginous tissue were seen in non-diabetic animals, and the majority of the articular cartilage was replaced by metaplastic fibrocartilaginous tissue, confirmed by the deeply amphophilic appearance of the tissue on toluidine blue stain (not shown). The tissue of diabetic animals was considerably less cellular, with a greater concentration of collagenous material, and although cartilaginous formations were present in the 30 day animals, they were noticeably reduced.

At 90 days, the tissues in both groups of animals showed signs of resolving, and there was a reduction in overall cellularity compared to day 30 tissues. The diabetic tissue showed signs of increased chondrogenic formation, as seen in the rounded chondrocyte-like cells and toluidine blue staining. By day 120, both groups showed an overall reduction in cellularity, and the phenotype of tissues resembled that of more normal tissue, with the reappearance of adipose tissue along the outer edge of the joint space. Overall, the tissues were less aggressive and appeared to switch from a

proliferative phase to one of remodeling. While most of the cartilaginous developments were resolved in the non-diabetic animals, this process seem to lag in the diabetic joints as many of the cartilaginous masses remained within the joint.

Decreases in Gene Expression at Onset of Fibrosis were seen between Diabetic and Non-Diabetic Animals Receiving Ad.TGF-β1

Counter to our expectations in the diabetic animals, several genes showed a much lower level of induction following delivery of Ad.TGF-β1 (Table 6-3 and Table 6-4). The most notable changes were seen at day 10 in the structural proteins, Collagen I, II and VIII, and Hapln1, all of which showed decreased expression from -2.6 to -326-fold. The decreased expression in Collagen II and Hapln1 is consistent with the lack of cartilaginous formation seen histologically in diabetic compared to non-diabetic.

Compared to non-diabetic animals, several matricellular proteins displayed decreased expression at day 10 including osteopontin, periostin and thrombospondins 1 and 2. Osteopontin and periostin also had decreased expression levels at day 90 and 120 respectively. N-cadherins, integrin α_V, and Ncam 1 were all slightly decreased at day 10 in diabetic animals. For the most part, MMPs displayed decreased expression levels compared to non-diabetic animals. At day 10, MMPs 8, 9, and 11-16 were all decreased -2 to -35-fold. Many of these remained decreased throughout the experiment.

Discussion

The experiments performed in the present study were designed to identify the effects of diabetes on arthrofibrosis. Diabetes has been identified as a risk factor for the development of IAC, and diabetics with frozen shoulder typically have more severe and persistent disease. Diabetes was induced in immunocompetent male Wistar rats using

the drug STZ. Studies have shown the resulting experimental diabetes from STZ injections has many similarities to type I human diabetes, including hyperglycemia, glucosuria, hypoinsulinemia, hyperlipidemia and weight loss. Animals also exhibit many of the same complications seen in the human disease, such as retinopathy, alterations in angiogenesis, reduced bone formation and cardiovascular disease[158, 159].

Using our model of arthrofibrosis and an animal model of diabetes, we examined the differences in the synovium of diabetic animals histologically and by alterations in expression patterns, and compared them to non-diabetic animals. Histologically no differences were observed between diabetic and normal synovium. Expression profiles in diabetic joints displayed alterations in ECM and adhesion genes, with many genes showing an overall increase in expression, including the majority of metalloproteinases and many integrins over the course of the 120 day experiment. This is consistent with studies in other tissues, including the kidney, that show increases in MMP and TIMP levels and various collagens, particularly collagen type IV. The elevated levels of expression of metalloproteinases and inhibitors, collagens and integrins, in the joint synovium of diabetic animals compared to non-diabetic synovium, suggests a reason for diabetic joints to be prone to development of arthrofibrosis. The altered expression patterns that occur in the joint may pre-dispose diabetics to IAC and result in a longer lasting fibrotic response.

Our initial hypothesis, that diabetic animals would suffer a more severe and longer lasting fibrotic response in our animal model of arthrofibrosis, proved inaccurate. Histologic comparisons of both diabetic-induced and non-diabetic animals in our TGF-β1 model, showed a robust fibrotic induction in both sets of animals with a few minor

differences. Overall the fibrotic response appeared to be very similar in both sets of animals. Non-diabetic animals appeared to have an overall more robust chondrometaplasia that onset earlier and resolved later; however, diabetic animals had overall less chondrogenic formation throughout the experiment as evidenced by histology and expression patterns. Day 90 tissues are very similar in both groups of animals and histologic examination shows signs of remodeling with a decrease in overall cellularity. By day 120, tissues in both groups show resolution of much of the fibrotic adhesions and the appearance of the fat pad can be seen on the outer layers of the joint space. While much of the chondrogenic tissue appears to have resolved in the non-diabetic animals, it is less resolved in diabetic animals and can still be seen in the joint space.

Expression data from PCR-arrays show few differences between diabetic and non-diabetic animals receiving Ad.TGF-β1. Consistent with the histology data showing decreased in chondrogenesis in diabetic animals, at day 10 both collagen type II and cartilage link protein (Hapln1) had decreased expression levels compared to non-diabetic synovium. Decreases in Osteopontin and MMPs -8-16 were also observed at day 10. Only a handful of changes in the expression profile are seen at days 30-90; however, by day 120 several genes, including MMP-1, NCAM2, collagen type II and Hapln1 showed increased expression.

The decreased cartilage formation observed in diabetic animals with fibrosis is consistent with current literature showing delayed fracture healing and increases in cartilage resorption[47]. These studies suggest there is an increase in chondrocyte apoptosis and osteoclastogenesis, accelerating the loss of cartilage during fracture

repair[47]. Others have suggested that hyperglycemia leads to increased bone resorption and osteopnia[160] and decreased bone and cartilage formation[161]. A study by Kayal et al. comparing diabetic and non-diabetic rats showed that while initial cartilage formation was similar, over time there was a decrease in bone volume, callus size and cartilage content corresponding with an increase in osteoclasts and an increase in cartilage resorption[47]. They found that ADAMSTS 4 and 5, major aggrecanases that degrade cartilage, were higher in diabetic animals, but there were no differences between mRNA levels of MMP13[47]. Type I diabetes in humans is associated with a decrease in skeletal mass and a delay in fracture healing[162, 163]. Models of Type I diabetes have demonstrated reduced bone turnover and impaired fracture repair and STZ diabetic rats showed abnormal bone repair to be insulin dependent[164, 165]. Diminished expression of osteocalcin, collagen type I and transcription factors that regulate osteoblast differentiation were evident in an STZ model of diabetes[166].

Altogether, altered expression patterns seen in diabetic joint synovium, combined with complications due to hyperglycemia, may predispose diabetics to arthrofibrotic development. Histology and expression data suggest diabetic animals may not necessarily suffer from a more severe case of IAC; however, the altered signaling and expression profiles in these animals and their elevated circulating glucose may affect the resolution. These joints may take a longer amount of time to resolve than non-diabetic joints.

Table 6-1. Mean of blood glucose in diabetic and normal Wistar rats.

Metabolic Parameter	Normal	Diabetic
Blood Glucose (mg/dL)		
Day 10	102	480
Day 30	110	600
Day 90	110	360
Day 120	111	480
Body Weight (g)		
Day 10	290	365
Day 30	370	340
Day 90	385	540
Day 120	490	485

Table 6-2. Relative signal values of ECM and adhesion genes in the joints of Diabetic Wistar rats compared to non-diabetic normal Wistar joints

Gene	Day 10	Day 30	Day 90	Day 120
Structural Proteins				
Collagen, type 1, alpha 1	-2.8	*-3.4	-1.9	-2.6
Collagen, type 2, alpha 1	1.4	1.1	1.8	*-13.1
Collagen, type 3, alpha 1	*1.7	-1.5	-2.1	-2.4
Collagen, type 4, alpha 1	-1.5	1.1	1.9	1.9
Collagen, type 4. alpha 2	-2.3	1.5	*2.1	2.1
Collagen, type 4, alpha 3	-1.8	-1.2	3.7	*5.4
Collagen, type 5, alpha 1	-1.8	-1.7	-1.2	-1.2
Collagen, type 6, alpha 1	*-3.9	-1.3	2.1	2.0
Collagen, type 8, alpha 1	*-3.2	*-3.3	**2.1	2.2
Hapln 1	1.2	1.1	5.9	-1.2
Versican	-1.8	-1.3	2.1	1.8
Matricellular Proteins				
CCN2 (CTGF)	1.8	1.9	2.6	1.8
Osteopontin 1	1.3	2.4	2.4	-3.8
Periostin	-1.5	-1.6	-1.7	-2.0
Sparc	-1.1	-1.5	-1.1	-1.1
Spock 1	5.2	2.5	3.0	*6.1
Tenascin-C	-4.3	-1.5	4.1	3.1
Thrombospondin 1	1.6	2.1	1.5	2.1
Thrombospondin 2	-1.1	1.2	2.6	2.0
Cell Adhesion Proteins				
E-Cadherin	3.8	-1.2	-1.1	1.6
N-Cadherin	**-12.9	**-31.7	2.0	3.7
P-Cadherin	2.3	-1.0	-1.1	1.1
R-Cadherin	*2.9	1.4	1.8	1.7
Catenin, alpha 1	1.6	*2.0	2.1	2.5
Catenin, alpha 2	9.7	1.0	2.0	*3.7
Catenin, beta 1	-1.6	1.6	*2.7	*3.1
Contactin 1	1.6	-1.3	*4.2	*4.3
Icam-1	-1.5	1.7	**3.6	**3.9
Integrin, alpha 2	1.5	-1.2	1.1	1.5
Integrin, alpha 3	**-2.7	1.2	**6.4	**5.0
Integrin, alpha 4	1.6	1.9	1.6	1.5
Integrin, alpha 5	*-1.9	1.0	1.9	1.9
Integrin, alpha D	**4.1	1.7	2.0	3.7
Integrin, alpha E	**26.7	**10.0	1.6	1.5
Integrin, alpha L	1.8	**4.0	1.9	*2.2
Integrin, alpha M	2.0	*2.9	2.7	3.2
Integrin, alpha V	-1.4	1.9	1.5	1.7
Integrin, beta 1	**-61.5	**-13.7	**12.0	*24.4
Integrin, beta 2	1.7	*2.7	2.4	2.3
Integrin, beta 3	1.4	1.4	1.8	1.8
Integrin, beta 4	*-1.8	1.6	**3.0	**3.1
Ncam 1	2.2	1.2	1.1	-1.1
Ncam 2	3.2	1.0	2.0	3.7

Table 6-2. Continued

Gene	Day 10	Day 30	Day 90	Day 120
Pecam	-1.3	2.1	*3.9	*5.1
E-Selectin	**-13.3	**-6.8	*5.2	*15.5
L-Selectin	*-7.9	**-17.4	2.0	*4.4
P-Selectin	-1.3	1.4	1.4	1.7
Vcam 1	-4.5	1.2	**4.7	**5.6
Vitronectin	*-6.4	-1.8	*6.4	**9.6
Extracellular Matrix Proteins				
Fibronectin 1	**-21.8	*-2.5	**9.2	*11.7
Laminin alpha 1	*17.7	2.9	2.0	3.7
Laminin alpha 2	-2.9	1.3	-1.0	1.1
Laminin alpha 3	1.6	2.0	1.9	1.9
Laminin beta 2	*5.8	3.0	1.5	1.4
Laminin beta 3	-1.2	2.7	1.9	**10.2
Laminin gamma 1	14.5	22.0	2.3	*4.2
Tgfbi	1.3	2.0	2.0	1.9
Metaolloproteinases and Inhibitors				
Adamts 1	7.0	7.6	1.5	*2.1
Adamts 2 (RGD1565950)	**-5.8	*-3.1	*4.0	*4.0
Adamts 5	-1.2	1.5	**9.5	**20.8
Adamts 8	*-4.8	**-18.7	1.7	3.1
Mmp 1a	16.1	1.3	2.0	3.7
Mmp 2	1.3	1.1	2.6	2.1
Mmp 3	2.0	3.1	2.1	2.7
Mmp 7	*20.8	3.3	1.7	3.2
Mmp 8	*12.2	1.5	2.2	3.8
Mmp 9	1.6	-3.4	3.7	-1.2
Mmp 10	21.0	1.2	1.7	3.0
Mmp 11	1.9	1.6	*3.0	2.6
Mmp 12	*22.9	11.7	-1.6	-3.5
Mmp 13	-3.3	1.4	21.9	4.7
Mmp 14	*-3.8	-1.1	4.1	4.3
Mmp 15	**-10.9	*-2.9	**8.3	*9.9
Mmp 16	-1.3	-2.2	1.3	1.1
Timp 1	**13.5	**8.1	2.4	2.9
Timp 2	**10.1	**35.1	*5.7	*8.0
Timp 3	1.2	1.9	2.0	*2.6
Elastic Fiber Proteins				
Emilin 1	1.5	6.7	*5.6	*7.0
Fibulin 1	1.0	1.1	*3.6	*3.0
Extracellular matrix protein 1	3.1	2.1	3.0	2.7
Other				
Synaptotagmin I	3.4	1.4	2.1	3.7
CD44 Antigen	*-3.3	-2.7	1.8	*3.1
Sarcogycan	1.4	1.7	2.8	*3.1
NTPDase-1 (CD39)	-1.1	*2.0	*3.3	*3.5

Values with an asterisk represent $p<0.05$. Values with two asterisks represent $p<0.01$. n=3 for each time point.

Table 6-3. Relative signal values of ECM and adhesion genes in the joints of Diabetic Wistar rats receiving Ad.TGF-β1 compared to untreated diabetic Wistar rats

Gene	Day 10	Day 30	Day 90	Day 120
Structural Proteins				
Collagen, type 1, alpha 1	**5.1	**9.7	**2.7	2.9
Collagen, type 2, alpha 1	-1.3	*57.7	-1.1	**171.3
Collagen, type 3, alpha 1	1.4	**3.4	1.4	*1.8
Collagen, type 4, alpha 1	-1.2	*-1.7	**-3.9	-*2.9
Collagen, type 4. alpha 2	1.8	-1.6	**-5.1	**-3.1
Collagen, type 4, alpha 3	-2.3	*-2.5	-1.3	1.0
Collagen, type 5, alpha 1	**2.5	**2.6	-1.5	1.2
Collagen, type 6, alpha 1	*5.4	6.9	-1.7	-1.0
Collagen, type 8, alpha 1	**12.7	**9.6	1.0	1.6
Hapln 1	1.5	**30.3	1.8	**25.5
Versican	*4.6	**4.3	-1.0	*2.8
Matricellular Proteins				
CCN2 (CTGF)	-1.1	-1.1	1.4	2.5
Osteopontin 1	*8.9	*36.9	9.2	*153.6
Periostin	**2.6	*2.6	-1.6	-1.5
Sparc	1.1	2.0	*-1.9	-1.4
Spock 1	-3.5	1.3	4.6	3.0
Tenascin-C	*14.0	**4.9	-1.7	1.6
Thrombospondin 1	**3.0	*3.7	1.4	*2.3
Thrombospondin 2	**4.6	**4.8	1.0	*2.1
Cell Adhesion Proteins				
E-Cadherin	1.0	**4.1	3.2	2.3
N-Cadherin	*-2.6	*3.6	1.9	-1.3
P-Cadherin	-5.3	1.1	2.3	3.5
R-Cadherin	**-17.1	-2.3	-1.2	1.3
Catenin, alpha 1	-2.0	**-2.2	**-3.5	*-2.1
Catenin, alpha 2	*-11.2	**6.5	**15.3	5.7
Catenin, beta 1	1.7	-1.1	**-3.4	-1.9
Contactin 1	**-3.4	-1.1	-3.4	*-1.9
Icam-1	1.9	-1.3	-3.4	*-1.9
Integrin, alpha 2	-1.8	1.0	-1.0	2.1
Integrin, alpha 3	-1.2	**-3.4	*-6.1	-1.9
Integrin, alpha 4	1.4	1.0	*-2.9	-1.4
Integrin, alpha 5	1.9	1.1	*-2.7	-1.3
Integrin, alpha D	**-6.2	*-1.9	**-2.9	-2.8
Integrin, alpha E	1.8	**6.7	2.7	4.3
Integrin, alpha L	**3.0	-1.0	*-3.7	**-2.4
Integrin, alpha M	1.1	-1.1	-3.0	-2.2
Integrin, alpha V	-1.3	*-2.1	*-2.6	*-1.6
Integrin, beta 1	7.1	**3.1	*2.8	-1.3
Integrin, beta 2	-1.3	-1.6	*-3.5	-1.8
Integrin, beta 3	-1.2	1.0	**-3.6	-1.4
Integrin, beta 4	1.4	-1.9	**-4.1	-1.5

Table 6-3. Continued

Gene	Day 10	Day 30	Day 90	Day 120
Ncam 1	**2.9	**7.0	3.2	**4.1
Ncam 2	**-7.1	1.2	*4.3	2.3
Pecam	1.1	*-1.9	*-1.7	-1.6
E-Selectin	7.4	*3.2	3.0	1.4
L-Selectin	1.5	1.4	1.1	-2.2
P-Selectin	3.4	1.6	-2.6	-1.6
Vcam 1	2.9	-1.3	**-2.9	-3.4
Vitronectin	-1.2	-3.3	-1.3	-2.2
Extracellular Matrix Proteins				
Fibronectin 1	5.9	1.2	-1.8	-1.1
Laminin alpha 1	*-8.6	2.9	2.6	2.1
Laminin alpha 2	5.3	*-1.6	-1.0	1.3
Laminin alpha 3	*-3.2	*-2.7	-2.2	-1.1
Laminin beta 2	**-7.9	**-2.9	*-1.9	1.2
Laminin beta 3	**-13.6	**-25.8	1.2	*-5.8
Laminin gamma 1	1.3	1.0	1.1	-2.8
Tgfbi	**2.0	*1.6	*-2.5	-1.4
Metaolloproteinases and Inhibitors				
Adamts 1	1.8	**2.1	**-2.7	-1.4
Adamts 2 (RGD1565950)	*5.1	**3.9	1.3	1.7
Adamts 5	-1.4	-1.5	-1.4	-2.1
Adamts 8	2.3	**21.7	5.4	3.9
Mmp 1a	*-17.5	2.6	*8.2	4.2
Mmp 2	-1.4	-1.2	*-3.2	-1.4
Mmp 3	1.6	**5.3	*1.8	1.3
Mmp 7	*-12.4	-1.1	1.8	3.2
Mmp 8	-3.1	5.1	5.1	3.0
Mmp 9	1.7	*52.5	3.8	**14.3
Mmp 10	-18.3	*6.4	**14.5	5.1
Mmp 11	1.5	*2.9	-1.2	*2.4
Mmp 12	2.2	20.5	**5.7	**23.2
Mmp 13	**38.1	*40.4	2.1	**6.5
Mmp 14	*7.4	**3.0	-1.3	-1.1
Mmp 15	1.5	-1.6	*-5.2	*-2.1
Mmp 16	*2.0	**6.6	1.5	**3.8
Timp 1	1.4	**3.4	1.5	1.4
Timp 2	*3.0	1.1	-1.7	-1.6
Timp 3	-2.9	**-3.6	**-3.1	*-1.9
Elastic Fiber Proteins				
Emilin 1	**19.5	**4.6	2.4	1.9
Fibulin 1	19.5	4.6	2.4	1.9
Extracellular matrix protein 1	-2.4	-1.2	1.0	1.5

Values with an asterisk represent $p<0.05$. Values with two asterisks represent $p<0.01$. n=3 for each time point.

Table 6-4. Relative signal values of ECM and adhesion genes in the joints of Diabetic Wistar rats receiving Ad.TGF-β1 compared to non-diabetic Wistar rats receiving Ad.TGF-β1

Gene	Day 10	Day 30	Day 90	Day 120
Structural Proteins				
Collagen, type 1, alpha 1	*-2.6	-1.2	1.3	-1.9
Collagen, type 2, alpha 1	**-326.5	1.3	-14.2	3.2
Collagen, type 3, alpha 1	-1.1	1.2	1.8	-1.3
Collagen, type 4, alpha 1	-1.3	1.3	1.4	1.1
Collagen, type 4. alpha 2	-1.4	1.3	1.4	1.2
Collagen, type 4, alpha 3	-2.0	-1.2	-1.0	1.5
Collagen, type 5, alpha 1	**-1.7	-1.3	1.1	-1.2
Collagen, type 6, alpha 1	-1.7	3.5	1.3	-1.0
Collagen, type 8, alpha 1	*-3.6	-1.7	-1.2	1.0
Hapln 1	**-57.7	1.5	-3.0	*2.6
Versican	-1.4	-1.8	-1.3	1.3
Matricellular Proteins				
CCN2 (CTGF)	-1.3	-1.2	1.7	*1.7
Osteopontin 1	*-9.7	1.8	-4.7	1.9
Periostin	**-3.0	-1.6	1.3	*-3.6
Sparc	**-1.8	-1.2	1.2	-1.3
Spock 1	1.1	-1.9	1.1	1.6
Tenascin-C	-1.5	*1.7	-1.0	1.3
Thrombospondin 1	*-2.6	-1.5	-1.9	1.4
Thrombospondin 2	**-2.4	-1.3	-1.1	-1.0
Cell Adhesion Proteins				
E-Cadherin	-1.1	-1.7	-1.2	2.1
N-Cadherin	**-10.5	-1.3	-1.0	1.3
P-Cadherin	-4.1	-2.7	1.2	1.6
R-Cadherin	3.96	-2.4	1.2	1.6
Catenin, alpha 1	-1.1	-1.2	1.2	1.1
Catenin, alpha 2	2.2	-3.0	1.5	4.5
Catenin, beta 1	*-1.9	-1.2	-1.1	-1.0
Contactin 1	1.4	-1.3	1.6	-1.0
Icam-1	1.4	1.2	-1.1	-1.2
Integrin, alpha 2	-1.4	-1.3	-1.1	1.8
Integrin, alpha 3	1.2	1.2	-1.2	1.3
Integrin, alpha 4	1.1	1.1	-1.3	-1.2
Integrin, alpha 5	-1.4	1.0	1.0	-1.0
Integrin, alpha D	1.1	-2.4	1.1	-1.3
Integrin, alpha E	1.7	1.1	1.6	-1.0
Integrin, alpha L	1.7	1.2	1.1	-1.1
Integrin, alpha M	1.3	1.5	1.0	-1.4
Integrin, alpha V	*-2.2	-1.1	1.2	1.0
Integrin, beta 1	-2.5	1.1	1.2	-1.3
Integrin, beta 2	1.4	1.4	1.2	1.1
Integrin, beta 3	-2.8	1.3	-1.2	1.1
Integrin, beta 4	1.0	1.1	-1.0	1.3
Ncam 1	**-2.8	-1.4	1.4	-1.7

Table 6-4. Continued

	Gene	Day 10	Day 30	Day 90	Day 120
	Ncam 2	1.5	-3.8	1.8	4.0
	Pecam	-1.3	-1.3	1.1	-1.3
	E-Selectin	-1.3	-1.4	1.4	-1.7
	L-Selectin	1.2	-3.8	1.8	4.0
	P-Selectin	1.8	-1.3	1.1	*-1.3
	Vcam 1	1.2	1.3	1.1	-1.2
	Vitronectin	-1.2	1.1	1.2	1.3
Extracellular Matrix Proteins					
	Fibronectin 1	-1.6	1.7	1.4	*2.0
	Laminin alpha 1	-1.1	-2.1	-1.3	1.5
	Laminin alpha 2	1.6	-1.7	1.5	-1.2
	Laminin alpha 3	-1.4	-1.3	1.1	1.8
	Laminin beta 2	1.5	-1.3	1.6	1.5
	Laminin beta 3	-1.5	-1.4	1.8	-1.1
	Laminin gamma 1	-8.4	1.2	1.3	-1.7
	Tgfbi	**-2.3	-1.3	1.4	-1.0
Metaolloproteinases and Inhibitors					
	Adamts 1	1.2	1.2	-1.4	-1.3
	Adamts 2 (RGD1565950)	-1.9	-1.3	1.5	-1.0
	Adamts 5	1.6	1.3	1.3	1.3
	Adamts 8	1.2	3.0	-1.1	-1.0
	Mmp 1a	1.9	-6.1	1.4	5.0
	Mmp 2	-1.3	-1.4	1.6	-1.4
	Mmp 3	1.3	*-2.4	1.1	-1.5
	Mmp 7	3.4	*-3.3	1.0	-2.3
	Mmp 8	**-34.9	*-3.2	-2.4	-1.1
	Mmp 9	**-24.4	1.3	-1.1	-1.6
	Mmp 10	-1.4	-2.7	1.4	1.5
	Mmp 11	*-3.4	-1.2	1.4	1.4
	Mmp 12	*-9.0	1.5	*-2.4	*-9.4
	Mmp 13	*-9.5	1.1	-2.3	*-5.0
	Mmp 14	*-3.4	-1.1	1.2	-1.5
	Mmp 15	-2.4	1.1	-1.2	1.4
	Mmp 16	**-2.7	-1.5	1.0	1.3
	Timp 1	-1.3	*-1.8	1.4	-1.0
	Timp 2	*-2.5	1.1	1.4	1.2
	Timp 3	-1.1	1.2	1.3	1.8
Elastic Fiber Proteins					
	Emilin 1	-4.1	-1.1	1.8	-1.1
	Fibulin 1	-1.3	-1.6	1.2	-1.3
	Extracellular matrix protein 1	1.0	1.4	2.0	1.3
Other					
	Synaptotagmin I	1.5	-2.7	-1.0	4.2
	CD44 Antigen	2.0	-1.0	1.0	1.1
	Sarcogycan	-1.2	-1.3	1.4	1.2
	NTPDase-1 (CD39)	-1.3	*2.8	1.1	-1.1

Values with an asterisk represent $p<0.05$. Values with two asterisks represent $p<0.01$. n=3 for each time point.

Table 6-5. Arbitrary scale measuring severity of fibrosis by a blinded observer. Scale represents 0 (Normal)-4 (severe fibrosis).

	Ad.TGF-β1 Treated	Scale (0-4)
Control	Non-Diabetic	0.0
	Diabetic	0.0
Day 10	Non-Diabetic	2.5
	Diabetic	2.25
Day 30	Non-Diabetic	4.0
	Diabetic	3.0
Day 90	Non-Diabetic	2.75
	Diabetic	2.75
Day 120	Non-Diabetic	2.25
	Diabetic	2.25

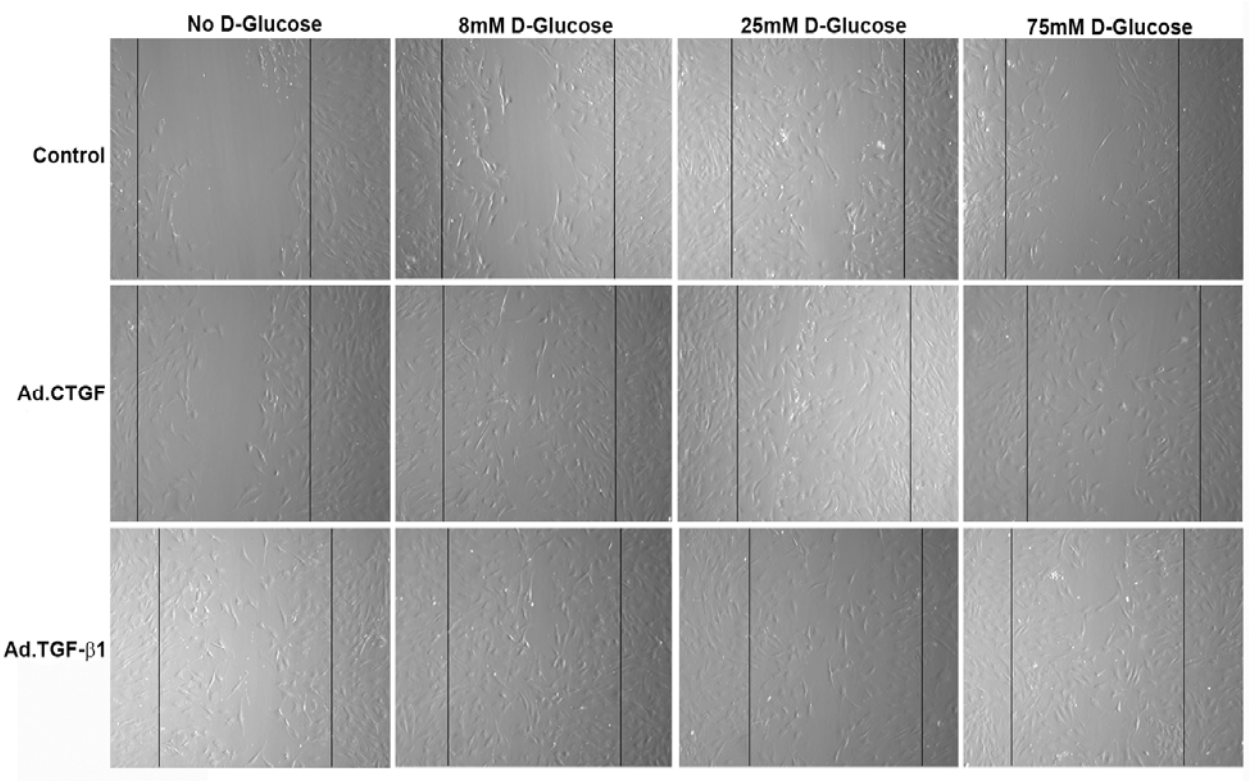

Figure 6-1. Glucose stimulates rat synovial fibroblast migration. Migration into the mock wound space is seen in the presence of Ad.CTGF and Ad.TGF-β1 alone. D-glucose stimulates migration into the wound space on its own, with 25mM having the greatest effect.

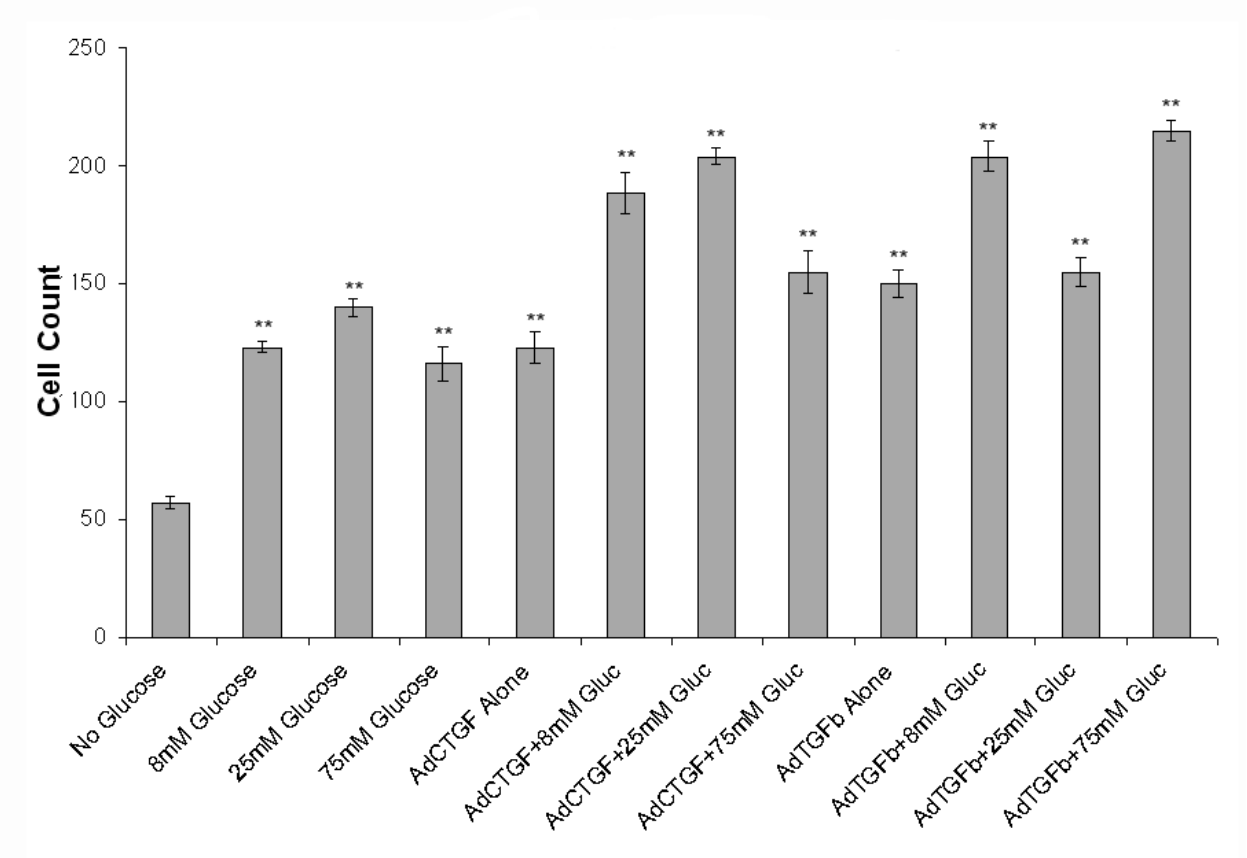

Figure 6-2. Glucose stimulates rat synovial fibroblast migration. Migration into the mock wound space is enhanced in the presence of Ad.CTGF and Ad.TGF-β1 alone. D-glucose stimulates migration into the wound space on its own, with 25mM having the greatest effect. Values are mean ± SEM. (One-way ANOVA, ** $P < 0.01$).

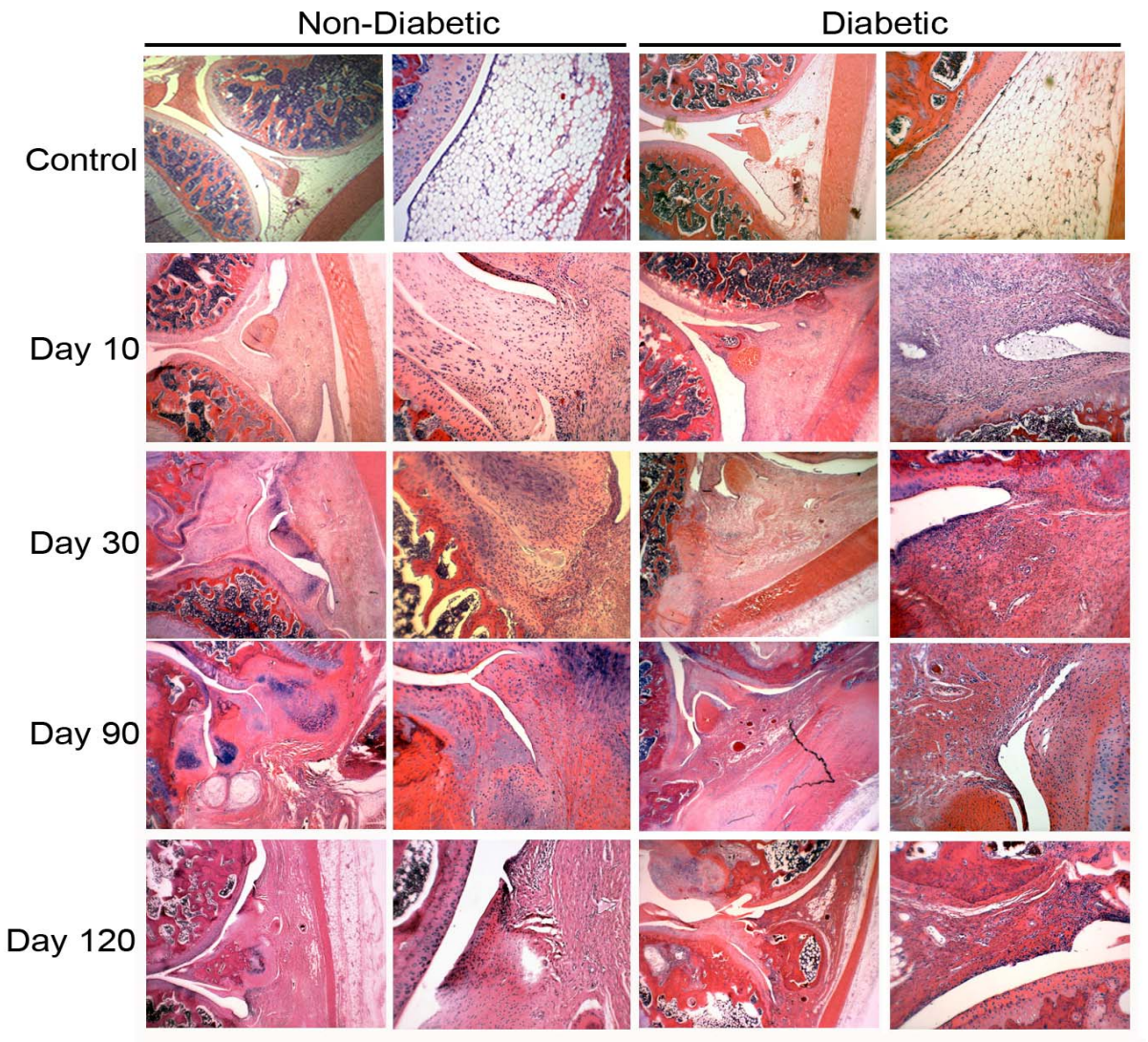

Figure 6-3. Capsular fibrosis induced by Ad.TGF-β1 in diabetic animals. Knees of diabetic and non-diabetic Wistar rats receiving Ad.TGF-β1 were harvested at various time points, decalcified and processed for histology. Sections were stained with H&E. At 10 days post injection, an expansion of fibroblastic cells from the synovial lining generated the bulk of the fibrotic mass, occluding the adipose layer in both groups and the formation of chondrocytic cells can be seen within the fibrotic tissue in non-diabetic animals. By day 30, the majority of fibroblastic cells had differentiated into chondrocytes in non-diabetic animals. Day 90 tissues are similar in both sets of animals, showing signs of resolving. Both show signs of chondrogenic formation. At day 120, both groups have resolved and display an overall decrease in cellularity and visualization of the fatpad; however, diabetic tissues appear to be less resolved and much of the chondrogenic tissue remains. Images in left two columns are at a magnification of 2.5x, and images in the right columns are at a magnification of 20x.

CHAPTER 7
ANTISENSE-OLIGONUCLEOTIDES LESSEN SEVERITY OF JOINT FIBROSIS WHEN DELIEVERED AT ONSET OF DISEASE

Introduction

Anti-fibrotic strategies have increased importance and relevance in many tissues throughout the body, including the joint. Arthrofibrosis, in particular IAC, is a complex disease of unknown origin that has not been fully characterized. Although it is known to be a fibrotic condition in the synovium of the joint, the mechanisms of onset are not well defined. Treatment options are limited and range from physical therapy to massive surgical release. Given the prevalence of IAC, identification of an effective fibrotic modulator would be beneficial in treatment of a significant portion of the population.

There is widespread evidence that enhanced synthesis of TGF-β1 leads to scarring and fibrosis in a variety of tissues throughout the body. In earlier chapters (Chapters 4-6) we demonstrated the potency of overexpression TGF-β1 on the tissues of the joint and its ability to induce an arthrofibrotic event in rodents. TGF-β1 has been observed in a variety of fibrotic disorders, thus, TGF-β1 has been the target of many therapeutic approaches designed to treat fibrosis. However, due to its pleiotropic nature and many beneficial effects on cells, systemic treatments could have deleterious effects. Along with TGF-β1, CTGF has also been observed in a variety of fibrotic disorders. Although not found to be highly expressed at the mRNA level in our model of arthrofibrosis (see Tables 4-1 and 5-1), it has been shown to modulate and enhance many of the effects of TGF-β1, and could prove to be a useful and specific target for modulating fibrosis seen in the joint.

Antisense oligonucleotides (ASO) could be a promising therapeutic strategy. ASOs have been used with some success in other diseases, including cancer and viral infections[167, 168]. In most renal cell types, treatment with a TGF-β1 antagonist ASO[59], reduces the rise in ECM expression due to high glucose. ASOs are short, single strands of DNA or RNA that are complementary to a particular sequence and upon specific hybridization with mRNA, inhibit gene expression. While ASOs were first described in 1978, modifications to their structure over the years have led to improvements in their pharmacokinetics and pharmacodynamics[169].

ASOs recognize and hybridize to target mRNA by Watson-Crick base pairing and trigger RNase H–mediated RNA destruction. First generation ASOs lack the nuclease resistance and tissue stability necessary for therapy. Second generation ASOs have been reengineered, improving potency, nuclease resistance, and tissue half-life. Second generation oligonucleotides used in this study have been modified to contain 2'-O-Methoxy ethyl (MOE) and phosphorothioate, which has been shown to enhance stability *in vivo*. Naturally occurring oligonucleotides are highly susceptible to rapid degradation by cellular nucleases. When the phoshodiester bond is modified by replacing one of the non-bridging oxygens with sulfur, there is a greater resistance to nuclease degradation. Because the 2'-MOE modification does not allow recruitment of RNase H when bound to mRNA, only the terminal residues of the ASO sequence are 2'MOE-modified, leaving the central region with only the phosphorothioate backbone modification, thereby coupling the resistance to degradation in tissues with improved potency while supporting activation of RNase H[170].

With the use our arthrofibrotic animal model, based on the overexpression of TGF-β1 in the joint space (Chapters 4-6), we evaluated the function of ASOs specific to TGF-β1 and CTGF in their ability to limit joint fibrotic induction.

Results

TGF-β1 Knockdown by Specific ELISA

As shown in Chapters 4-7, overexpression of Ad.TGF-β1 in the joints of rodents, leads to a pathology similar to that seen in human arthrofibrosis. Consequently, we hypothesized that treatment with ASOs specific to TGF-β1 and CTGF would reduce the severity of fibrosis seen in our animal model of IAC. Prior to undertaking *in vivo* experimentation we tested the effectiveness of TGF-β1 ASO *in vitro*. Twelve-well plates of rat synovial fibroblasts (RSFs) were grown to confluence prior to treatment with ASO. TGF-β1 ASO at 100nM (0.825μg/ml) and 300nM (2.47μg/ml) was transfected into the appropriate wells using lipofectamine transfection reagent. Twenty-four hours post transfection cells were infected with Ad.TGF-β1 at a dose of 1.3×10^7 viral particles (vp). The culture medium was replaced with serum free medium 24 hours after transduction, and harvested forty-eight hours post-transduction for specific ELISA. As seen in Figure 7-1, knockdown of TGF-β1 expression was observed after treatment with both the 100nM and 300nM concentrations of TGF-β1 ASO compared to Ad.TGF-β1 alone.

Intra-articular Injection of Reporter ASO is Retained in the Joint Space

After confirming the ability of the ASO to knockdown of TGF-β1 expression in cultured cells, we worked to determine the functionality of ASO delivery intra-articularly in the Ad.TGF-β1 fibrosis model *in vivo*. We first examined their distribution within the

joint following intra-articular injection of a reporter ASO generously provided by Dr. Gregory Schultz and Dr. Nick Dean. Approximately 10μg/μl of reporter ASO was diluted in 50μl of PBS and injected into the joint space of adult male Wistar rats. 10 days post injection, the animals were killed and joint tissues were harvested and processed for further immunohistochemical analysis using antibodies specific to the reporter ASO. Antibody staining demonstrated the reporter ASO was retained within the joint space and its detection was seen throughout the fibrous synovium and fat pad and radiated outward from the joint space (Figure 7-2). IHC staining was not observed outside the joint space.

ASOs were Effective at Inhibiting Arthrofibrosis in Animal Model

Knowing the relative location of the ASOs within the joint and their ability to knockdown TGF-β1 expression in rat synovial fibroblasts in culture, we wanted to determine their ability to inhibit fibrosis within our animal model. For this, animals were divided into 6 categories: (1) normal controls receiving PBS, (2) animals receiving 5.0 x 10^7 vp of Ad.TGF-β1 alone, (3) animals receiving 5.0 x 10^7 vp of Ad.TGF-β1 and 10μg/μl TGF-β1 ASO, (4) animals receiving 5.0 x 10^7 vp of Ad.TGF-β1 and 10μg/μl CTGF ASO, (5) animals receiving 5.0 x 10^7 vp of Ad.TGF-β1, 10μg/μl TGF-β1 ASO and 10μg/μl CTGF ASO, (6) and finally those animals receiving 5.0 x 10^7 vp of Ad.TGF-β1 and 10μg/μl scramble ASO.

At 5 days post injection, animals were killed and tissues were harvested and processed for histology. H&E staining differences in fibrotic severity between joints treated with ASOs and untreated joints. Normal control animals show a thin layer of synovial cells, overlying layer of adipose. In animals treated with Ad.TGF-β1 alone, the

joint space was filled with a thick, hypercellular tissue populated primarily by elongated fibroblastic cells expanding into the adipose layer (Figure 7-3). Upon co-injection with the TGF-β1 ASO, and slightly less so with CTGF ASO, a reduction in the cellularity and overall fibrotic development was seen, resulting in less displacement of adipose tissue. When the oligos were co-injected together (Figure 7-3), results were similar to TGF-β1 ASO alone. There was a reduction in the overall fibrotic induction, such that the fibrotic expansion was minor and did not over-ride the joint space. As expected, no differences were observed between the scramble ASO and Ad.TGF-β1 alone (Figure 7-3).

Discussion

The second generation ASOs selected for these studies appeared to effectively target TGF-β1 expression *in vitro* and reduce TGF-β1 mediated fibrosis *in vivo*. Knockdown activity disappeared when a scrambled ASO was tested, indicating this inhibition occurs through a sequence specific hybridization-dependent mechanism. Using the reporter oligonucleotide we showed that these molecules permeate the joint tissues and were largely contained within and along the joint space. Interestingly, the oligos were detected up to 10 days post injection. ASOs specific for TGF-β1 and CTGF resulted in a decrease in development of fibrosis in our arthrofibrotic animal model.

An antisense-based approach to arthrofibrosis, in particular IAC, is an intriguing alternative to current therapies, which are based on physical manipulation and surgical release of adhesions. Targeting mRNA using ASOs is an appealing approach to study cell signaling, since an inhibitor can be designed for any gene for which a partial sequence in available. Cell and tissue type must be optimized to ensure cellular uptake of ASO, as this can vary. Prior to being considered a therapeutic agent, important

considerations regarding relevance of animal models for human disease must be considered, as well as characterization of potency, tissue distribution, administration and dosing, and clearance and metabolism along with various other parameters. Clinical experiences with second generation oligonucleotides, such as the ones used here, have thus far revealed little dose-limiting toxicity[171]. Additionally, ASOs can be repeatedly administered, as neutralizing antibody responses are not mounted against ASOs. Clinical trials have been tested in patients with Crohn's disease using an ASO targeting ICAM-1, which proved to be well tolerated and capable of producing long-lasting disease remissions[168].

However promising these initial experiments in our animal model of arthrofibrosis appear, many more rigorous tests need to be performed to fully examine the success of ASOs in our model. Preliminary data shown here examines inhibition of *fibrotic induction* by simultaneous injection of each ASO and Ad.TGF-β1 into the knee joints of Wistar rats. TGF-β1 blockade was effective at ameliorating the induction of acute fibrosis, as was CTGF blockade although to a lesser extent. However, since patients are typically not seen by physicians until they are experiencing pain and stiffness (Stages 2 or 3 of IAC), adhesions and scar tissue have already formed within their joint capsule. Therefore it would be prudent to check the effectiveness of ASOs at varying levels of fibrotic severity, including progression and resolution. For example, it would be necessary validate ASOs in our animal model at onset of fibrosis (similar to Stage 1 in humans), at a frozen state (similar to Stage 3 and 4) and even determine if it enhances the rate of resolution of joint fibrosis. While simultaneous injection of either TGF-β1 or CTGF ASO with our fibrotic stimulator (Ad.TGF-β1) appears to lessen the severity of

fibrosis, more replicates and further experiments need to be performed to tighten this preliminary data and determine fibrotic knockdown at each stage of disease.

Table 7-1. Arbitrary scale in which a blinded observer measured severity of fibrosis. Scale represents 0 (normal)-4 (severe fibrosis).

Substance Intra-articularly Injected	Scale (0-4)
Ad.TGF-β1 Alone	3.5
Ad.TGF-β1 with TGF-β1 ASO	1.5
Ad.TGF-β1 with CTGF ASO	2.5
Ad.TGF-β1 with both TGF-β1 ASO and CTGF ASO	1.5
Ad.TGF-β1 with scramble ASO	3.0
Normal Control	0.0

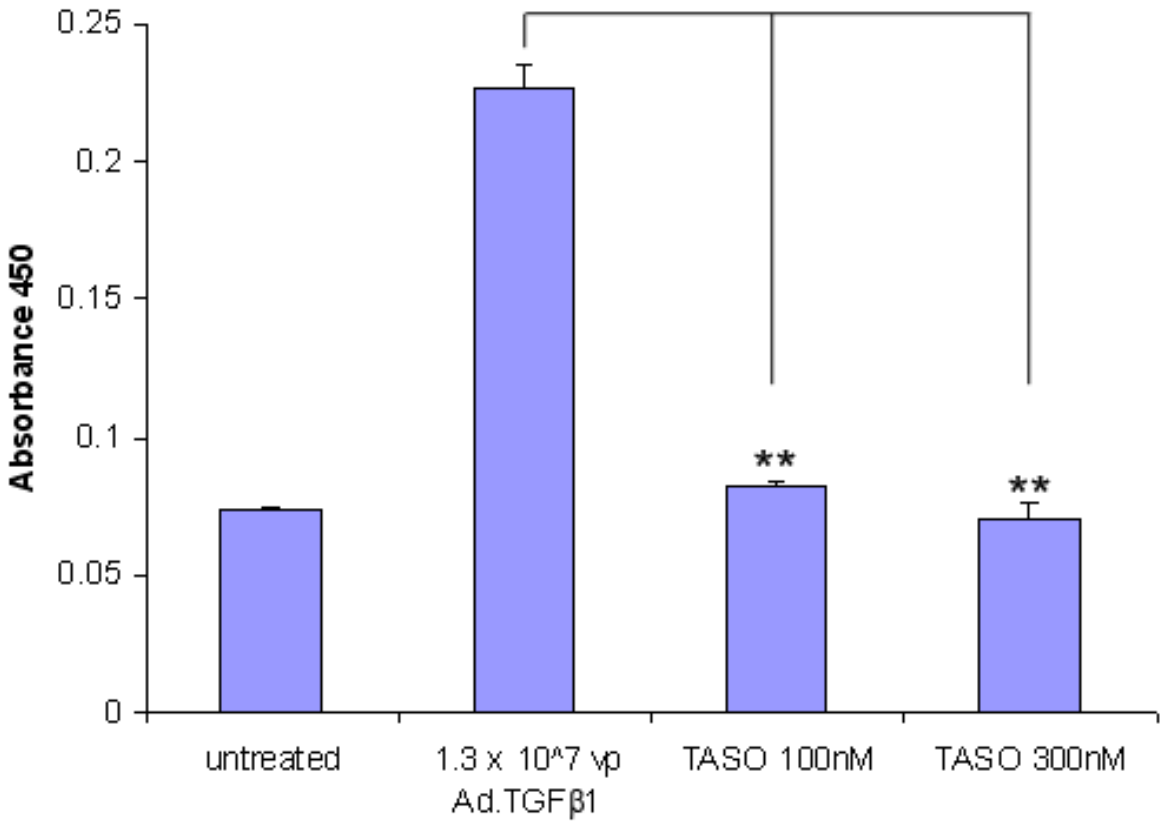

Figure 7-1. Transgene expression following transduction of rat synovial fibroblasts with Ad.TGF-β1 and/or transfection with an antisense oligonucleotide specific for TGF-β1. Following isolation of fibroblasts from rat synovium, the cells were grown in monolayer in 12-well plates and transfected with either 100nM or 300nM TGF-β1 ASO using Lipofectamine. At 24hrs post transfection, cells were transduced with 1.3 x 10^7 vp of Ad.TGF-β1. The next day, medium was replaced by 0.5 ml of serum-free medium. At 48hrs post transduction, the conditioned medium was harvested and TGF-β1 content measured by specific ELISA. Results are expressed as the mean of 3 replicates. Error bars represent ± S.E.M. (One-way ANOVA, ** $P < 0.01$).

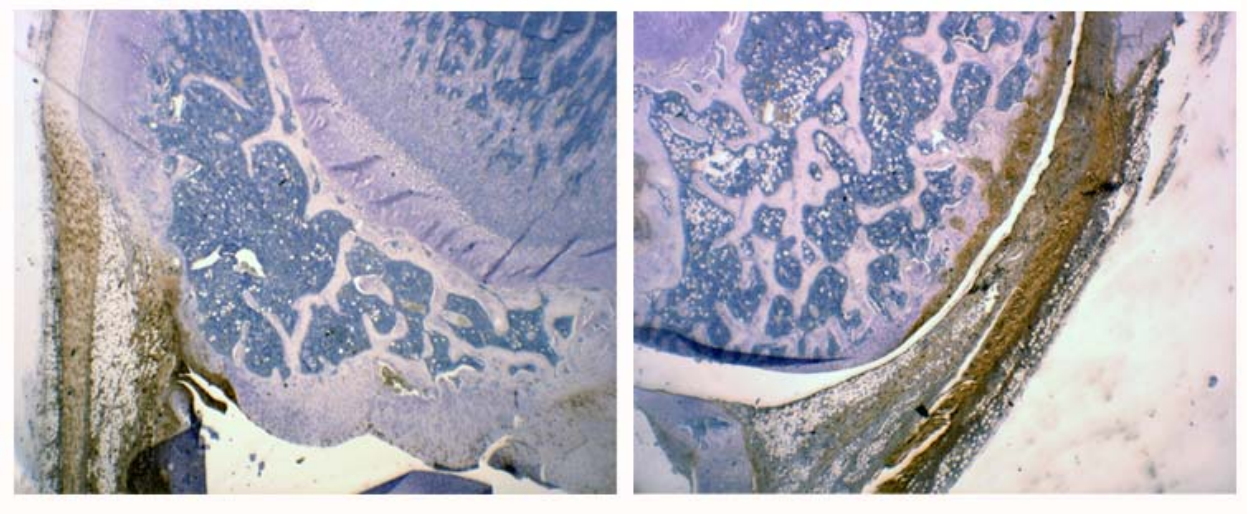

Figure 7-2. Immunohistochemical staining of reporter anti-sense oligonucleotide. Knee joints of Wistar rats intra-articularly injected with 10μg/μl of reporter ASO were harvested at day 10, paraffin embedded, sectioned and immunologically stained for the presence of reporter ASO.

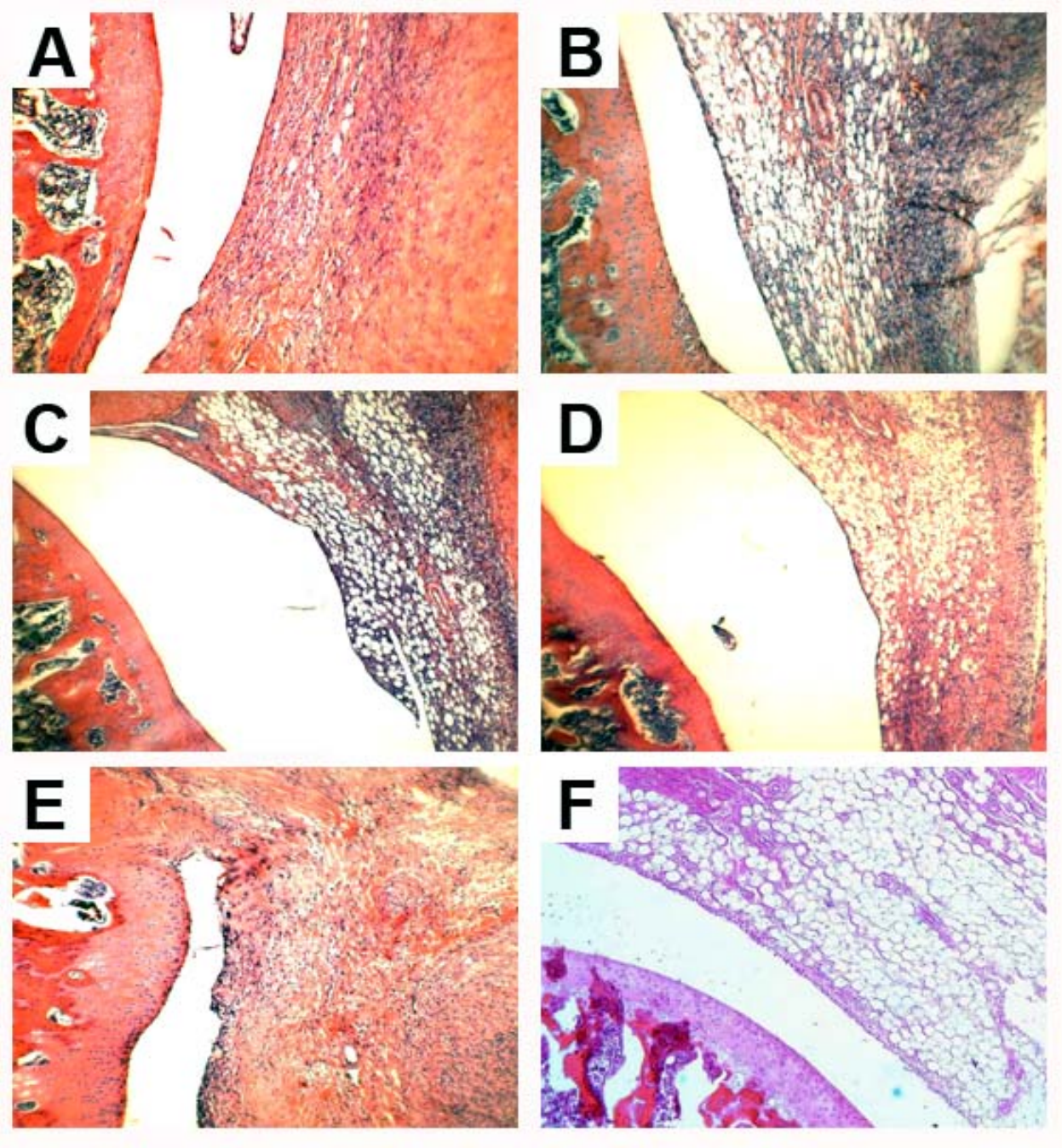

Figure 7-3. Capsular fibrosis induced by Ad.TGF-β1 in Wistar rats is inhibited by co-intra-articular injection of ASOs. Knees of Wistar rats receiving Ad.TGF-β1 alone (a), Ad.TGF-β1 and TGF-β1 ASO (b), Ad.TGF-β1 and CTGF ASO (c), Ad.TGF-β1, CTGF ASO and TGF-β1 ASO (d), Ad.TGF-β1 and scramble ASO (e), or PBS control (f) were harvested 5 days post injection, decalcified and processed for histology. Sections were stained with H&E. Images are at a magnification of 20x.

CHAPTER 8
SUMMARY AND FUTURE DIRECTIONS

Arthrofibrosis is a condition that arises from the development of excess fibrous tissue intra-articularly, which leads to chronic joint pain and loss of range of motion. The prevalence of arthrofibrosis has been sited to occur in up to 35% of the population, and has been described in joints throughout the body[83, 84, 85, 86]. In an effort to establish an animal model of IAC, an arthrofibrotic condition affecting ~3% of the population, and develop an understanding of the cellular and molecular events contributing to arthrofibrosis, we used an adenovirus to deliver and over-express TGF-β1 cDNA (Ad.TGF-β1) in the knee joints of athymic nude rats and immunocompetent Wistar rats. We were able to both model fibrotic induction and resolution in the joints of Wistar rats and obtain an expression profile of ECM genes and their altered signaling patterns.

We initially hypothesized that prolonged release of TGF-β1 was responsible for initiating and maintaining the fibrotic phenotype; however, our data do not necessarily support this. Rather, it appears that acute overexpression of TGF-β1 is sufficient to induce a very severe fibrosis. Its maintenance is not reliant on the sustained presence of TGF-β1, but appears to arise from a lack of mechanisms that remove the collagenous ECM that has been deposited. Indeed, over time, we observe a reduction in the cellularity of the fibrotic mass, but the fibrous matrix still remained. Without a resident or infiltrating cell population to effect degradation of the fibrotic ECM, there is no mechanism in place for its removal and this is destined to persist.

In this regard, treatment options would appear most effective when administered prophylactically to high risk patients prior to the synthesis of constricting fibrotic matrix. This scenario would be applicable in both the fibrosis arising post knee surgery or from

IAC. Preliminary experiments examining the effects of ASO technology in our animal model of fibrosis proved to be modestly successful. Co-injection of ASOs and Ad.TGF-β1 resulted in knock down of fibrotic induction compared to Ad.TGF-β1 alone. However, more experiments need to be performed in order to determine the usefulness of ASOs as a potential therapy for IAC. Examining their function when injected into the joint at varying levels and stages of fibrosis would be ideal, as patients with IAC will not typically see their physician until they are in the middle to late stages of IAC. Currently the only therapy available to patients with IAC is physical manipulation under anesthesia and surgical release by arthroscopy. This technology, if successful, could provide a much needed alternative treatment for IAC.

Concerning the molecules that contribute to fibrosis, a widely held opinion is that the activities of TIMPs become dominant over proteolytic enzymes, and this enables the build-up of excess ECM associated with fibrosis. Our data, however, strongly contradict this idea. Rather it appears that fibrosis is very heavily dependent upon the activities of the MMPs. These molecules appear necessary to allow the dramatic expansion, motility and overgrowth of fibroblasts, as well as destruction of pre-existing matrix. It appears that the MMPs, in conjunction with matricellular proteins, are the primary mediators in the induction of fibrosis and that these molecules offer strong targets for intervention. Indeed these molecules are expressed only during tissue growth and remodeling, allowing drugs to selectively target their activities without risk to normal adult tissues.

Somewhat surprisingly, despite the dramatic effects of TGF-β1 on the joint tissues, expression of CCN2/CTGF remained relatively unchanged. CCN2/CTGF is thought to be a major activator of TGF-β1 activity and mediator of fibrosis in other tissues[21, 118, 119].

Initially, we believed that CCN2/CTGF would play a larger role in the development of joint fibrosis. However injection of Ad.CTGF resulted in little change to the joint space and expression analysis showed little difference in our model. Its relatively low induction here suggests that CCN2/CTGF may not play a major role in arthrofibrosis, and that its absence may be compensated for by other members of the matricellular proteins.

Although our data provide a severe representation of joint fibrosis, the pathologies observed are consistent with those seen clinically[98]. Procedures involving the knee, are particularly vulnerable to the development of this type of fibrosis[98]. Histological examination of tissues recovered from fibrotic knee joints following surgical release frequently identifies fibrosis, vascular proliferation and synovial chondrometaplasia[99]. In primary synovial chondromatosis, metaplastic hyaline cartilage expands the subsynovial connective tissue. While histologically primary synovial chondromatosis appears similar to chondrosarcoma, it is a benign condition that is typically self-limiting and true malignant transformation is rare. In many cases the fibro-chondrogenic tissues also contain endochondral bone formations[100-102]. The similarities between the tissue phenotype of the rat TGF-β1 overexpression model shown here and human arthrofibrosis, indicate that the data generated in the rat knee have relevance to human conditions.

Articular cartilage has a poor ability to self-regenerate and is frequently damaged as a result of trauma or pathological situations, such as osteoarthritis and rheumatoid arthritis; therefore, a method of repairing articular cartilage is of clinical relevance. Since articular cartilage has little capacity for self repair, a variety of cell based approaches are being investigated. Currently, chondrocytes isolated from healthy

cartilage and mesenchymal stem cells from bone marrow, fat, and other tissues are being tested in animal models. Our data in Chapter 4 demonstrate the enormous proliferative potential of fibroblastic cells resident in the joint capsule and synovium. Moreover, these cells appear predisposed to differentiation along a chondrogenic lineage. These cells appear to offer distinct advantages for regenerative applications, relative to progenitor cells isolated from bone marrow or adipose tissue that may be fated toward osteoblastic or adipogenic pathways respectively or to chondrocytes isolated from a very limited supply of healthy non-weight bearing cartilage.

Our findings further demonstrate that delivery of the growth factor TGF-β1 stimulates local proliferation and induces chondrogenesis. Our observations are consistent with data obtained from cultures of both embryonic and adult fibroblasts that are able to undergo differentiation into a chondrogenic phenotype in the presence of chondrogenic inducers[172] and other results which show that TGF-β1 is able to induce chondrogenic differentiation in mesenchymal progenitors[173, 174]. A phase I clinical trial is being presented using an *ex vivo* therapeutic approach to initiate cartilage repair by infecting primary chondrocytes with a virus modified to express TGF-β1 and then injecting these TGF-β1 expressing chondrocytes into the knee joint (TissueGene, Gaithersburg, MD). From the data we have presented, the application of TGF-β1 as a chondrogenic agent *in vivo*, either as a recombinant protein or transgene product, should be explored with extreme caution. Our results serve dramatize the sensitivity of connective tissue fibroblasts to growth factor stimulation, and that protocols designed to induce cellular differentiation in cartilage and bone repair *in vivo* should be aware of the high capacity for toxic side effects of these pleiotropic agents in adjacent tissues.

While the animal model of joint fibrosis described in Chapter 5 resembles the phenotype of IAC and shows signs of resolving, comparing the expression profiles of our model of arthrofibrosis to what occurs in human patients should provide a valuable insight into the signaling of this disease and, perhaps, highlight potential targets for therapy. To enable a comprehensive description of the biology of IAC at the molecular level, we will use microarray analyses to determine the differences in global transcription patterns between normal capsular tissues and those from patients with IAC. Capsular tissues from affected joints have been recovered from patients with IAC and to allow for comparative controls, tissue from the glenohumoral capsule was similarly collected from surgical patients without IAC. These tissue samples collected from patients with and without IAC, are currently being analyzed using Agilent one-color microarrays. By determining the genes and gene classes that are over and under expressed in IAC and comparing those with the biological analyses performed here, a clearer understanding of the pathogenesis and progression of the disease should emerge with respect to inflammation, fibrosis, fibrotic signaling, and TGF-β1. It would be of interest to measure endogenous TGF-$\beta 1$ expression in the long term fibrotic model to determine its levels of activity during the remodeling process and compare to expression data obtained in humans. These studies should provide direct information about the profibrotic condition in IAC and perhaps allow insight into its relationship to other fibrotic, autoimmune or hyperplastic conditions, such as scleroderma.

LIST OF REFERENCES

1. Hannafin, J. A. & Chiaia, T. A. Adhesive capsulitis. A treatment approach. *Clin Orthop Relat Res*, 95-109 (2000).

2. Dias, R., Cutts, S. & Massoud, S. Frozen shoulder. *Bmj* **331**, 1453-6 (2005).

3. Siegel, L. B., Cohen, N. J. & Gall, E. P. Adhesive capsulitis: a sticky issue. *Am Fam Physician* **59**, 1843-52 (1999).

4. van Royen, B. J. & Pavlov, P. W. Treatment of frozen shoulder by distension and manipulation under local anaesthesia. *Int Orthop* **20**, 207-10 (1996).

5. Binder, A. I., Bulgen, D. Y., Hazleman, B. L. & Roberts, S. Frozen shoulder: a long-term prospective study. *Ann Rheum Dis* **43**, 361-4 (1984).

6. Bulgen, D. Y., Binder, A. I., Hazleman, B. L., Dutton, J. & Roberts, S. Frozen shoulder: prospective clinical study with an evaluation of three treatment regimens. *Ann Rheum Dis* **43**, 353-60 (1984).

7. Placzek, J. D. *et al.* Long-term effectiveness of translational manipulation for adhesive capsulitis. *Clin Orthop Relat Res*, 181-91 (1998).

8. Helbig, B., Wagner, P. & Dohler, R. Mobilization of frozen shoulder under general anaesthesia. *Acta Orthop Belg* **49**, 267-74 (1983).

9. Rhind, V., Downie, W. W., Bird, H. A., Wright, V. & Engler, C. Naproxen and indomethacin in periarthritis of the shoulder. *Rheumatol Rehabil* **21**, 51-3 (1982).

10. Binder, A., Hazleman, B. L., Parr, G. & Roberts, S. A controlled study of oral prednisolone in frozen shoulder. *Br J Rheumatol* **25**, 288-92 (1986).

11. de Jong, B. A., Dahmen, R., Hogeweg, J. A. & Marti, R. K. Intra-articular triamcinolone acetonide injection in patients with capsulitis of the shoulder: a comparative study of two dose regimens. *Clin Rehabil* **12**, 211-5 (1998).

12. Quigley, T. B. Indications for Manipulation and Corticosteroids in the Treatment of Stiff Shoulders. *Surg Clin North Am* **43**, 1715-20 (1963).

13. Steinbrocker, O. & Argyros, T. G. Frozen shoulder: treatment by local injections of depot corticosteroids. *Arch Phys Med Rehabil* **55**, 209-13 (1974).

14. Franklin, T. J. Therapeutic approaches to organ fibrosis. *Int J Biochem Cell Biol* **29**, 79-89 (1997).

15. Clark, R. A. Cutaneous tissue repair: basic biologic considerations. I. *J Am Acad Dermatol* **13**, 701-25 (1985).

16. Desmouliere, A., Darby, I. A. & Gabbiani, G. Normal and pathologic soft tissue remodeling: role of the myofibroblast, with special emphasis on liver and kidney fibrosis. *Lab Invest* **83**, 1689-707 (2003).

17. Border, W. A. & Noble, N. A. Transforming growth factor beta in tissue fibrosis. *N Engl J Med* **331**, 1286-92 (1994).

18. Czaja, M. J. *et al. In vitro* and *in vivo* association of transforming growth factor-beta 1 with hepatic fibrosis. *J Cell Biol* **108**, 2477-82 (1989).

19. Isaka, Y. *et al.* Gene therapy by skeletal muscle expression of decorin prevents fibrotic disease in rat kidney. *Nat Med* **2**, 418-23 (1996).

20. Johnson, R. J., Floege, J., Couser, W. G. & Alpers, C. E. Role of platelet-derived growth factor in glomerular disease. *J Am Soc Nephrol* **4**, 119-28 (1993).

21. Ihn, H. Pathogenesis of fibrosis: role of TGF-beta and CTGF. *Curr Opin Rheumatol* **14**, 681-5 (2002).

22. Miyazono, K., Kusanagi, K. & Inoue, H. Divergence and convergence of TGF-beta/BMP signaling. *J Cell Physiol* **187**, 265-76 (2001).

23. Piek, E., Heldin, C. H. & Ten Dijke, P. Specificity, diversity, and regulation in TGF-beta superfamily signaling. *Faseb J* **13**, 2105-24 (1999).

24. Nunes, I., Gleizes, P. E., Metz, C. N. & Rifkin, D. B. Latent transforming growth factor-beta binding protein domains involved in activation and transglutaminase-dependent cross-linking of latent transforming growth factor-beta. *J Cell Biol* **136**, 1151-63 (1997).

25. Saitoh, M. *et al.* Identification of important regions in the cytoplasmic juxtamembrane domain of type I receptor that separate signaling pathways of transforming growth factor-beta. *J Biol Chem* **271**, 2769-75 (1996).

26. Wrana, J. L., Attisano, L., Wieser, R., Ventura, F. & Massague, J. Mechanism of activation of the TGF-beta receptor. *Nature* **370**, 341-7 (1994).

27. Holmes, A. *et al.* CTGF and SMADs, maintenance of scleroderma phenotype is independent of SMAD signaling. *J Biol Chem* **276**, 10594-601 (2001).

28. Dennler, S. *et al.* Direct binding of Smad3 and Smad4 to critical TGF beta-inducible elements in the promoter of human plasminogen activator inhibitor-type 1 gene. *Embo J* **17**, 3091-100 (1998).

29. Jonk, L. J., Itoh, S., Heldin, C. H., ten Dijke, P. & Kruijer, W. Identification and functional characterization of a Smad binding element (SBE) in the JunB promoter that acts as a transforming growth factor-beta, activin, and bone morphogenetic protein-inducible enhancer. *J Biol Chem* **273**, 21145-52 (1998).

30. Nagarajan, R. P., Zhang, J., Li, W. & Chen, Y. Regulation of Smad7 promoter by direct association with Smad3 and Smad4. *J Biol Chem* **274**, 33412-8 (1999).

31. Taylor, L. M. & Khachigian, L. M. Induction of platelet-derived growth factor B-chain expression by transforming growth factor-beta involves transactivation by Smads. *J Biol Chem* **275**, 16709-16 (2000).

32. Lai, C. F. *et al.* Transforming growth factor-beta up-regulates the beta 5 integrin subunit expression via Sp1 and Smad signaling. *J Biol Chem* **275**, 36400-6 (2000).

33. Takagawa, S. *et al.* Sustained activation of fibroblast transforming growth factor-beta/Smad signaling in a murine model of scleroderma. *J Invest Dermatol* **121**, 41-50 (2003).

34. Verrecchia, F., Chu, M. L. & Mauviel, A. Identification of novel TGF-beta /Smad gene targets in dermal fibroblasts using a combined cDNA microarray/promoter transactivation approach. *J Biol Chem* **276**, 17058-62 (2001).

35. Verrecchia, F. & Mauviel, A. Transforming growth factor-beta signaling through the Smad pathway: role in extracellular matrix gene expression and regulation. *J Invest Dermatol* **118**, 211-5 (2002).

36. Postlethwaite, A. E., Keski-Oja, J., Moses, H. L. & Kang, A. H. Stimulation of the chemotactic migration of human fibroblasts by transforming growth factor beta. *J Exp Med* **165**, 251-6 (1987).

37. Jester, J. V., Huang, J., Petroll, W. M. & Cavanagh, H. D. TGFbeta induced myofibroblast differentiation of rabbit keratocytes requires synergistic TGFbeta, PDGF and integrin signaling. *Exp Eye Res* **75**, 645-57 (2002).

38. Zhang, H. Y. & Phan, S. H. Inhibition of myofibroblast apoptosis by transforming growth factor beta(1). *Am J Respir Cell Mol Biol* **21**, 658-65 (1999).

39. Rodeo, S. A., Hannafin, J. A., Tom, J., Warren, R. F. & Wickiewicz, T. L. Immunolocalization of cytokines and their receptors in adhesive capsulitis of the shoulder. *J Orthop Res* **15**, 427-36 (1997).

40. Bunker, T. D., Reilly, J., Baird, K. S. & Hamblen, D. L. Expression of growth factors, cytokines and matrix metalloproteinases in frozen shoulder. *J Bone Joint Surg Br* **82**, 768-73 (2000).

41. Ryu, J. D. *et al.* Expression of vascular endothelial growth factor and angiogenesis in the diabetic frozen shoulder. *J Shoulder Elbow Surg* **15**, 679-85 (2006).

42. Foulis, A. K., McGill, M. & Farquharson, M. A. Insulitis in type 1 (insulin-dependent) diabetes mellitus in man--macrophages, lymphocytes, and interferon-gamma containing cells. *J Pathol* **165**, 97-103 (1991).

43. Matthaei, S., Stumvoll, M., Kellerer, M. & Haring, H. U. Pathophysiology and pharmacological treatment of insulin resistance. *Endocr Rev* **21**, 585-618 (2000).

44. Galkowska, H., Wojewodzka, U. & Olszewski, W. L. Chemokines, cytokines, and growth factors in keratinocytes and dermal endothelial cells in the margin of chronic diabetic foot ulcers. *Wound Repair Regen* **14**, 558-65 (2006).

45. Maruyama, K. *et al.* Decreased macrophage number and activation lead to reduced lymphatic vessel formation and contribute to impaired diabetic wound healing. *Am J Pathol* **170**, 1178-91 (2007).

46. Twigg, S. M. *et al.* Advanced glycosylation end products up-regulate connective tissue growth factor (insulin-like growth factor-binding protein-related protein 2) in human fibroblasts: a potential mechanism for expansion of extracellular matrix in diabetes mellitus. *Endocrinology* **142**, 1760-9 (2001).

47. Kayal, R. A. *et al.* Diminished bone formation during diabetic fracture healing is related to the premature resorption of cartilage associated with increased osteoclast activity. *J Bone Miner Res* **22**, 560-8 (2007).

48. Lobmann, R. *et al.* Expression of matrix-metalloproteinases and their inhibitors in the wounds of diabetic and non-diabetic patients. *Diabetologia* **45**, 1011-6 (2002).

49. Roestenberg, P. *et al.* Connective tissue growth factor is increased in plasma of type 1 diabetic patients with nephropathy. *Diabetes Care* **27**, 1164-70 (2004).

50. Gilbert, R. E. *et al.* Urinary connective tissue growth factor excretion in patients with type 1 diabetes and nephropathy. *Diabetes Care* **26**, 2632-6 (2003).

51. Riser, B. L. *et al.* Regulation of connective tissue growth factor activity in cultured rat mesangial cells and its expression in experimental diabetic glomerulosclerosis. *J Am Soc Nephrol* **11**, 25-38 (2000).

52. Ito, Y. *et al.* Expression of connective tissue growth factor in human renal fibrosis. *Kidney Int* **53**, 853-61 (1998).

53. Ziyadeh, F. N. Mediators of diabetic renal disease: the case for tgf-Beta as the major mediator. *J Am Soc Nephrol* **15 Suppl 1**, S55-7 (2004).

54. Isono, M., Chen, S., Hong, S. W., Iglesias-de la Cruz, M. C. & Ziyadeh, F. N. Smad pathway is activated in the diabetic mouse kidney and Smad3 mediates TGF-beta-induced fibronectin in mesangial cells. *Biochem Biophys Res Commun* **296**, 1356-65 (2002).

55. McLennan, S. V. *et al.* Effects of glucose on matrix metalloproteinase and plasmin activities in mesangial cells: possible role in diabetic nephropathy. *Kidney Int Suppl* **77**, S81-7 (2000).

56. Ayo, S. H., Radnik, R., Garoni, J. A., Troyer, D. A. & Kreisberg, J. I. High glucose increases diacylglycerol mass and activates protein kinase C in mesangial cell cultures. *Am J Physiol* **261**, F571-7 (1991).

57. Ziyadeh, F. N., Sharma, K., Ericksen, M. & Wolf, G. Stimulation of collagen gene expression and protein synthesis in murine mesangial cells by high glucose is mediated by autocrine activation of transforming growth factor-beta. *J Clin Invest* **93**, 536-42 (1994).

58. Han, D. C., Isono, M., Hoffman, B. B. & Ziyadeh, F. N. High glucose stimulates proliferation and collagen type I synthesis in renal cortical fibroblasts: mediation by autocrine activation of TGF-beta. *J Am Soc Nephrol* **10**, 1891-9 (1999).

59. Han, D. C., Hoffman, B. B., Hong, S. W., Guo, J. & Ziyadeh, F. N. Therapy with antisense TGF-beta1 oligodeoxynucleotides reduces kidney weight and matrix mRNAs in diabetic mice. *Am J Physiol Renal Physiol* **278**, F628-34 (2000).

60. Sharma, K., Jin, Y., Guo, J. & Ziyadeh, F. N. Neutralization of TGF-beta by anti-TGF-beta antibody attenuates kidney hypertrophy and the enhanced extracellular matrix gene expression in STZ-induced diabetic mice. *Diabetes* **45**, 522-30 (1996).

61. Zhang, J., Liu, Z., Liu, H., Li, Y. & Li, L. [Regulation of the expression and function of glucose transporter-1 by TGF-beta 1 and high glucose in mesangial cells]. *Chin Med J (Engl)* **113**, 508-13 (2000).

62. Gnudi, L., Thomas, S. M. & Viberti, G. Mechanical forces in diabetic kidney disease: a trigger for impaired glucose metabolism. *J Am Soc Nephrol* **18**, 2226-32 (2007).

63. Ziyadeh, F. N., Han, D. C., Cohen, J. A., Guo, J. & Cohen, M. P. Glycated albumin stimulates fibronectin gene expression in glomerular mesangial cells: involvement of the transforming growth factor-beta system. *Kidney Int* **53**, 631-8 (1998).

64. Isono, M., Mogyorosi, A., Han, D. C., Hoffman, B. B. & Ziyadeh, F. N. Stimulation of TGF-beta type II receptor by high glucose in mouse mesangial cells and in diabetic kidney. *Am J Physiol Renal Physiol* **278**, F830-8 (2000).

65. Dyer, D. G. *et al.* Accumulation of Maillard reaction products in skin collagen in diabetes and aging. *J Clin Invest* **91**, 2463-9 (1993).

66. Vlassara, H., Bucala, R. & Striker, L. Pathogenic effects of advanced glycosylation: biochemical, biologic, and clinical implications for diabetes and aging. *Lab Invest* **70**, 138-51 (1994).

67. Vlassara, H., Brownlee, M. & Cerami, A. Nonenzymatic glycosylation of peripheral nerve protein in diabetes mellitus. *Proc Natl Acad Sci U S A* **78**, 5190-2 (1981).

68. Kreisberg, J. I., Garoni, J. A., Radnik, R. & Ayo, S. H. High glucose and TGF beta 1 stimulate fibronectin gene expression through a cAMP response element. *Kidney Int* **46**, 1019-24 (1994).

69. Oh, J. H., Ha, H., Yu, M. R. & Lee, H. B. Sequential effects of high glucose on mesangial cell transforming growth factor-beta 1 and fibronectin synthesis. *Kidney Int* **54**, 1872-8 (1998).

70. Ha, H., Yu, M. R. & Lee, H. B. High glucose-induced PKC activation mediates TGF-beta 1 and fibronectin synthesis by peritoneal mesothelial cells. *Kidney Int* **59**, 463-70 (2001).

71. Yung, S., Liu, Z. H., Lai, K. N., Li, L. S. & Chan, T. M. Emodin ameliorates glucose-induced morphologic abnormalities and synthesis of transforming growth factor beta1 and fibronectin by human peritoneal mesothelial cells. *Perit Dial Int* **21 Suppl 3**, S41-7 (2001).

72. Li, J. H. *et al.* Advanced glycation end products activate Smad signaling via TGF-beta-dependent and independent mechanisms: implications for diabetic renal and vascular disease. *Faseb J* **18**, 176-8 (2004).

73. Evans, C. H. *et al.* Gene therapy for rheumatic diseases. *Arthritis Rheum* **42**, 1-16 (1999).

74. Ghivizzani, S. C., Oligino, T. J., Glorioso, J. C., Robbins, P. D. & Evans, C. H. Direct gene delivery strategies for the treatment of rheumatoid arthritis. *Drug Discov Today* **6**, 259-267 (2001).

75. Bandara, G. *et al.* Intraarticular expression of biologically active interleukin 1-receptor-antagonist protein by ex vivo gene transfer. *Proc Natl Acad Sci U S A* **90**, 10764-8 (1993).

76. Otani, K. *et al.* Suppression of antigen-induced arthritis in rabbits by ex vivo gene therapy. *J Immunol* **156**, 3558-62 (1996).

77. Ghivizzani, S. C. *et al.* Constitutive intra-articular expression of human IL-1 beta following gene transfer to rabbit synovium produces all major pathologies of human rheumatoid arthritis. *J Immunol* **159**, 3604-12 (1997).

78. Gouze, E. *et al.* Lentiviral-mediated gene delivery to synovium: potent intra-articular expression with amplification by inflammation. *Mol Ther* **7**, 460-6 (2003).

79. Hardy, S., Kitamura, M., Harris-Stansil, T., Dai, Y. & Phipps, M. L. Construction of adenovirus vectors through Cre-lox recombination. *J Virol* **71**, 1842-9 (1997).

80. Ng, P. & Graham, F. L. Construction of first-generation adenoviral vectors. *Methods Mol Med* **69**, 389-414 (2002).

81. Heng, E. C., Huang, Y., Black, S. A., Jr. & Trackman, P. C. CCN2, connective tissue growth factor, stimulates collagen deposition by gingival fibroblasts via module 3 and alpha6- and beta1 integrins. *J Cell Biochem* **98**, 409-20 (2006).

82. Moussad, E. E. & Brigstock, D. R. Connective tissue growth factor: what's in a name? *Mol Genet Metab* **71**, 276-92 (2000).

83. Gholve, P. A. *et al.* Arthrofibrosis of the knee after tibial spine fracture in children: a report of two complicated cases. *Hss J* **4**, 14-9 (2008).

84. Lee, S. K., Gargano, F. & Hausman, M. R. Wrist arthrofibrosis. *Hand Clin* **22**, 529-38; abstract vii (2006).

85. Schiavone Panni, A., Cerciello, S., Vasso, M. & Tartarone, M. Stiffness in total knee arthroplasty. *J Orthop Traumatol* **10**, 111-8 (2009).

86. Boldt, J. G., Munzinger, U. K., Zanetti, M. & Hodler, J. Arthrofibrosis associated with total knee arthroplasty: gray-scale and power Doppler sonographic findings. *AJR Am J Roentgenol* **182**, 337-40 (2004).

87. Neviaser, R. J. & Neviaser, T. J. The frozen shoulder. Diagnosis and management. *Clin Orthop Relat Res*, 59-64 (1987).

88. Wynn, T. A. Cellular and molecular mechanisms of fibrosis. *J Pathol* **214**, 199-210 (2008).

89. Pohlers, D. *et al.* TGF-beta and fibrosis in different organs - molecular pathway imprints. *Biochim Biophys Acta* **1792**, 746-56 (2009).

90. Gressner, O. A., Rizk, M. S., Kovalenko, E., Weiskirchen, R. & Gressner, A. M. Changing the pathogenetic roadmap of liver fibrosis? Where did it start; where will it go? *J Gastroenterol Hepatol* **23**, 1024-35 (2008).

91. Rahimi, R. A. & Leof, E. B. TGF-beta signaling: a tale of two responses. *J Cell Biochem* **102**, 593-608 (2007).

92. Leivonen, S. K. & Kahari, V. M. Transforming growth factor-beta signaling in cancer invasion and metastasis. *Int J Cancer* **121**, 2119-24 (2007).

93. Bonniaud, P. *et al.* TGF-beta and Smad3 signaling link inflammation to chronic fibrogenesis. *J Immunol* **175**, 5390-5 (2005).

94. Gouze, E. *et al.* Transgene persistence and cell turnover in the diarthrodial joint: implications for gene therapy of chronic joint diseases. *Mol Ther* **15**, 1114-20 (2007).

95. Spessotto, P. *et al.* beta 1 Integrin-dependent cell adhesion to EMILIN-1 is mediated by the gC1q domain. *J Biol Chem* **278**, 6160-7 (2003).

96. Zhang, H. Y., Gharaee-Kermani, M., Zhang, K., Karmiol, S. & Phan, S. H. Lung fibroblast alpha-smooth muscle actin expression and contractile phenotype in bleomycin-induced pulmonary fibrosis. *Am J Pathol* **148**, 527-37 (1996).

97. Gouze, E. *et al. In vivo* gene delivery to synovium by lentiviral vectors. *Mol Ther* **5**, 397-404 (2002).

98. Magit, D., Wolff, A., Sutton, K. & Medvecky, M. J. Arthrofibrosis of the knee. *J Am Acad Orthop Surg* **15**, 682-94 (2007).

99. Murphey, M. D., Vidal, J. A., Fanburg-Smith, J. C. & Gajewski, D. A. Imaging of synovial chondromatosis with radiologic-pathologic correlation. *Radiographics* **27**, 1465-88 (2007).

100. Vargas-Gonzalez, R. & Sanchez-Sosa, S. Fibrocartilaginous dysplasia (fibrous dysplasia with extensive cartilaginous differentiation). *Pathol Oncol Res* **12**, 111-4 (2006).

101. Zoricic, S., Maric, I., Bobinac, D. & Vukicevic, S. Expression of bone morphogenetic proteins and cartilage-derived morphogenetic proteins during osteophyte formation in humans. *J Anat* **202**, 269-77 (2003).

102. Matsui, Y. *et al.* Intrapatellar tendon lipoma with chondro-osseous differentiation: detection of HMGA2-LPP fusion gene transcript. *J Clin Pathol* **59**, 434-6 (2006).

103. Wirrig, E. E. *et al.* Cartilage link protein 1 (Crtl1), an extracellular matrix component playing an important role in heart development. *Dev Biol* **310**, 291-303 (2007).

104. Gueders, M. M., Foidart, J. M., Noel, A. & Cataldo, D. D. Matrix metalloproteinases (MMPs) and tissue inhibitors of MMPs in the respiratory tract: potential implications in asthma and other lung diseases. *Eur J Pharmacol* **533**, 133-44 (2006).

105. Hemmann, S., Graf, J., Roderfeld, M. & Roeb, E. Expression of MMPs and TIMPs in liver fibrosis - a systematic review with special emphasis on anti-fibrotic strategies. *J Hepatol* **46**, 955-75 (2007).

106. English, J. L. *et al.* Individual Timp deficiencies differentially impact pro-MMP-2 activation. *J Biol Chem* **281**, 10337-46 (2006).

107. Pardo, A. & Selman, M. Matrix metalloproteases in aberrant fibrotic tissue remodeling. *Proc Am Thorac Soc* **3**, 383-8 (2006).

108. Bornstein, P. & Sage, E. H. Matricellular proteins: extracellular modulators of cell function. *Curr Opin Cell Biol* **14**, 608-16 (2002).

109. Alford, A. I. & Hankenson, K. D. Matricellular proteins: Extracellular modulators of bone development, remodeling, and regeneration. *Bone* **38**, 749-57 (2006).

110. Mo, F. E. & Lau, L. F. The matricellular protein CCN1 is essential for cardiac development. *Circ Res* **99**, 961-9 (2006).

111. Moura, R., Tjwa, M., Vandervoort, P., Cludts, K. & Hoylaerts, M. F. Thrombospondin-1 activates medial smooth muscle cells and triggers neointima formation upon mouse carotid artery ligation. *Arterioscler Thromb Vasc Biol* **27**, 2163-9 (2007).

112. Bradshaw, A. D. & Sage, E. H. SPARC, a matricellular protein that functions in cellular differentiation and tissue response to injury. *J Clin Invest* **107**, 1049-54 (2001).

113. Bornstein, P. Matricellular proteins: an overview. *Matrix Biol* **19**, 555-6 (2000).

114. Agnihotri, R. *et al.* Osteopontin, a novel substrate for matrix metalloproteinase-3 (stromelysin-1) and matrix metalloproteinase-7 (matrilysin). *J Biol Chem* **276**, 28261-7 (2001).

115. Pardo, A. *et al.* Up-regulation and profibrotic role of osteopontin in human idiopathic pulmonary fibrosis. *PLoS Med* **2**, e251 (2005).

116. Castellano, G. *et al.* Activation of the osteopontin/matrix metalloproteinase-9 pathway correlates with prostate cancer progression. *Clin Cancer Res* **14**, 7470-80 (2008).

117. Gao, Y. A., Agnihotri, R., Vary, C. P. & Liaw, L. Expression and characterization of recombinant osteopontin peptides representing matrix metalloproteinase proteolytic fragments. *Matrix Biol* **23**, 457-66 (2004).

118. Kobayashi, T. *et al.* Connective tissue growth factor mediates the profibrotic effects of transforming growth factor-beta produced by tubular epithelial cells in response to high glucose. *Clin Exp Nephrol* **9**, 114-21 (2005).

119. Leask, A., Parapuram, S. K., Shi-Wen, X. & Abraham, D. J. Connective tissue growth factor (CTGF, CCN2) gene regulation: a potent clinical bio-marker of fibroproliferative disease? *J Cell Commun Signal* **3**, 89-94 (2009).

120. Woods, A., Wang, G. & Beier, F. Regulation of chondrocyte differentiation by the actin cytoskeleton and adhesive interactions. *J Cell Physiol* **213**, 1-8 (2007).

121. Lehembre, F. *et al.* NCAM-induced focal adhesion assembly: a functional switch upon loss of E-cadherin. *Embo J* **27**, 2603-15 (2008).

122. Frame, M. C. & Inman, G. J. NCAM is at the heart of reciprocal regulation of E-cadherin- and integrin-mediated adhesions via signaling modulation. *Dev Cell* **15**, 494-6 (2008).

123. Shintani, N. & Hunziker, E. B. Chondrogenic differentiation of bovine synovium: bone morphogenetic proteins 2 and 7 and transforming growth factor beta1 induce the formation of different types of cartilaginous tissue. *Arthritis Rheum* **56**, 1869-79 (2007).

124. Fiorito, S., Magrini, L., Adrey, J., Mailhe, D. & Brouty-Boye, D. Inflammatory status and cartilage regenerative potential of synovial fibroblasts from patients with osteoarthritis and chondropathy. *Rheumatology (Oxford)* **44**, 164-71 (2005).

125. Mochizuki, T. *et al.* Higher chondrogenic potential of fibrous synovium- and adipose synovium-derived cells compared with subcutaneous fat-derived cells: distinguishing properties of mesenchymal stem cells in humans. *Arthritis Rheum* **54**, 843-53 (2006).

126. Shirasawa, S. *et al. In vitro* chondrogenesis of human synovium-derived mesenchymal stem cells: optimal condition and comparison with bone marrow-derived cells. *J Cell Biochem* **97**, 84-97 (2006).

127. Jiang, X. *et al.* [Study on the directed inducing process of cartilage cells differentiated from human marrow mesenchymal stem cells]. *Zhonghua Er Bi Yan Hou Ke Za Zhi* **37**, 137-9 (2002).

128. De Bari, C., Dell'Accio, F., Tylzanowski, P. & Luyten, F. P. Multipotent mesenchymal stem cells from adult human synovial membrane. *Arthritis Rheum* **44**, 1928-42 (2001).

129. Karystinou, A. *et al.* Distinct mesenchymal progenitor cell subsets in the adult human synovium. *Rheumatology (Oxford)* **48**, 1057-64 (2009).

130. Crawford, A., Frazer, A., Lippitt, J. M., Buttle, D. J. & Smith, T. A case of chondromatosis indicates a synovial stem cell aetiology. *Rheumatology (Oxford)* **45**, 1529-33 (2006).

131. Krampera, M., Pizzolo, G., Aprili, G. & Franchini, M. Mesenchymal stem cells for bone, cartilage, tendon and skeletal muscle repair. *Bone* **39**, 678-83 (2006).

132. Ahmed, N., Stanford, W. L. & Kandel, R. A. Mesenchymal stem and progenitor cells for cartilage repair. *Skeletal Radiol* **36**, 909-12 (2007).

133. Patel, T. & Gores, G. J. Apoptosis and hepatobiliary disease. *Hepatology* **21**, 1725-41 (1995).

134. Vaux, D. L. & Strasser, A. The molecular biology of apoptosis. *Proc Natl Acad Sci U S A* **93**, 2239-44 (1996).

135. Evan, G. I., Brown, L., Whyte, M. & Harrington, E. Apoptosis and the cell cycle. *Curr Opin Cell Biol* **7**, 825-34 (1995).

136. Fraser, A. & Evan, G. A license to kill. *Cell* **85**, 781-4 (1996).

137. Cole, A. A. *et al.* Chondrocyte matrix metalloproteinase-8. Human articular chondrocytes express neutrophil collagenase. *J Biol Chem* **271**, 11023-6 (1996).

138. Hanemaaijer, R. *et al.* Matrix metalloproteinase-8 is expressed in rheumatoid synovial fibroblasts and endothelial cells. Regulation by tumor necrosis factor-alpha and doxycycline. *J Biol Chem* **272**, 31504-9 (1997).

139. Sasano, Y. *et al.* Gene expression of MMP8 and MMP13 during embryonic development of bone and cartilage in the rat mandible and hind limb. *J Histochem Cytochem* **50**, 325-32 (2002).

140. Poczatek, M. H., Hugo, C., Darley-Usmar, V. & Murphy-Ullrich, J. E. Glucose stimulation of transforming growth factor-beta bioactivity in mesangial cells is mediated by thrombospondin-1. *Am J Pathol* **157**, 1353-63 (2000).

141. Sharma, K. *et al.* Increased renal production of transforming growth factor-beta1 in patients with type II diabetes. *Diabetes* **46**, 854-9 (1997).

142. Yamamoto, T. *et al.* Expression of transforming growth factor-beta isoforms in human glomerular diseases. *Kidney Int* **49**, 461-9 (1996).

143. Iwano, M. *et al.* Quantification of glomerular TGF-beta 1 mRNA in patients with diabetes mellitus. *Kidney Int* **49**, 1120-6 (1996).

144. McLennan, S. V. *et al.* Decreased matrix degradation in diabetic nephropathy: effects of ACE inhibition on the expression and activities of matrix metalloproteinases. *Diabetologia* **45**, 268-75 (2002).

145. Ziyadeh, F. N. *et al.* Long-term prevention of renal insufficiency, excess matrix gene expression, and glomerular mesangial matrix expansion by treatment with monoclonal antitransforming growth factor-beta antibody in db/db diabetic mice. *Proc Natl Acad Sci U S A* **97**, 8015-20 (2000).

146. Milgrom, C. *et al.* Risk factors for idiopathic frozen shoulder. *Isr Med Assoc J* **10**, 361-4 (2008).

147. Lee, J. S., Oum, B. S. & Lee, S. H. Mitomycin c influence on inhibition of cellular proliferation and subsequent synthesis of type I collagen and laminin in primary and recurrent pterygia. *Ophthalmic Res* **33**, 140-6 (2001).

148. Nieto, A. *et al.* Effect of mitomycin-C on human foreskin fibroblasts used as feeders in human embryonic stem cells: immunocytochemistry MIB1 score and DNA ploidy and apoptosis evaluated by flow cytometry. *Cell Biol Int* **31**, 269-78 (2007).

149. Heilmann, C., Schonfeld, P., Schluter, T., Bohnensack, R. & Behrens-Baumann, W. Effect of the cytostatic agent idarubicin on fibroblasts of the human Tenon's capsule compared with mitomycin C. *Br J Ophthalmol* **83**, 961-6 (1999).

150. Blacker, K. L., Williams, M. L. & Goldyne, M. Mitomycin C-treated 3T3 fibroblasts used as feeder layers for human keratinocyte culture retain the capacity to generate eicosanoids. *J Invest Dermatol* **89**, 536-9 (1987).

151. Chen, T. C. & Chang, S. W. Mitomycin C Modulates IL-1R Expression on Corneal Fibroblasts and Modifies Corneal Epithelial Cell Migration via IL-1 Related Hepatocyte Growth Factor. *Invest Ophthalmol Vis Sci* (2009).

152. Ha, T. S. *et al.* Regulation of renal laminin in mice with type II diabetes. *J Am Soc Nephrol* **10**, 1931-9 (1999).

153. van Det, N. F. *et al.* Regulation of glomerular epithelial cell production of fibronectin and transforming growth factor-beta by high glucose, not by angiotensin II. *Diabetes* **46**, 834-40 (1997).

154. Suzuki, D. *et al.* In situ hybridization studies of matrix metalloproteinase-3, tissue inhibitor of metalloproteinase-1 and type IV collagen in diabetic nephropathy. *Kidney Int* **52**, 111-9 (1997).

155. Del Prete, D. *et al.* Down-regulation of glomerular matrix metalloproteinase-2 gene in human NIDDM. *Diabetologia* **40**, 1449-54 (1997).

156. Shankland, S. J., Ly, H., Thai, K. & Scholey, J. W. Glomerular expression of tissue inhibitor of metalloproteinase (TIMP-1) in normal and diabetic rats. *J Am Soc Nephrol* **7**, 97-104 (1996).

157. Knoll, K. E., Pietrusz, J. L. & Liang, M. Tissue-specific transcriptome responses in rats with early streptozotocin-induced diabetes. *Physiol Genomics* **21**, 222-9 (2005).

158. Mosci, P., Vecchiarelli, A., Cenci, E., Puliti, M. & Bistoni, F. Low-dose streptozotocin-induced diabetes in mice. I. Course of Candida albicans infection. *Cell Immunol* **150**, 27-35 (1993).

159. Kunjathoor, V. V., Wilson, D. L. & LeBoeuf, R. C. Increased atherosclerosis in streptozotocin-induced diabetic mice. *J Clin Invest* **97**, 1767-73 (1996).

160. Krakauer, J. C. *et al.* Bone loss and bone turnover in diabetes. *Diabetes* **44**, 775-82 (1995).

161. Gooch, H. L., Hale, J. E., Fujioka, H., Balian, G. & Hurwitz, S. R. Alterations of cartilage and collagen expression during fracture healing in experimental diabetes. *Connect Tissue Res* **41**, 81-91 (2000).

162. Herskind, A. M., Christensen, K., Norgaard-Andersen, K. & Andersen, J. F. Diabetes mellitus and healing of closed fractures. *Diabete Metab* **18**, 63-4 (1992).

163. Soejima, K. & Landing, B. H. Osteoporosis in juvenile-onset diabetes mellitus: morphometric and comparative studies. *Pediatr Pathol* **6**, 289-99 (1986).

164. Goodman, W. G. & Hori, M. T. Diminished bone formation in experimental diabetes. Relationship to osteoid maturation and mineralization. *Diabetes* **33**, 825-31 (1984).

165. Funk, J. R., Hale, J. E., Carmines, D., Gooch, H. L. & Hurwitz, S. R. Biomechanical evaluation of early fracture healing in normal and diabetic rats. *J Orthop Res* **18**, 126-32 (2000).

166. Lu, H., Kraut, D., Gerstenfeld, L. C. & Graves, D. T. Diabetes interferes with the bone formation by affecting the expression of transcription factors that regulate osteoblast differentiation. *Endocrinology* **144**, 346-52 (2003).

167. Tamm, I., Dorken, B. & Hartmann, G. Antisense therapy in oncology: new hope for an old idea? *Lancet* **358**, 489-97 (2001).

168. Yacyshyn, B. R. *et al.* A placebo-controlled trial of ICAM-1 antisense oligonucleotide in the treatment of Crohn's disease. *Gastroenterology* **114**, 1133-42 (1998).

169. Stephenson, M. L. & Zamecnik, P. C. Inhibition of Rous sarcoma viral RNA translation by a specific oligodeoxyribonucleotide. *Proc Natl Acad Sci U S A* **75**, 285-8 (1978).

170. Dean, N. M. & Griffey, R. H. Identification and characterization of second-generation antisense oligonucleotides. *Antisense Nucleic Acid Drug Dev* **7**, 229-33 (1997).

171. Henry, S. *et al.* Chemically modified oligonucleotides exhibit decreased immune stimulation in mice. *J Pharmacol Exp Ther* **292**, 468-79 (2000).

172. Lengner, C. J. *et al.* Primary mouse embryonic fibroblasts: a model of mesenchymal cartilage formation. *J Cell Physiol* **200**, 327-33 (2004).

173. Tuli, R. *et al.* Transforming growth factor-beta-mediated chondrogenesis of human mesenchymal progenitor cells involves N-cadherin and mitogen-activated protein kinase and Wnt signaling cross-talk. *J Biol Chem* **278**, 41227-36 (2003).

174. Barry, F., Boynton, R. E., Liu, B. & Murphy, J. M. Chondrogenic differentiation of mesenchymal stem cells from bone marrow: differentiation-dependent gene expression of matrix components. *Exp Cell Res* **268**, 189-200 (2001).

175. Brittberg, M. *et al.* Treatment of deep cartilage defects in the knee with autologous chondrocyte transplantation. *N Engl J Med* **331**, 889-95 (1994).

BIOGRAPHICAL SKETCH

Rachael Susan Watson was raised in Bainbridge Township, Ohio. She graduated summa cum laude of Kenston High School's class of 1999. Her undergraduate studies began the following fall at the University of Mount Union, Alliance, Ohio, where she majored in biology and minored in chemistry. During the summers of her junior and senior years, Rachael began working as a research assistant at the NASA Glenn Research Center in Cleveland, Ohio in the lab of Dr. Greg Zimmerli, where she contributed to the understanding of loss of bone density in microgravity. After graduating magna cum laude and receiving her Bachelor of Science in May 2003, she began work for Dr. Yung Huang at Case Western Reserve University in Cleveland, Ohio developing a cell based vaccine for influenza, until joining the Interdisciplinary Program in Biomedical Sciences (IDP) at the University of Florida in August of 2004. In May of 2005, Rachael began her doctoral study under the guidance Dr. Steven C. Ghivizzani, in the Department of Orthopaedics and Rehabilitation where she investigated the idiopathic disease, Adhesive Capsulitis. During the course of her graduate studies she received extensive training in the use of techniques to study arthrofibrosis, including the development viral vectors for gene transfer, techniques to study *in vivo* gene signaling and the development of animal models. She received a graduate student research grant from Clinical and Translation Science Institute at the University of Florida. Rachael presented her research at a talk for a Keystone Symposia on TGF-beta and received a scholarship from the Keystone Symposia for her work. She also presented her research at a poster presentation for the American Society of Gene and Cell Therapy. Her graduate research characterizing the role of TGF-beta in arthrofibrosis is currently in submission. Rachael received her Ph.D. in the spring of 2010.